COMPARISON OF STRESS-PATH METHOD OF SETTLEMENT ANALYSIS WITH OTHER METHODS APPLIED TO A LIGHTLY OVER-CONSOLIDATED CLAY

A Thesis

by

MUHAMMED HUMAYUN KABIR

Submitted to the Department of Civil Engineering,
Bangladesh University of Engineering and Technology, Dacca
in partial fulfilment of the requirements for the degree
of
MASTER OF SCIENCE IN CIVIL ENGINEERING

August, 1978

COMPARISON OF STRESS-PATH METHOD OF SETTLEMENT ANALYSIS WITH OTHER METHODS APPLIED TO A LIGHTLY OVER-CONSOLIDATED CLAY

A Thesis

by

MUHAMMED HUMAYUN KABIR

Approved as to style and content by:

Chairman of the Committee	DR. S.H.K. EUSUFZAI Member, Planning Commission, Govt. of the Peoples' Republic of Bangladesh.
Member	DR. J.R. CHOUDHURY Professor and Head, Dept. of Civil Engineering, BUET.
Member	DR. WAHIDUDDIN AHMAD Vice-Chancellor, BUET.
Member	DR. ALAMGIR HABIB Professor, Dept. of Civil Engineering, BUET.
Member	MR. A.F.M. ABDUR RAUF Associate Professor, Dept. of Civil Engineering, BUET.

August, 1978.

ABSTRACT

A comparison of the stress path method of settlement analysis with the other methods has been presented in this study. For this purpose a typical foundation was choosen at a site near Narayanganj about ten miles from Dacca City.

For conducting the stress path tests a set-up with most of the components fabricated locally was successfully installed and it worked smoothly. The locally made components included a null indicator, a control cylinder, a K_0-Cell, a volume change indicator and a twin manometer.

Stress paths were obtained for elements of soil due to undrained foundation loading and subsequent consolidation.

The magnitudes of immediate and primary consolidation settlement were obtained by stress path, Davis and Poulos, Skempton and Bjerrum and the Conventional Methods. The results were found to agree to a considerable degree with the findings of other investigators. A fairly reasonable conclusion could be made that the stress path method is likely to predict with sufficient accuracy the magnitude of both the immediate and the consolidation settlements whereas the Conventional and Skempton and Bjerrum methods are likely to overestimate those.

The test results further revealed that the three-dimensional consolidation theory yields a faster time-rate of settlement than that obtained from conventional one-dimensional theory

and the actual time-rate in the field is closer to that predicted by the three-dimensional theory.

The effect of sample disturbance on the oedometer consolidation settlement was also investigated and it was found that the magnitude of the settlement may be very much overestimated due to the effect of sample disturbances during sampling and handling.

ACKNOWLEDGEMENTS

The investigation reported herein was carried out under the supervision of Prof. S.H.K. Eusufzai, former Head of Civil Engineering Department, BUET, now Member, Planning Commission, Govt. of the People's Republic of Bangladesh. During the concluding stages of the study, Prof. J.R. Choudhury, Head of the Civil Engineering Department, BUET, acted as the supervisor. The author wishes to express his sincere and profound gratitude to them for their guidence, invaluable suggestions and encouragement throughout the investigation. Their efforts to help procure literature from abroad is also gratefully acknowledged.

Sincere gratitude is expressed to Prof. Alamgir Habib and Prof. A.F.M. Abdur Rauf of the Civil Engineering Department for their suggestions and encouragement at the various stages of the study.

The help rendered by Mr. A.M.M. Safiullah and Mr. Aminul Islam of the Civil Engineering Department, BUET, at the various stages of the work is gratefully acknowledged.

Sincere appreciation is due to M/S Foundation Consultants Ltd., for collecting soil samples from the project site for the study.

The help rendered by Mr. Nurul Islam of the Department of Chemistry and the Technicians of the Machine and Foundry Shops in various stages of the construction of the test set-up is gratefully acknowledged.

The author is indebted to Mr. A. Malek and Mr. Shahiduddin of the Civil Engineering Department for the help rendered in typing the manuscript and preparing the figures.

TABLE OF CONTENTS

Table of Contents (Contd...)

Table of Contents (Contd...)

LIST OF TABLES

LIST OF FIGURES

LIST OF PLATES

NOTATIONS

A	Skempton's pore pressure parameter
B	Skempton's pore pressure parameter
B	Width of foundation
c_u	Undrained cohesion
C_{V1}	Coefficient of consolidation under 1-D condition
C_{V2}	Coefficient of consolidation under 2-D condition
C_{V3}	Coefficient of consolidation under 3-D condition
C_{CF}	Compression index from field curve
C_{CL}	Compression index from laboratory curve
C_{CR}	Compression index from rebound curve
E_u	Undrained elastic modulus
E'	Drained elastic modulus
e_o	Initial void ratio
f	Initial shear ratio
H,h	Thickness of layer/stratum
I	Influence factor
K	Coefficient of permeability
K_o	Coefficient of earth pressure at rest
K'_o	Coefficient of earth pressure at rest under effective stress condition
LL	Liquid limit
m_{V1}	Coefficient of volume compressibility under 1-D condition
m_{V3}	Coefficient of volume compressibility under 3-D condition
μ	Consolidation settlement correction factor
N.M.C	Natural moisture content
$p'_o, \bar{p}_o$	In-situ effective overburden pressure

$\bar{p}_c$	Preconsolidation pressure
PI	Plasticity index
q	Applied foundation pressure
q_u	Ultimate bearing capacity
q_y	Local yield stress
S_R	Correction factor for immediate settlement
S_u	Magnitude of immediate settlement
S_{CF}	Magnitude of final consolidation settlement
S_{TF}	Magnitude of total final settlement
S_{Tt}	Magnitude of total settlement at any time t
S_{oed}	Oedometer consolidation settlement
S_s	Secondary consolidation settlement
t	Time
T_v	Time factor
u	Excess pore-water pressure
u_o	Initial pore-pressure
u_t	Pore-pressure at any time t
U_p	Degree of pore-pressure dissipation
U_s	Degree of settlement
U_1	Degree of settlement under 1-D condition
U_3	Degree of settlement under 3-D condition
$\Delta\bar{\sigma}_1, \Delta\bar{\sigma}_v$	Increase in effective vertical stress
$\Delta\bar{\sigma}_3, \Delta\bar{\sigma}_h$	Increase in effective horizontal stress
$\bar{\sigma}_x, \bar{\sigma}_y, \bar{\sigma}_z$	Principal stresses
ϵ_1	Axial strain
ϵ_v	Volume strain
ν_u	Poisson's ratio under undrained condition
ν'	Poisson's ratio under drained condition

CHAPTER I

INTRODUCTION

1.1 General

The two most important problems foundation engineers are required to deal with are the prediction of the settlement of structures and the analysis of the stability of foundations. The complexity of the problem of settlement computation has been appreciated by engineers right from the beginning. From historic past, innumerable structures have been damaged due to excessive settlement resulting from the consolidation of the underlying soil. The most classic example of such a failure is the case of the "Leaning Tower of Pisa" which suffered a total settlement of almost ten feet and a differential settlement of the order of six feet in a time span of about eight hundred years.

A large number of case histories of settlement failure of structures like buildings, bridges and storage tanks containing hazardous inflammeable fluid have been reported from different parts of the world. In the modern world, Mexico City has become a meuseum of settlement failures as the subsoil of the city consists of very highly compressible underconsolidated volcanic ash.

In Bangladesh, settlement failures are more common than stability failures. Tilting of several oil storage tanks due to excessive settlement of the foundation has been reported from Chittagong area. Structural and functional damage of several buildings due to differential settlement of the foundation beyond tolerable limits have been reported from Dacca City. The river transport Terminal Building of the Inland Water Transport Authority at Narayanganj has suffered considerable damage of the superstructure due to differential settlement of the foundation.

In most places surface deposits in this country are composed of underconsolidated to slightly overconsolidated fine-grained materials. Reliable settlement prediction is therefore very important for satisfactory performance of structures built on them. At present the country is moving forward with large development projects involving construction of heavy industrial structures, power stations, transmission towers, oil storage tanks, jetties, harbour and port structures. Construction of high rise buildings and long span bridges are also being taken up. A detailed knowledge of the process of consolidation and settlement is, therefore, of great importance for a foundation engineer in this country.

1.2 Methods of Settlement Analysis

Terzaghi initiated the modern era of laboratory methods of settlement analysis when he built the first crude oedometer to demonstrate the process of consolidation of clays and presented the famous one-dimensional consolidation theory over fifty years ago. This method known as Conventional Method has undergone very little change since then and is still the main basis of settlement analysis in most design offices. Field conditions in many cases differ from the simplifying assumptions that are made in the Conventional Method, specially from the condition of one-dimensional strain.

An important improvement over the Conventional Method was made by Skempton and Bjerrum (1957) when they recognized that an element of soil undergoes lateral deformation as a result of applied foundation loading and the subsequent consolidation is a function of the excess pore-water pressure developed in the clay. However in this method, the relationship between axial compressibility and effective stress was determined from the standard oedometer test, where the influence of lateral stresses on the axial compressibility are not taken into account.

Davis and Polous (1963, 1968) suggested a method of settlement analysis considering the actual three dimensional strain condition to which an element of soil is subjected in the field rather than the one-dimensional strain condition assumed by Terzaghi. In this analysis the soil being considered as an elastic continuum, the elastic displacement and stress distribution theory is extensively used to predict settlement. The use of this theory for a non-elastic material as soil is justified, to the accuracy required in practical problems, provided the elastic soil parameters are determined over a range of stress representative of the change in state of stress occuring in the actual problem, and provided the foundation load at which local yield first occurs is not seriously exceeded.

A better laboratory procedure to predict the deformation of a soil under a given foundation loading, would be to test the soil under the same stress changes to which the soil will be subjected in the field. Moreover, soil behaviour being generally non-linear, deformation properties will vary with stress level. It is therefore desirable that a soil specimen after sampling, be first brought back to the stress system initially prevailing in the ground, before subjecting it to the stress changes it is likely to undergo on loading. This concept, termed as stress path testing, was pointed out by Lambe (1964, 1967) and the method of settlement analysis based on this concept is known as the 'Stress-path Method'.

1.3 Statement of the Problem

A large number of publications present disagreement between observed settlement and that predicted by the Conventional Method for structures founded on clays (Art. 2.6). The stress-path method has been established theoretically as more accurate compared to the other methods of settlement analysis as the field condition is more closely duplicated in the laboratory in this method of settlement analysis. Although some amount of work has been reported stating the stress-path method as a more reliable method of predicting settlement on heavily over consolidated clays virtually no data is available for normally consolidated to moderately overconsolidated clays. No publication concerning reliable estimate of settlement of structures founded on soil with small clay content but behaving like clay layers, similar to those in many places in Bangladesh, is available. So it was felt necessary to study the settlement characteristics of a typical structure on such a soil. For this a site was selected at Narayanganj about ten miles from Dacca City where an elevated water tower is being constructed.

The stress-path method of calculation of settlement requires an elaborate laboratory test set-up. These facilities being non-available in the country, the first task was to fabricate and calibrate the components necessary for the test set-up, using indigenous materials wherever applicable.

1.4 Objective of the Research

After successful installation of a test setup with components made locally and on the assumption that the settlement predicted by the stress-path method may be closer to the actual settlement of the structure the following objectives were fixed for this research work:

(i) Determination of field stress-path experienced by soil elements due to foundation loading.

(ii) Comparison of immediate settlement obtained from the stress-path method with that obtained from the other available methods of settlement analysis.

(iii) Comparison of the primary consolidation settlement obtained from the stress-path method with those obtained from the other methods of settlement analysis.

(iv) Comparison of the rate of settlement obtained by the three-dimensional consolidation theory with that obtained by one-dimensional consolidation theory.

(v) Determination of the error in the estimation of consolidation settlement by the conventional method due to sample disturbance.

CHAPTER II

REVIEW OF LITERATURE

2.1 The Conventional Method

The method of settlement analysis advanced by Terzaghi in 1925, popularly known as the Conventional Method assumes one-dimensional strain (K_o) and drainage condition. The settlement is calculated on this assumption from the results of oedometer tests and is termed as S_{oed}.

Under true one-dimensional condition the immediate or undrained settlement $S_U = 0$ and therefore,

$$\left.\begin{aligned} S_{TF} &= S_{oed} \\ S_{Tt} &= U_1 S_{oed} \end{aligned}\right\} \qquad 2.1$$

Where,

S_{TF} = total final settlement,

S_{Tt} = total settlement at any time t after application of foundation load,

U_1 = degree of consolidation given by one-dimensional consolidation theory

and $$S_{oed} = \int_0^z m_{v1} \, \Delta\sigma_1' \, dz \qquad 2.2$$

Where,

m_{v1} = coefficient of compressibility in the oedometer test.

$\Delta\sigma_1'$ = increase in vertical effective stress,

z = depth below the footing level.

Where conditions are not even approximately one-dimensional, it is still often (Skempton and Bjerrum, 1957, Davis and Poulos, 1968 and Simons, 1971) assumed that,

$$\left.\begin{aligned} S_{TF} &= S_U + S_{oed} \\ S_{Tt} &= S_U + U_1 S_{oed} \end{aligned}\right\} \qquad 2.3$$

Where, S_U is the immediate or undrained settlement which occurs without significant dissipation of excess pore water pressure due to sudden application of load.

Linear elastic displacement theory is widely used for predicting initial settlement by the conventional method. In this theory the soil is characterized as an uniform layer having an elastic modulus determined either from conventional undrained triaxial test or from unconfined compression test (Davis and Poulos, 1968).

The elastic displacement theory gives the initial settlement in the form:

$$S_U = \frac{q\ B\ I}{E_U} \qquad 2.4$$

Where,

q = applied foundation pressure,

B = some chosen dimension of the foundation,

I = influence factor given by elastic theory which depends on the shape of the loaded area, the Poisson's ratio ν of the soil and the depth of the clay bed, and E_U = undrained elastic modulus of the foundation clay.

Many solutions are available for the influence factor I, but a very convenient (Simons, 1974) form of this solution has been given by Janbu et.al (1956) which is expressed as follows,

$$I = \mu_0 \mu_1 \qquad 2.5$$

For Poisson's ratio equal to 0.5 which is true for all saturated clays the factors μ_0 and μ_1, given in Fig. 2.1, are functions of the geometry and depth of the footing and the thickness of the layer. By using the principle of superposition, as demonstrated by Simons and Menzies (1975), it is possible to carry out calculations for multilayered soil system.

There are still some controversies (Skempton and Bjerrum, 1957 and Davis and Poulos, 1968) on the point whether immediate settlement should be included in the conventional method of settlement analysis.

D'Appolonia et al (1971) state that evaluation of the initial settlement of structures on clay is important for the following reasons:

(i) Initial settlement may constitute a large portion of the total final settlement, depending on the nature of the soil, the loading geometry and the thickness of the compressible layer.

(ii) Analysis of initial settlement is an integral part of the analysis of overall time-settlement behavior of foundation.

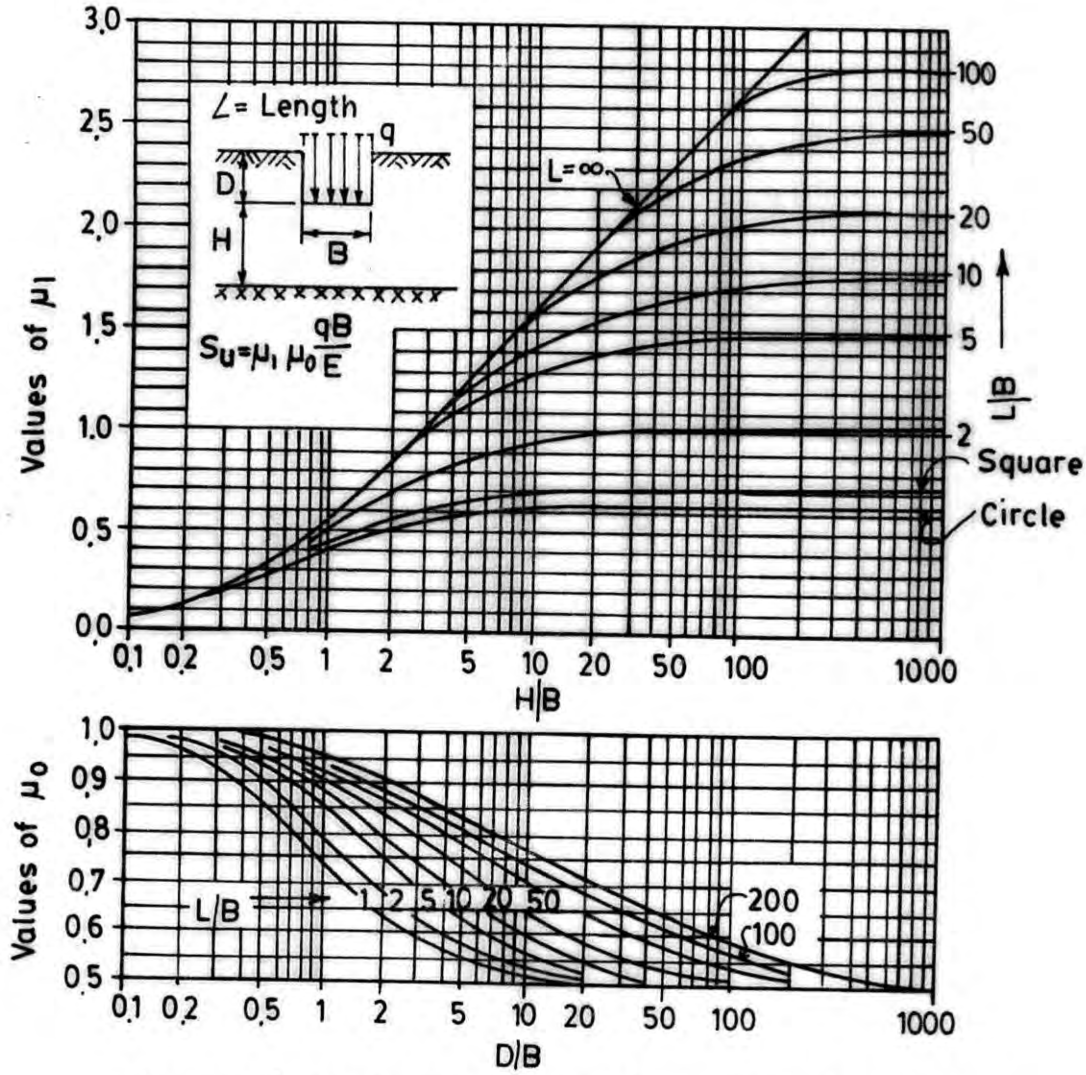

Fig. 2.1 Diagrams for the Factors μ_0 and μ_1 Used in the Calculation of Immediate Average Settlement of Uniformly Loaded Flexible Areas on Homogeneos Isotropic Saturated clays (after Janbu et. al. 1956)

(iii) Initial settlement is closely related to the undrained stability of a foundation, Excessive initial settlement may be a warning to impending failure.

Depending on the type of soil Flaate (1963) presented the following to demonstrate the relative importance of different types of settlement, which is shown in Table 2.1. It is evident that immediate settlement is important for all types of soil condition and it is very important in case of overconsolidated clays.

Table 2.1. Relative Importance of Different Types of Settlement (after Flaate, 1963)

Type of soil	Immediate settlement S_U	Primary consolidation settlement S_{CF}	Secondary consolidation settlement S_S
O.C. clays	V. Imp.	?	?
N.C. clays	Imp.	V. Imp.	Imp.
Organic clays	Imp.	Imp.	Imp.
Granular soils	Imp.	-	?

To establish the relative importance of immediate settlement, Davis and Poulos (1968) plotted its ratio to the total final settlement as a function of drained Poisson's ratio ν', for various thickness of supporting soil (Fig. 2.2). From the curves it is evident that the immediate settlement contributes a much higher proportion to the total final settlement when

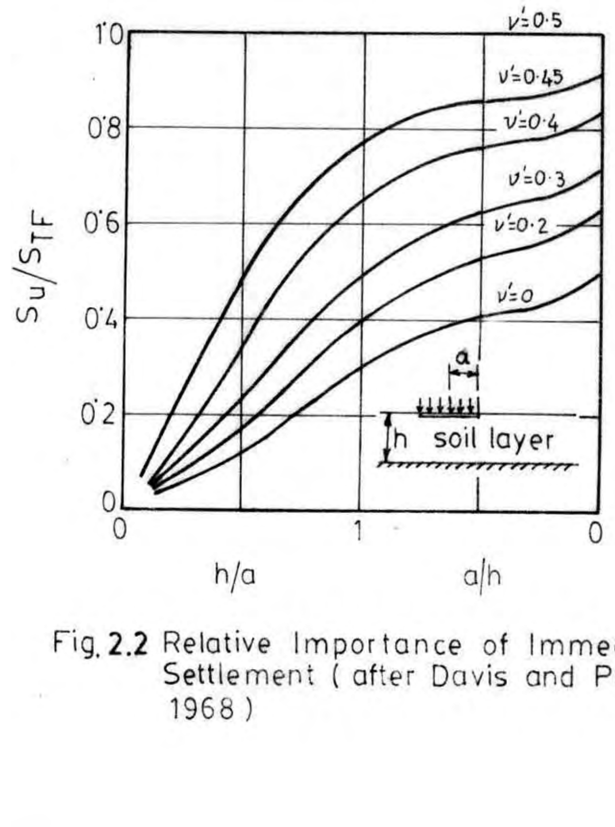

Fig. 2.2 Relative Importance of Immediate Settlement (after Davis and Polous 1968)

Poisson's ratio is high asis the case for O.C.clays (Lambe and Whitman 1969), and for shallow layers, the immediate settlement is relatively small. McNamee and Gibson (1960) also showed that the ratio for a semi-infinite supporting soil was,

$$\frac{S_U}{S_{TF}} = \frac{1}{2(1 - \nu')} \qquad 2.6$$

2.2 Skempton and Bjerrum Method

Skempton and Bjerrum in 1957 first pointed out that as the consolidation of clay results from dissipation of excess-porewater pressure the consolidation settlement is due to increase in effective stress rather than due to increase in net vertical pressure. The pore-pressure developed in a clay is dependent not only on the applied stresses but also on the type of clay. Thus, if there are two identical footings, carrying identical loads, and these footings rest on two clays with identical compressibilities, yet if the pore-pressure set up in the two cases are different, the consolidation settlement will also be different. And this is true inspite of the fact that no difference would be seen in the results of the oedometer test. They also pointed out that although the effective vertical stress increases as soon as the foundation load is applied, there is a decrease in effective horizontal stress. So during the period of pore-pressure dissipation a soil element experiences a recompression followed by a virgin compression in the horizontal direction. However Skempton and Bjerrum failed to take into account the consequences of these effects and opined that the lateral strains during consolidation are so small that they may be neglected without involving an error of more than roughly 20% in the value of vertical consolidation settlement. Taking these into consideration they suggested the following equation analogous to Eq. 2.2 for the consolidation settlement

$$S_{CF} = \int_0^z m_{v1} \, u \, dz \qquad 2.7$$

where u is the increase in pore-water pressure due to applied loading which may be represented by the expression

$$u = B\left[\Delta\sigma_3 + A\left(\Delta\sigma_1 - \Delta\sigma_3\right)\right] \qquad 2.8$$

Where A and B are Skempton's pore-pressure parameters, $\Delta\sigma_1$ and $\Delta\sigma_3$ are net increase in effective vertical and horizontal stresses respectively.

Putting the value of u from Eq. 2.8 and assuming B=1 (for saturated clays) Eq. 2.7 takes the form

$$S_{CF} = \int_0^z m_{v1} \Delta\sigma_1 \left[A + \frac{\Delta\sigma_3}{\Delta\sigma_1} (1 - A)\right] dz \qquad 2.9$$

Equation 2.9 can be written in the form

$$S_{CF} = \mu \, S_{oed} \qquad 2.10$$

where S_{oed} is given by equation 2.2. From Eq. 2.9 and 2.10 it follows that

$$\mu = \frac{\int_0^z m_{v1} \Delta\sigma_1 \left[A + \frac{\Delta\sigma_3}{\Delta\sigma_1} (1 - A) \right] dz}{\int_0^z m_{v1} \Delta\sigma_1 \, dz} \qquad 2.11$$

by assuming constant values of m_{v1} and A with depth, it is possible to express μ by the simple equation

$$\mu = A + \alpha (1 - A) \qquad 2.12$$

Where $$\alpha = \frac{\int_0^z \Delta\sigma_3 \, dz}{\int_0^z \Delta\sigma_1 \, dz} \qquad 2.13$$

The coefficient α depends on the shape of the footing and depth of the compressible layer below foundation level.

Scott (1963) showed that the above expressions are valid only for radially symmetrical (circular) loading. For long strip foundation the expression for μ should be changed to

$$\mu = N + \alpha (1 - N) \qquad 2.14$$

Where, $$N = \frac{\sqrt{3}}{2} \left(A - \frac{1}{3}\right) + 1/2 \qquad 2.15$$

This modification, which is due to the influence of intermediate principal stress increase of long strip loading, was not taken into consideration in the original work of Skempton and Bjerrum.

The semi-empirical factor μ as presented by Scott (1963) after correcting that given by Skempton and Bjerrum (1957) is presented in Fig. 2.3.

Skempton and Bjerrum suggested the following formula for computation of total settlement.

$$\left.\begin{aligned} S_{TF} &= S_U + \mu\, S_{oed} \\ S_{Tt} &= S_U + U_1 \mu\, S_{oed} \end{aligned}\right\} \qquad 2.16$$

Where S_U is the immediate settlement calculated in the conventional manner, and U_1 is the degree of consolidation settlement obtained by Terzaghi's one dimensional consolidation theory.

2.3 Elastic Method by Davis and Poulos

Davis and Poulos (1963, 1968) have emphasized that a three-dimensional treatment is desirable in the analysis of settlement of foundations on deep beds of compressible soil. They have proposed a three-dimensional method of settlement analysis which relies largely on the elastic displacement theory for a homogeneous isotropic elastic body. Despite the questionable use of elastic theory to soils which are in general non-homogeneous, anisotropic and inelastic, the method appears to be extremely promising for engineering application. The logic behind adoption of a three-dimensional approach for settlement calculation is to take care the effect of lateral stresses on the load - settlement characteristics of a foundation. To show

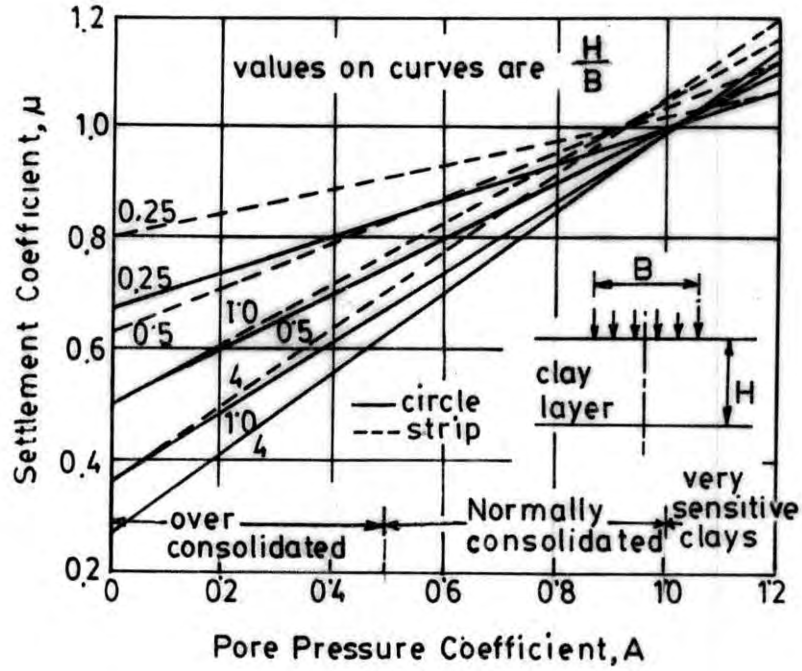

Fig.2.3 Correction Factor for Pore-Pressure Set-Up Under a Foundation (after Skempton and Bjerrum, 1957 and Scott, 1963)

the relative importance of a three dimensional settlement analysis they have plotted the ratio of S_{oed}/S_{TF}(3-Dimn.) for all depths of an elastic layer subject to uniform loading on the surface over a circular area which is shown in Fig. 2.4. From Fig. 2.4 it can be seen that the errors in the one dimensional approach increases rapidly as ν' increases beyond 0.25. For high values of ν', (O.C. clays) even quite shallow layers deserve three dimensional treatment.

Under the three-dimensional conditions in which a soil element is subject to strains in the three co-ordinate direction, the total settlement S_{TF} of a foundation on saturated clay soil is given by

$$\left.\begin{aligned} S_{TF} &= S_U + S_{CF} \\ S_{Tt} &= S_U + U_3\, S_{CF} \end{aligned}\right\} \qquad 2.17$$

Where U_3 is the degree of consolidation settlement appropriate to three-dimensional conditions.

Davis and Poulos (1963, 1968) suggested that in three-dimensional problems involving several strata of different types, the total final settlement may be obtained from the elastic stress distribution theory by summation of the strains in the individual strata.

$$S_{TF} = \sum \frac{1}{E'}\left[\sigma_z - \nu'(\sigma_x + \sigma_y)\right]\delta h \qquad 2.18$$

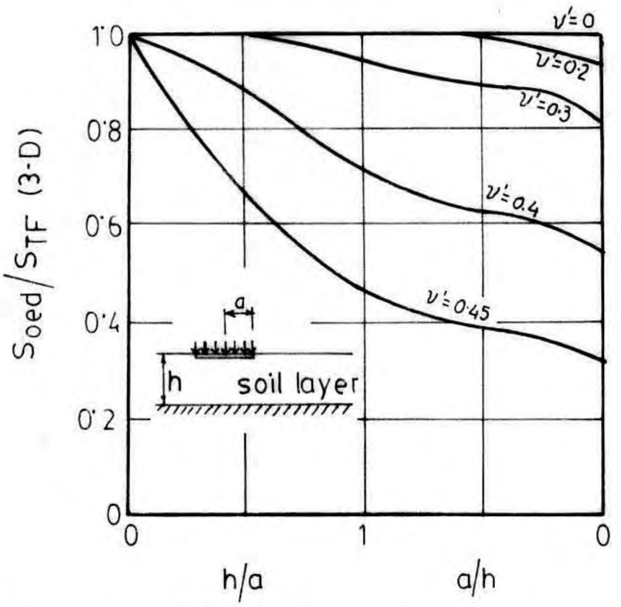

Fig.2.4 Errors in Conventional One Dimensional Approach for Total Final Settlement of an Elastic Consolidating Soil (after Davis and Poulos 1968)

Where E' and ν' are the elastic modulus and Poissons ratio of the soil skeleton appropriate to the changes of stress or stress level in each layer, σ_x, σ_y and σ_z are the stress increments due to the foundation loading, estimated from the three dimensional elastic stress distribution theory and ∂h is the thickness of each stratum or layer. If, however the clay stratum is reasonably homogeneous, an appropriate average values of E' and ν' can be assigned to the clay for the whole depth of the stratum, S_{TF} may be calculated from elastic displacement theory as

$$S_{TF} = \frac{qBI}{E'} \qquad 2.19$$

where I is the influence factor given by the elastic displacement theory for $\nu = \nu'$.

For calculating immediate settlement Davis and Poulos suggested appropriate version of equation 2.18 and 2.19.

A numerical integration approach analogous to equation 2.18 can be used when dealing with several strata of different types

$$S_U = \sum \frac{1}{E_U}\left[\sigma_z - 0{\cdot}5\left(\sigma_x + \sigma_y\right)\right] \delta h \qquad 2.20$$

when dealing with a homogenious isotropic semi-infinite mass Eq. 2.4 can be used inplace of equation 2.19. The only difference being in the value of E_U which should be determined from

CK_0U test following the same stress-path which is expected to be experienced by a soil element in the field.

The prerequisite for the use of the method is a knowledge of the stresses and surface displacements of an elastic continuum. Poulos (1967a, 1967b) suggested a method which provide sufficient data to allow the calculation of the stresses within a layer and the surface displacement due to normal surface loading over an area of any shape. The method is called sector method as loaded sectors are used in the calculation.

Poulos also took into account the effect of depth to the base of the footing on the influence factors by using the type of correction proposed by Fox (1948).

The elastic theory has two major limitations as pointed out by D' Appolonia et. al. (1971). First, solutions for materials exhibiting some of the important characteristics of soils e.g. nonlinearity, nonhomogeneity and anisotropy are not readily available. The second important limitation of elastic theory is that the stress redistribution and the strains occuring after local yielding cannot be evaluated. On the point of stress redistribution Hoeg et. al. (1968) writes that the vertical stresses remain relatively unchanged even during the development of plastic flow in the soil mass. Horizontal stresses, however, change markedly as the result of plastic yielding under increased load. Thus elastic theory does not provide satisfactory estimates for horizontal stresses, which has got marked influence on the stress-deformation characteristics of clays as pointed out by Simons and Som (1969). In the absence of any formal elastic-plastic solution of a footing on clay Davis and Poulos (1968) observed that, it is important to examine the magnitude of footing pressure g_y at which the first local yield occurs.

In an assesment of the footing pressure q_y, for a strip footing which depends on the initial state of stress, Davis established that

$$q_y = \pi(1 - f)\ C_u \text{ for } 0 \leqslant f \leqslant 1$$
$$= \pi(1 - f^2)\ C_u \text{ for } -1 \leqslant f \leqslant 0 \qquad 2.21$$

where f is a factor $(-1 \leqslant f \leqslant 1)$ which defines the initial stress-state as

$$\sigma_{1i} - \sigma_{3i} = 2 f C_u \qquad 2.22$$

Eq. 2.22 can easily be written in the form

$$2f = \frac{(1 - K'_o)}{C_u/\bar{P}} \qquad 2.23$$

Where K'_o is the coefficient of earth pressure at rest with respect to effective stresses and $C_u/\bar{P}$ is the ratio of undrained shear strength to the effective overburden pressure on the element under consideration.

Equations 2.21 are plotted in Fig. 2.5a to give the theoretical minimum factor of safety against ultimate bearing capacity failure required to ensure that local yield does not occur. From this figure it can be seen that with the commonly used minimum factor of safety of 3, it is necessary to have $-0.33 < f < +0.45$ if local yield is not to influence the results of settlement computation by the elastic theory.

Equation 2.23 is plotted in Fig. 2.5b.

To overcome the limitations of elastic theory in calculation of initial settlement D' Appolonia et.al. (1971) presented finite element solutions which have been extended to include the effects of local yield, for loadings beyond the so-called elastic limit, by considering non-linear and elastic-plastic behavior of soils.

The proposed method for estimating initial settlement utilizes conventional elastic theory together with a series of finite element solutions. These solutions are plotted in a dimensionless form that indicates the deviation of the actual load-initial settlement curve from the settlement predicted by elastic theory. Using these curves, the initial settlement at any load upto the failure load can be estimated. To apply the method, three parameters are required, the elastic undrained Young's modulus E_U, the ultimate bearing stress q_u and the initial shear stress ratio, f. The dimensionless initial settlement curves, as obtained by D' Appolonia et.al. (1971) are presented in Fig. 2.6.

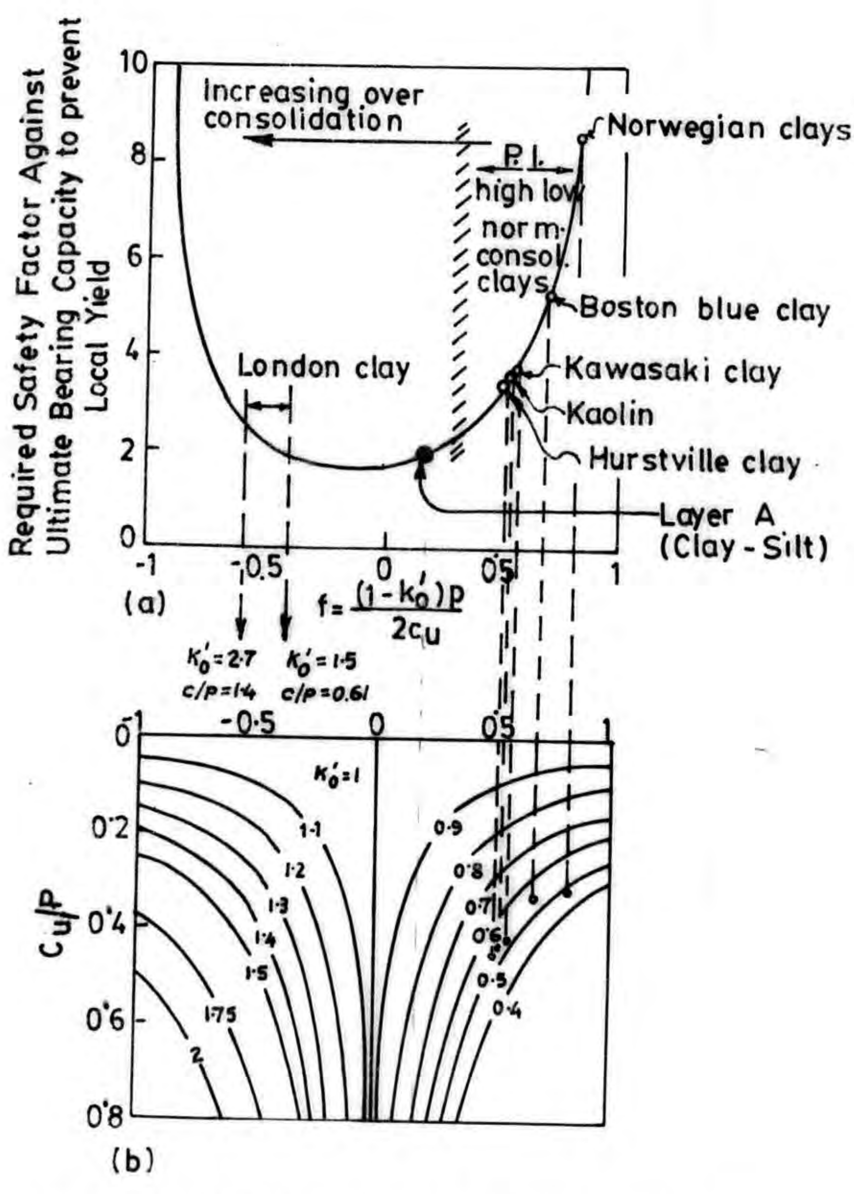

Fig.2.5 Factor of Safety to Prevent Local Yield
(after Davis and Poulos 1968)

They show the settlement ratio S_R, plotted as a function of an applied stress ratio, q/q_u, for three values of H/B where H is the layer depth and B is the foundation width. The settlement ratio, S_R, expresses the ratio of the elastic settlement computed by the elastic theory without considering local yield to the actual settlement that occurs. Curves are presented for a range of values of the initial shear stress ratio f. They also found that the ratio, H/B does not have a large influence and that the results of H/B = 1.5 will apply for all values of $H/B > 1.5$.

This method of estimating initial settlement may be expressed as

$$S_U = S_R \cdot \frac{q\ B\ I}{E_u} \qquad 2.24$$

From the range of literature reviewed, it appears that no similar solution is available for the calculation of consolidation settlement for stress range beyond local yield.

As regards the experimental measurement of the elastic effective stress parameters E' and ν', Davis and Poulos (1968) write that as these are stress-dependent, the values must be established in a test simulating the field stress-state. As the state of stress is a function of depth, it is necessary to determine a suitable representative depth at which the values of the parameters could be determined to obtain a suitable average. For an one-dimensional analysis . Davis and Poulos

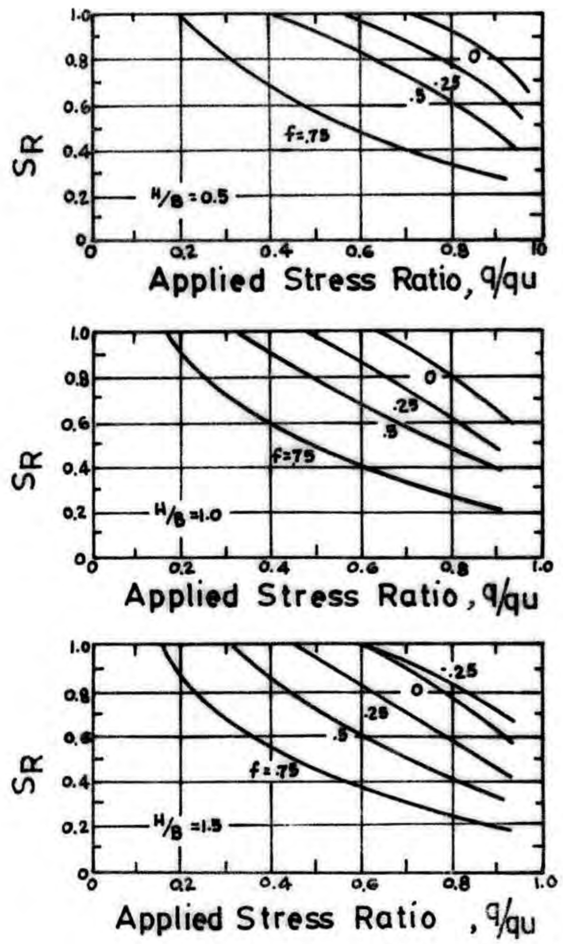

Fig.2.6 Relationship Between Settlement Ratio and Applied Stress Ratio for Strip Foundation on Homogeneous Isotropic Elastic Layer (after D Appolonia et. al. 1971)

concluded that the representative depth should be between 1/4 and 1/3 of the full stratum depth, depending on whether the distribution of vertical stress with depth is triangular or uniform. Davis and Poulos also assumed that this rule is applicable to three-dimensional analysis, although an approximate determination for a footing on a deep stratum showed that the representative depth should not exceed 0.9 time the footing width.

2.4 Lambe's Stress-Path Method

The use of stress-paths in the settlement analysis was evolved by Lambe (1964 and 1967). One of the most important advantages of this method is that the design engineer can develop a 'feel' of the problem instead of blindly applying formulae.

A stress path is essentially a line drawn through points on a plot of stress changes and shows the relationship between components of stresses of various stages in moving from one stress point to another. Stress-paths can be plotted in a variety of ways, but the following methods are common and suitable for studying deformation problems:

(i) A plot of normal stress (effective or total) against shear stress as used by Lambe (1964, 1967).

(ii) A plot of vertical (effective or total) stress to horizontal (effective or total) stress as used by Simons and Som (1970).

Fig. 2.7 shows the effective and total stress-paths of an element of over-consolidated London clay in the field during undrained loading by a circular loaded area and subsequent consolidation. The insitu effective stresses, p' and K_o' p', before the application of the surface loading, is represented by point A and the corresponding total stresses by A_1 in Fig. 2.7. Owing to the applied foundation pressure, q, the stresses on the element will increase by $\Delta\sigma_v$ and $\Delta\sigma_{h1}$. If the foundation pressure is applied sufficiently quickly so that no drainage occurs during the load application, the element will deform without any volume change and any vertical compression will be associated with lateral expension. The increase in stresses $\Delta\sigma_v$ and $\Delta\sigma_{h1}$ will set up an excess pore-water pressure u in the element of clay. Since for most clays, and certainly for London clay the value of parameter A is positive and less than unity for the range of stresses normally encountered in practice, u is greater than $\Delta\sigma_{h1}$. Consequently, the effective vertical stress increases and the effective horizontal stress decreases during load application, and the stress point moves from A to B. The vertical strain during undrained loading is, therefore, a function of the stress path AB. The element now begins to consolidate. During the early stages, the increase in horizontal stress is a recompression until the original value K_o' p' is restored, beyond which the further increase in effective stress is net, while the element is subjected to a net increase in effective vertical stress during the entire process of consolidation. During load application under undrained conditions,

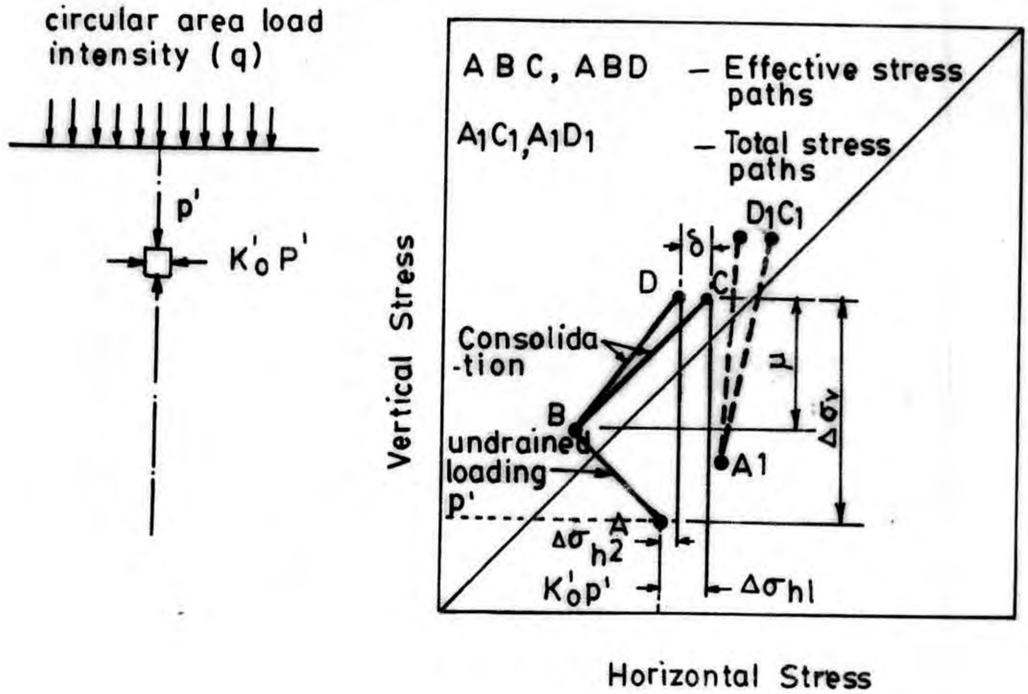

Fig.2.7 Stress Path of an Element of London Clay in the Field During Loading and Consolidation (after Simons & Som 1970)

a saturated clay behaves as an incompressible medium with Poisson's ratio $\nu = 0.5$. As the excess pore-water pressure dissipates the Poisson's ratio decreases and finally falls to its fully drained value at the end of consolidation. This change in Poisson's ratio is unlikely to effect significantly the vertical stress but the horizontal stress will decrease by an amount ∂. Therefore during consolidation, the element will follow the effective stress path BD instead of BC. The total stress-path is represented by A_1D_1.

To illustrate the approach used by Lambe (1964, 1967), the effective stress-path for an element of soil undergoing undrained loading followed by consolidation is shown in Fig. 2.8.

Point I represents the initial state of stress (on K_o-line) of the element prevailing in-situ. Point B represents the state of stress after the application of loading under undrained condition. So IB is the stress-path due to undrained or shear loading. As the element consolidates with pore pressure dissipation, the stress path moves horizontally from B as there is no change in shear stress. Finally F represents the state of stress after full dissipation of pore-pressure. The stress-path during consolidation is denoted by BF.

The method of settlement analysis proposed by Lambe (1964) suggests two approaches to calculate immediate settlement (from stress-path IB Fig. 2.8) as well as consolidation settlement (from stress-path BF).

The first approach which is rather approximate in nature involves the use of stress-strain contours, consists of the following steps:

(i) Running a series of consolidated undrained triaxial tests with pore-pressure measurements and from the results, plotting a pattern of stress strain contours of the type shown in Fig. 2.9.

(ii) Superimposing on the stress-strain contours the predicted effective stress path for field loading.

(iii) Estimating the axial strain due to undrained loading directly from the figures on the strain contours.

(iv) Estimating the volumetric strain from consolidation test results using the expression $\epsilon_v = \frac{\Delta e}{1 + eo}$ for the relevent stress changes obtained from the Fig. 2.9 following the K_o - line.

(v) Estimating the axial strain by multiplying the volume strain ϵ_v by λ which is the ratio of axial to volumetric strain.

(vi) Multiplying the vertical strain, which is obtained by adding the two components of strain obtained in steps (iii) and (v) by the thickness of the layer under consideration to get the total settlement.

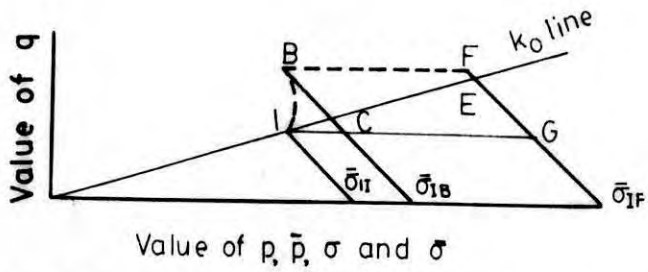

Fig.28 Stress Path of an Element of Soil in the Field, During Loading and Consolidation (after Lambe, 1964)

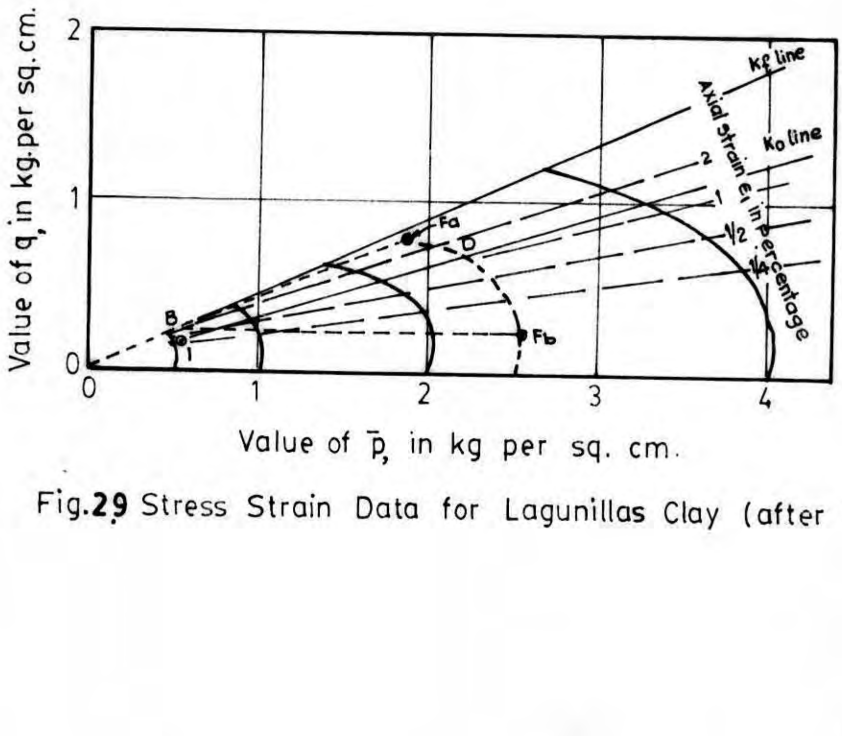

Fig.29 Stress Strain Data for Lagunillas Clay (after Lambe, 1964)

The expression for λ may be presented in the form of Eq.2.25 which is developed by Lambe (1964) for drained compression for any given radial stress-path, Fig. 2.9.

$$\lambda = \frac{\epsilon_1}{\epsilon_v} = \frac{\frac{\Delta L}{L_o}}{\frac{\Delta V}{V_o}} = \frac{1 + K'_o - 2KK'_o}{(1-K'_o)(1+2K)} \qquad 2.25$$

where $K = \frac{\bar{\sigma}_3}{\bar{\sigma}_1}$ at final point of stress-path.

For a truly isotropic soil under a hydrostatic stress system, ϵ_1 should be equal to $\epsilon_v/3$, for an effective stress-path along the horizontal axis that is for a isotropic stress system. Lambe (1964) observed that for typical undistrubed sedimentary soils, which are not, however, isotropic, the value of ϵ_1 may be nearer to $\epsilon_v/2$ rather than $\epsilon_v/3$. He suggested that the most reasonable way of calculating λ is by direct measurement in the laboratory by duplicating the field effective stress-path.

The second and the most precise method of estimating settlement suggested by Lambe is by using results of laboratory test duplicating the field effective stress-path. The method may be described by the following steps:

(i) Estimating the effective stress-path for the field loading,

(ii) Running a laboratory compression test duplicating the field effective stress-path and

(iii) Computing the settlement by multiplying the thickness of the layer under consideration by the axial strain from the laboratory test.

Simons (1971) presented an indirect approach of calculating immediate and consolidation settlement. Duplicating the field stress-path in laboratory testing as suggested by Lambe, he suggested that the immediate and consolidation settlements can be calculated by the following equations:

$$S_u = \sum \frac{\Delta\sigma_1 - \Delta\sigma_3}{E(z)} dz \qquad 2.26$$

$$S_{CF} = \int_0^z \lambda \, m_{v_3} \, u \, dz . \qquad 2.27$$

and finally

$$S_{TF} = S_u + S_{CF} \qquad 2.28$$

2.5 Rate of Primary Consolidation Settlement

In the conventional and Skempton and Bjerrum methods of settlement analyses the one-dimensional consolidation theory evolved by Terzaghi is used to compute the time rate of settlement. Lambe (1964) did not specify any method for calculating the rate of settlement in his stress-path method. However from the closeness of his method to the elastic method by Davis and Poulos (1963, 1968), it could be concluded that the three dimensional approach suggested by Davis and Poulos (1963,1968, 1972) may logically be used to predict time rate of settlement in the stress-path method.

By the three-dimensional consolidation theory, Biot (1941), the basic differential equation of consolidation for a two-phase material having constant permeability may be written as (Lee, 1968)

$$\frac{K}{\gamma_w} \nabla^2 u + \frac{\partial \epsilon_v}{\partial t} = 0 \qquad 2.29$$

where $\nabla^2 = \frac{\partial^2}{\partial x^2} + \frac{\partial^2}{\partial y^2} + \frac{\partial^2}{\partial z^2}$

K = coefficient of permeability

t = time

ϵ_v = volume strain of soil due to changes in effective stress

u = excess pore pressure

For three dimensional strain condition

$$\epsilon_v = \frac{(1-2\nu')}{E'} \theta' = \frac{(1-2\nu')}{E'} (\theta - 3u) \qquad 2.30$$

where $\theta = \sigma_x + \sigma_y + \sigma_z$, the changes in total stress causing consolidation. Substituting the value of ϵ_v from Eq. 2.30 to Eq. 2.29.

$$\frac{\partial u}{\partial t} = c_{v3} \nabla^2 u + \frac{1}{3} \frac{\partial \theta}{\partial t} \qquad 2.31$$

where $\quad C_{V3} = \dfrac{KE'}{3\gamma_w(1-\nu')}$ 2.32

which is the coefficient of consolidation for three-dimensional strain conditions.

For two and one-dimensional strain conditions, equation of the same form as Eq. 2.31 can be obtained.

For two-dimensional (Plane) strain condition, assuming $\epsilon_y = 0$ Eq. 2.31 takes the form

$$\frac{\partial u}{\partial t} = C_{v2}\left(\frac{\partial^2 u}{\partial x^2} + \frac{\partial^2 u}{\partial z^2}\right) + \frac{1}{2}\frac{\partial(\sigma_x+\sigma_z)}{\partial t} \qquad 2.33$$

where $C_{V2} = \dfrac{KE'}{2\gamma_w(1-2\nu')(1+\nu')}$ 2.34

For one-dimensional (K_o) strain condition assuming $\epsilon_x = \epsilon_y = 0$ Eq. 2.31 takes the form

$$\frac{\partial u}{\partial t} = C_{V1}\frac{\partial^2 u}{\partial z^2} + \frac{\partial \sigma_z}{\partial t} \qquad 2.35$$

where

$$C_{V1} = \frac{KE'(1-\nu')}{\gamma_w(1+\nu')(1-2\nu')} \qquad 2.36$$

From Eqs. 2.32, 2.34 and 2.36 the three coefficient of consolidation may be related as follows:

$$C_{V1} = 2(1-\nu')\,C_{v2} = \frac{3(1-\nu')}{(1+\nu')}\,C_{v3} \qquad 2.37$$

It can be seen from Eq. 2.37 that as ν' tends to 0.5 these three values become identical but for $\nu' = 0$, $C_{V1} = 2C_{V2} = 3C_{V3}$.

Davis and Poulos (1968, 1972) write that the difference between these values of coefficient of consolidation may be important. Which they have showed by the example that, the theoretical curve relating degree of consolidation to time factor for a triaxial consolidation test with end drainage only is identical with the ordinary curve in one-dimensional oedometer test. However, the value of coefficient of consolidation in the definition of time factor for the triaxial test is C_{v3} whereas that for oedometer test is C_{v1}.

Davis and Poulos suggested that $\frac{\partial \theta}{\partial t}$ in Eq. 2.31 or its equivalent in Eqs. 2.33 and 2.35 is generally not zero, even when the foundation load remains constant, since stress redistribution will generally take place within the soil mass during consolidation.

Davis and Poulos (1968) further suggested that as ν' tends to 0.5, $\frac{\partial \theta}{\partial t}$ tends to zero and further more even when $\nu' < 0.5$ the overall change in the distribution of θ, from the start to finish of consolidation, is not very great, so $\frac{\partial \theta}{\partial t}$ may be ignored. Then Eq. 2.31 simplifies to:

$$\frac{\partial u}{\partial t} = C_{v3} \times \nabla^2 u \qquad 2.38$$

Equation 2.38 can be solved as an ordinary diffusion equation using numerical finite difference methods (Gibson and Lumb, 1953).

For such solutions the average degree of pore-pressure dissipation U_p on the centre line beneath of foundation may be calculated for any time t as,

$$U_p = 1 - \frac{\int u_t \; dz}{\int u_o \; dz} \qquad 2.39$$

where u_t = pore-pressure at any time t

u_o = initial excess pore-pressure

Davis and Poulos (1968) presented a series of curves for U_p for different ratios of the depth of layer h to radius a of a circular footing obtained by numerical finite difference method as used by Gibson and Lumb (1953). The curves which are presented in Fig. 2.10 is for the hydraulic boundary condition of a permeable base to the layer and a permeable footing and upper surface. The curves are correct for $\nu' = 0.5$ and approximately correct for $\nu' < 0.5$, the possible error increases as the ratio h/a decreases. For small values of h/a, the error can be largely removed by substituting C_{v1} for C_{v3} in the definition of the time factor. Since the time factor T_v is defined in terms of the depth of layer, Fig. 2.10 can be regarded as giving the effect of changing the layer depth on the rate of consolidation beneath a footing of constant radius. It is evident from Fig. 2.10 that the three dimensional effects are very strong, the ability of the pore-pressure to dissipate laterally as well as vertically producing a very considerable increase in the rate of consolidation even for quite shallow layers.

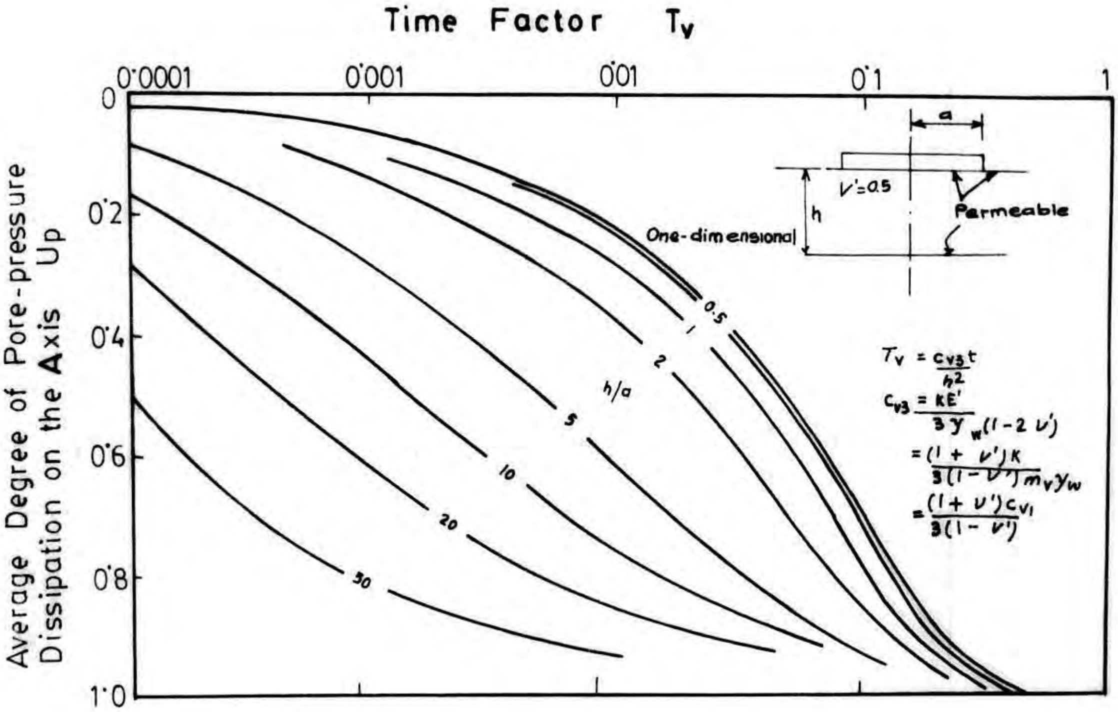

Fig.2.10 Three Dimensional Effects on Rate of Consolidation (after Davis and Poulos, 1968)

Davis and Poulos (1972) presented a series of curves similar to those in Fig. 2.10. The curves were obtained by numerical finite difference solution of the simple diffusion equation. The solutions are presented for two types of footing geometry viz. circular and strip. Four types of hydraulic boundary condition were considered for each type of footing. The curves are plotted for a wide range of depth of layer to width of the footing ratio, taking $\nu' = 0.5$. Davis and Poulos also presented an approximate basis to take care of the effect of Poisson's ratio different from $\nu' = 0.5$

Although according to Biot's theory U_p is not, in general, equal to the degree of settlement U_3, Davis and Poulos (1963, 1968, 1972) suggested that U_p may be equated approximately to U_3 for the degree of accuracy required in all practical purpose.

2.6 Reliability of the Methods of Settlement Analysis

A reliable method of settlement analysis should include the following aspects which are very important in predicting the magnitude as well as the time rate of settlement. These are

(i) the relative importance of initial settlement,

(ii) the magnitude of excess pore-water pressure that is expected to be developed in the field due to imposed loading,

(iii) the effect of lateral stresses on the stress deformation characteristics of saturated clays and

(iv) the effect of relative depth of the compressible layer to the geometry of the footing, Poisson's ratio of the soil and the actual hydraulic boundary condition, on time rate of settlement.

The conventional method of settlement analysis given by Eq.2.1 assumes true one dimensional strain condition, so the immediate settlement S_u is neglected. From the observations of Skempton and Bjerrum (1957), McNamee and Gibson (1960), Flaate (1963) Lambe (1964), Davis and Poulos (1968) and D' Appolonia et.al (1971), it can be concluded that the importance of initial settlement should not be ignored. The initial settlement may constitute a large portion of total final settlement if the soil is overconsolidated (large ν') and if the depth of the compressible layer is large compared to the geometry of the foundation.

The conventional method of settlement analysis given by Eq.2.1 and 2.3 assumes that the excess pore-water pressure, u is equal to the net increase in the vertical pressure, $\Delta\sigma_1$, due to imposed foundation loading. This may be true in case of oedometer test but may be far away from the actual condition developed in an element of soil in the field. The expression for excess pore-water pressure given by Eq. 2.8 depicts that u is always less than $\Delta\sigma_1$ for the type of clays normally encountered in practice. In case of heavily overconsolidated clays the value of u may be very much less than $\Delta\sigma_1$. However, in very sensitive underconsolidated clays the value of u may become equal to or even exceed $\Delta\sigma_1$. The consolidation settlement, which is proportional to the excess pore-water pressure developed in the clay, as pointed out by Skempton and Bjerrum (1957), is bound to be miscalculated if u is taken equal to $\Delta\sigma_1$ in all types of clays. Skempton and Bjerrum took this fact into account in their method of estimating settlement.

The importance of lateral stress on the stress-deformation characteristics of soils was pointed out by Hruban as far back as 1948 when he commented that those methods of settlement computation, which disregard the very important effect of horizontal pressures on the compressibility of soil elements, are bound to give unreliable results. They fail in all cases when horizontal stresses in a natural soil layer differ from those produced in samples tested in the laboratory. The difference may amount to several times the value of the real settlement. Simons and Som (1969) while working on London clay found that the vertical consolidation settlement is greatly influenced by the relative magnitude of vertical and lateral stress increments during consolidation. They also opined that direct use of oedometer test result will not, therefore, result in accurate prediction of settlement, even if account is taken of the different excess porewater pressure set up in the oedometer and in the field. This aspect of behavior has been taken into account in the elastic method by Davis and Poulos and the stress-path method by Lambe. The Skempton and Bjerrum method and the conventional method failed to take these into consideration.

Lambe (1964) presented a theoretical comparison between the conventional method given by Eqs. 2.1 and 2.3, the Skempton and Bjerrum method given by Eq. 2.16 and the stress-path method. The comparison is shown in Fig. 2.11 (a), (b) and (c) and Table 2.2 which depicts the closeness of the stress path method to the actual field condition.

A consistent rate theory should take into account the effect of the relative dimension of the footing to the thickness of the layer below the footing, Poisson's ratio of the soil and the hydraulic boundary condition actually prevailing in the field. Davis and Poulos (1963, 1968, 1972) presented solutions to the basic differential equation of three dimensional condition. They however failed to take into account the effect of stress redistribution due to consolidation and suggested that such simplification would not impair the results very much. They have advocated the need for a three-dimensional approach even for shallow layers and suggested that the one-dimensional solution given by Terzaghi will give reasonable estimate of the rate of consolidation only when the layer is less than about one footing radius deep.

Skempton and Bjerrum (1957) presented a survey of observed final settlement for eight structures, four of which are founded on normally consolidated clays and the other four on over-consolidated clays. The informations, which are based on works of Cooling and Gibson (1955) and Skempton et.al.(1955), are presented in Table 2.3.

Table 2.2 Comparison of the Methods of Settlement Analysis (After Lambe - 1964)

Method	Basis of Method	Excess Pore Pressure Δu	Immediate Settlement S_u	Consolidation Settlement S_{CF}	Reference
Conventional Method Eq. (2.1)	All settlement from one-dimensional strain	$u = \Delta\sigma_1$ (IG)*	0 (0)	$S_{CF} = \int_0^H m_v \Delta\sigma_1 \delta H$ ($S_{CF} \sim$ IE)	Fig. 2.11 (a)
Conventional Method Eq. (2.3)	Immediate settlement from undrained shear during load application. Long-term settlement from one-dimensional strain.	$u = f(\Delta\sigma_1 - \Delta\sigma_3)$ or $u = \Delta\sigma_1$ (BF or IG)	$S_u = \int_0^H \frac{\Delta\sigma_1 - \Delta\sigma_3}{E_u} \delta H$ or $S_u = \mu_0 \mu_1 \frac{qB}{E_u}$ ($S_u \sim$ IB)	$S_{CF} = \int_0^H m_v \Delta\sigma_1 \delta H$ ($S_{CF} \sim$ IE)	Fig. 2.11 (b)
Skempton and Bjerrum Method Eq. (2.16)	Immediate settlement from undrained shear during load application. Long-term settlement from one-dimensional strain.	$u = B[\Delta\sigma_3 + A(\Delta\sigma_1 - \Delta\sigma_3)]$ (BF)	$S_u = \int_0^H \frac{\Delta\sigma_1 - \Delta\sigma_3}{E_u} \delta H$ or $S_u = \mu_0 \mu_1 \frac{qB}{E_u}$ ($S_u \sim$ IB)	$S_{CF} = \int_0^H m_v \, u \, \delta H$ ($S_{CF} \sim$ CE)	Fig. 2.11 (c)
Lambes Stress Path Method	Use of effective stress path	From stress paths (BF)	From stress paths ($S_u \sim$ IB)	From stress paths ($S_{CF} \sim$ BF)	Fig. 2.11 (c)

* The terms in ( ) are shown in Fig. 2.11.

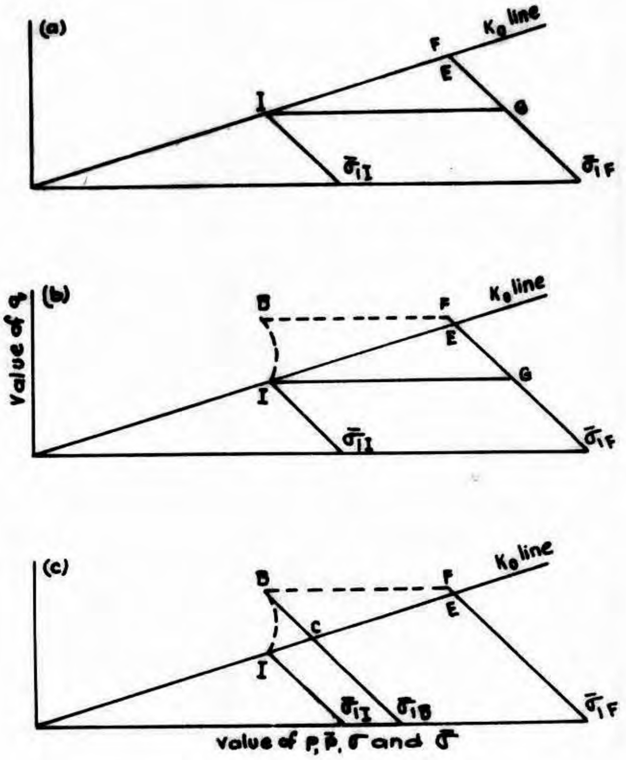

Fig.2.11 Comparison of the Methods of Settlement Analysis (Lambe 1964)

Table 2.3. Comparison of Calculated and Observed Settlements for Eight Structures (after Skempton and Bjerrum,1957)

Basis	Average cal/obs. total final settlement for four structures	
	N.C. clays	O.C. clays
Conventional method Eq. 2.1	0.81	1.25
Conventional method Eq.2.3	1.10	1.59
Skempton and Bjerrum method Eq.2.16	0.99	0.99

From the observations of Table 2.3 it can be concluded that the conventional method by Eq. 2.1 tends to underestimate the magnitude of settlement in N.C. clays and overestimate in O.C. clays. The conventional method given by Eq. 2.3 leads to severe error in O.C. clays but gives somewhat satisfactory results in N.C. clays. The method advanced by Skempton and Bjerrum seems to give reliable results in both types of clay.

Skempton et.al (1955) presented settlement records of three structures on O.C. London clay and three on N.C. Chicago clay. In all the six cases they found the observed rate to be faster than that calculated by one-dimensional consolidation theory.

Simons (1957) presented information on settlement studies of two structures founded on normally consolidated Norwegian clays. He found reasonable results by using Eq. 2.3 and expressed the need to include the initial settlement in the calculation. In both the two cases the calculated time rates of consolidation underestimated the observed rates.

Simons (1963) reports observed and calculated settlement for a nine story apartment building in Oslo. The structure is founded on O.C. clay overlying a layer of N.C. clay. Both the calculated immediate and consolidation settlements were found greater than those observed and the calculated time rate was much slower than the field rate.

Haswell (1963) presented the predicted and actual settlements of three thermal power stations founded on O.C. clays. The predicted settlements were too large compared to that observed.

Davis and Poulos (1968, 1972) presented results of model footing tests on two types of normally consolidated clay. The three-dimensional elastic approach advanced by them predicted reasonably both the total final and the time rate of settlement compared to the conventional and Skempton and Bjerrum method.

Davis and Poulos (1968) presented a rivew of 14 cases in which a reasonably reliable comparison could be made between the rate predicted from Terzaghi's one-dimensional consolidation theory and the observed rate. Eight of these cases showed that the observed rate was faster, four being very much faster. In the six remaining cases the observed rate was either very close to or only slightly slower than the predicted. In these cases the thickness of the clay layer and its depth below the foundation was such that the condition of the problem was close to being one-dimensional.

They also found that out of four cases where the rate was predicted by three-dimensional theory, three showed reasonably good agreement with the observed rates.

Simons (1974) writes that the use of stress-path testing results in smaller (and more reliable) predictions of settlement for structures on heavily O.C. clays which has been shown by Lambe (1967) and Simons and Som (1970). Simons further writes that fewer data are available for normally and lightly O.C. clays, although Lambe (1973) showed for the North East Test Embankment that settlements predicted from oedometer tests and stress path triaxial tests did not differ greatly.

CHAPTER III

THE EXPERIMENTAL SET UP

3.1 General

Simons (1971), when commenting on the relative merits and demerits of the stress path method, writes that although it is an important improvement over the other methods of settlement analysis, it suffers from the practical disadvantage that very sophisticated, time consuming and expensive laboratory techniques are required. Lambe (1964) also emphasised the need for good technician and proper equipment for carrying out test along a predetermined stress-path. Simons and Lambe did not, however, prescribe any test set-up to carry out these stress-path tests.

Davis and Poulos (1963, 1968) when presenting the three-dimensional elastic method of settlement analysis, described a layout of apparatus for determining the elastic parameters for settlement computation from tests which are essentially stress-path tests as described by Simons (1971) and Lambe (1964, 1967).

Bishop and Henkel (1964) presented a layout of apparatus for the triaxial consolidation of samples against a back-pressure.

In light of the layouts of apparatus presented by Davis and Poulos (1963) and Bishop and Henkel (1964), a test set-up was designed and is shown in Fig. 3.6.

Most of the component parts of the set-up were designed and fabricated locally and are described in the following sections.

3.2 The K_o - Cell

Direct experimental determination of K_o, the lateral earth-pressure at rest, had been a great problem for research workers for many years.

Thin walled oedometer rings fitted with electrical resistance strain gages were used by Som (1970) and Simons and Som (1970) to determine K_o during oedometer consolidation tests.

Sherif and Koch (1970) described an apparatus, called stress meter, where a semi-circular soil container fitted with a proving ring was used to measure K_o. Bishop and Henkel (1964) described the use of lateral strain indicator to achieve K_o - consolidation and also to determine K_o.

Davis and Poulos (1963) presented the most versatile, instrument which they called K_o-cell. The apparatus which permits ready determination of K_o and is capable of loading a specimen under K_o condition is shown in Fig. 3.1 and Plate 3.1. In a K_o-cell the condition of no lateral strain (K_o) of the specimen is imposed by preventing any change in the volume of the cell fluid, by using a loading plunger of the same diameter as the specimen. An entire top platen of a conventional triaxial cell was fabricated where the plunger diameter was made equal to 1.4 in, which is the diameter of the sample. During load application, there is practically no volume change of the incompressible cell fluid (glycerine) which acts as a non-yielding wall around the specimen. To accomodate the movement

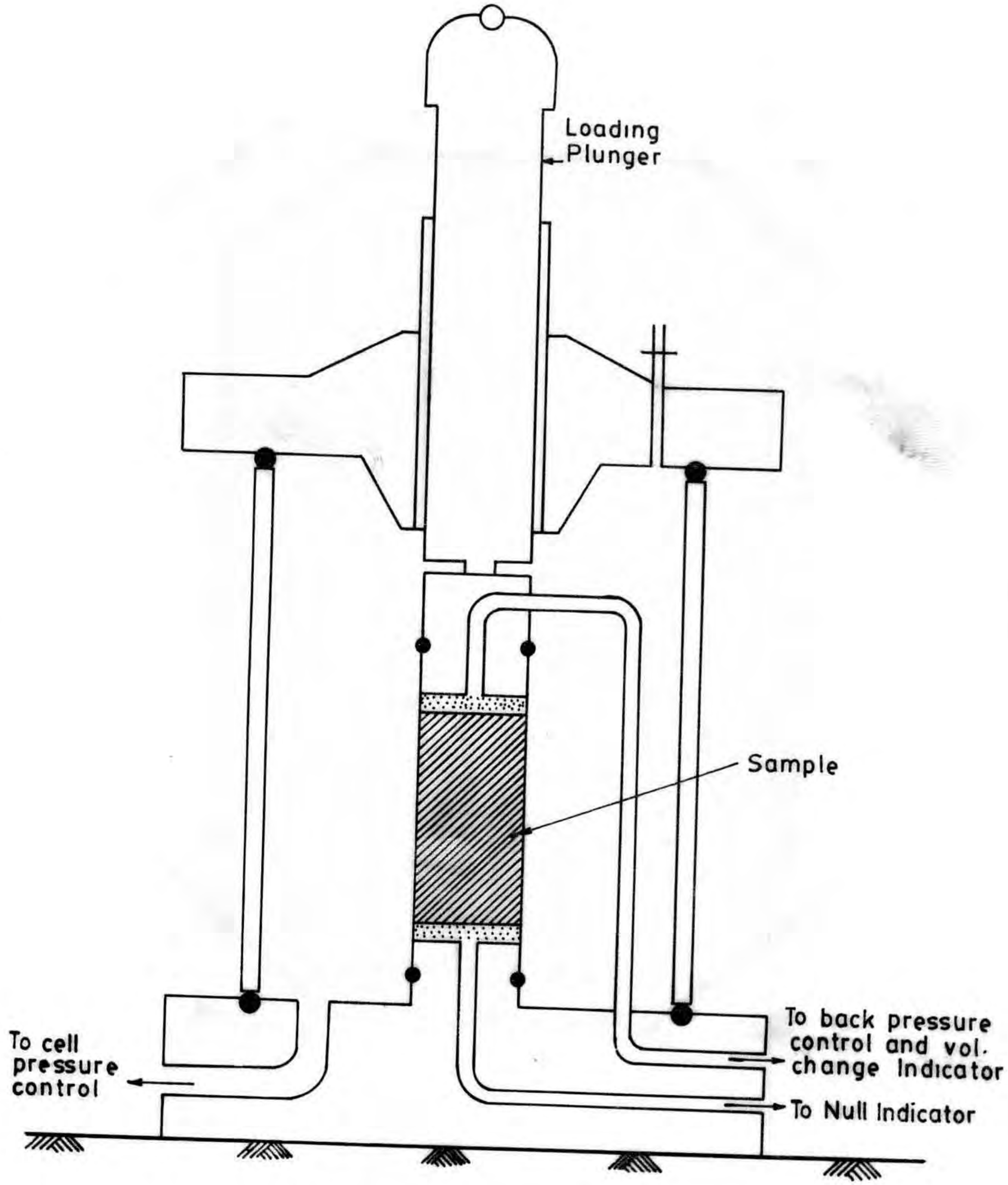

Fig.3.1 The K_o - Cell

Plate 3.1 The K_o - Cell.

of the plunger under undrained condition the cell pressure will increase. The ratio between the increase in total axial stress and increase in the developed cell pressure is the coefficient K_o under undrained condition. The final value of the ratio, when all excess pore pressure has dissipated, is the coefficient K_o' under drained condition.

3.3 Apparatus for Measuring Pore-water Pressure

A null method of pore-pressure measurement which was first used at Imperial College, London and subsequently developed by Bishop and Eldin (1950) was used in this study. The main components of the apparatus, a null indicator, a control cylinder and a twin manometer was constructed.

The principal features of the null indicator which is shown in Fig. 3.2 and Plate 3.2 are

(i) the upper body, A,
(ii) glass tube, B and end seals, E and
(iii) the lower body, C.

(i) The upper body, A:

The upper body which was machined from a brass rod, houses connections from a triaxial cell and a pipette via Klinger Cocks.

(ii) Glass tube, B and end Seals, E:

A section of 1 mm bore glass tubing about 7" long, having outside diameter about 10 mm, was ground flat at each end. The glass tube was connected to the upper and lower body by inserting, through each end, a short length of 1 mm O.D. Stainless steel tubing (hypodermic needle), F. At the lower end the hypodermic needle passes into the lower body and extends below the mercury surface (Fig. 3.2). The connection between the glass tubing and the upper and lower bodies were sealed by axial compression between two rubber washers, E, through which the hypodermic needles passed. For extra safety an epoxy adhesive (Araldite) was used to make the whole system pressure tight. The 1 mm. bore glass tubing was used because it gives adequate sensitivity and minimized capillary effects.

3. The lower body, C:

The lower body was connected to the upper body by an internally threaded tube, D, by which the seals on the glass tube could be adjusted. It contains a cylindrical chamber, into the lower end of which the mercury through, G, was sealed by a rubber O-ring. The trough may be raised and lowered by a Knurled nut, H, running on the screw thread on the outside of the chamber. The upper part of the chamber, which is filled with water, is connected to the pressure gage, the manometer and the control cylinder. The mercury trough was made from stainless steel to avoid rust and deterioration due to contact with mercury. To observe the mercury level in the capillary tube a window was cut in the threaded tube, D, which was fitted with a paper scale.

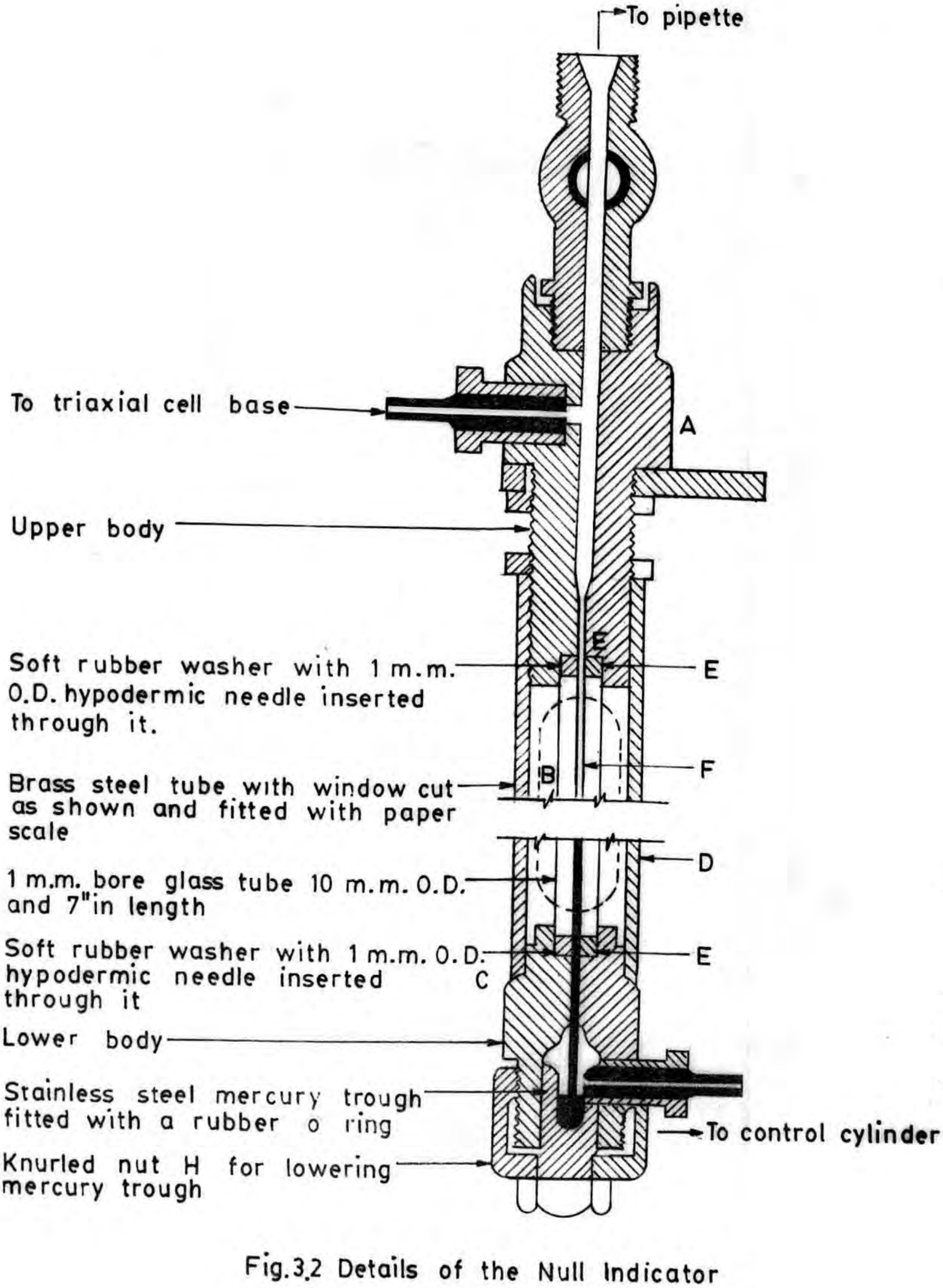

Fig.3.2 Details of the Null Indicator

Plate 3.2 The Null Indicator.

The principal features of the control cylinder which is shown in Fig. 3.3 and Plate 3.3 are:

(i) the cylinder, A,

(ii) the piston, B and

(iii) the piston rod, C.

(i) The cylinder A:

The cylinder which was made of brass, is a tube $1\frac{1}{2}$ in. I.D. and $\frac{1}{8}$ in. in thickness, was screwed and sweated on to the brass base E.

(ii) The piston, B:

The brass piston, B, was fitted with a rubber O-ring. A deep groove ball bearing was used to avoid rotation of the piston during screwing of the piston rod. A smooth running and leak-proof seal, essential to the performance of the apparatus was obtained from commercial rubber O-sealing rings.

(iii) The piston rod, C:

The stainless steel piston rod which was machined to have 20 threads per inch passes through the brass nut, F, which forms the cap of the cylinder. An 8 in dia. perspex hand wheel, D, was provided to turn the screwed rod and has a total travel of 6 in.

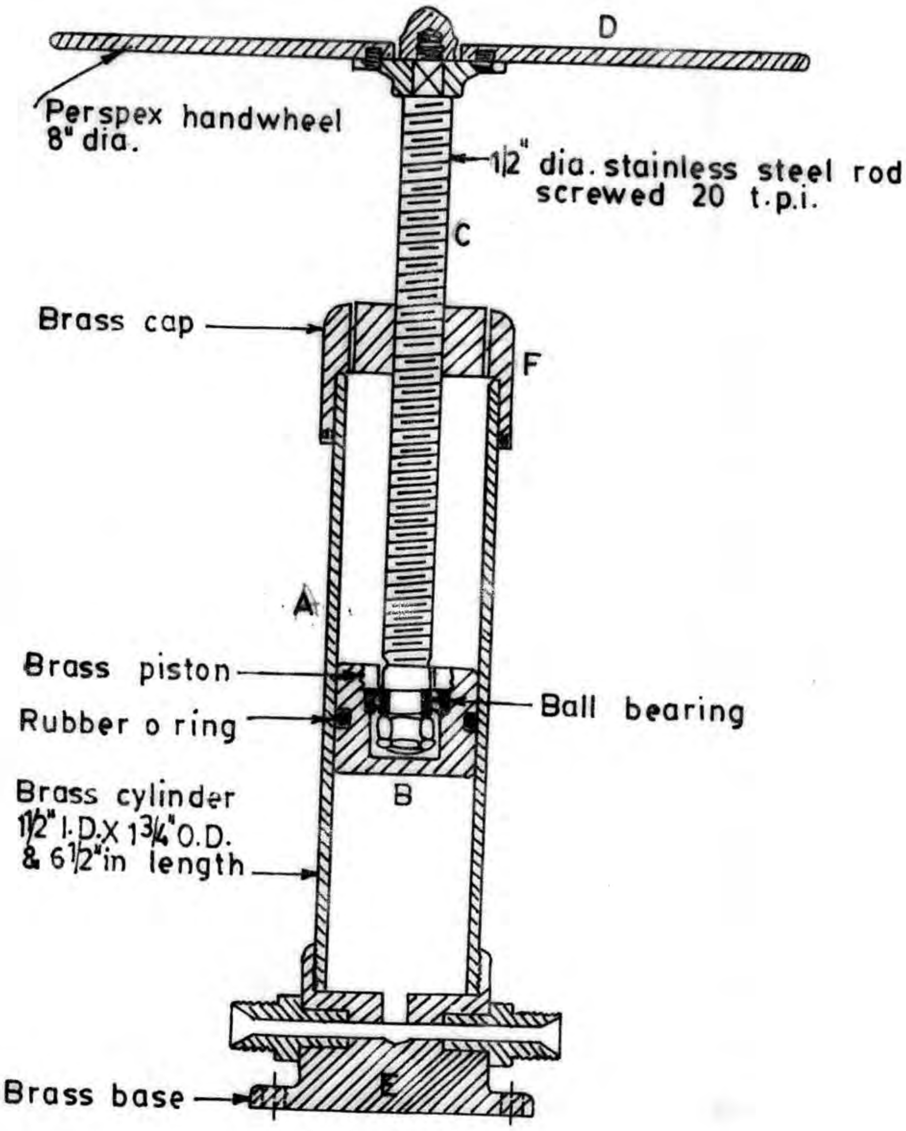

Fig.3.3 Details of the Control Cylinder

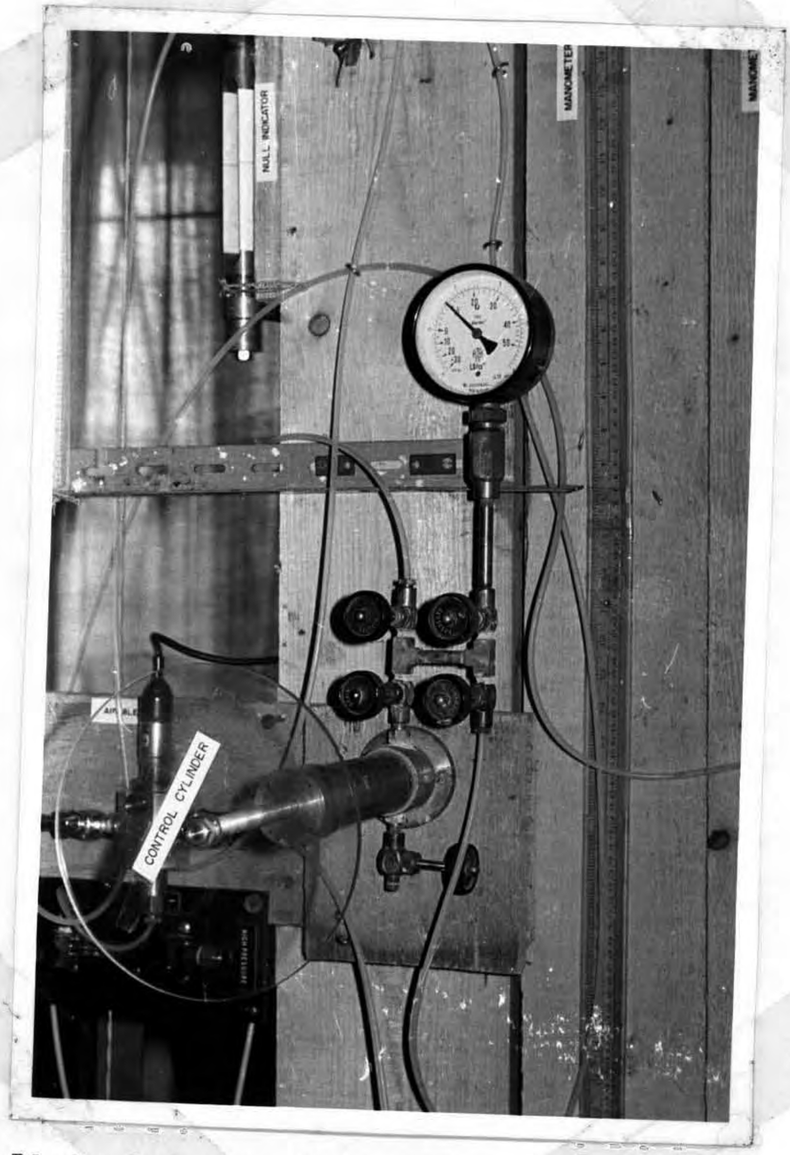

Plate 3.3 The Control Cylinder.

The construction details, deairing and cleaning, calibration and principle of operation is presented in details by Bishop and Henkel (1964).

To obtain a sensitive pore water pressure measuring device a twin manometer was designed and constructed. Transparent polythene tube, 3 mm I.D& wooden scales graduated both in millimeters and inches were used to construct the twin manometer, which is essentially two U-tube manometers connected in series. The zero reading of the null indicator was obtained at 3 psi of the pressure gage reading. The calibration curves for the manometer is presented in Fig. 3.4. Limbs L_1 and L_3 of the manometer are graduated in inches and upto 1/10th of an inch, and limbs, L_2 and L_4 are graduated in centimeters and millimeters. The calibration factor for the inch scale was obtained as 0.18 psi per 0.1 in and that for millimeter scale was obtained as 0.071 psi per mm.

3.4 The Volume-Change Indicator

The volume change indicator for the test set-up was constructed from the design presented by Davis and Poulos (1963), which enables ready measurement of volume change when the sample is under a back-pressure. The volume change indicator, N (Fig.3.6), (Plate 3.4), used to measure the volume strain during consolidation merely consists of an open ended tube 2.62 mm I.D. attached to a horizontal scale. The tube was connected by flexible polythene tubing 3 mm I.D. to the top pot(Plate 3.5)of Bishop

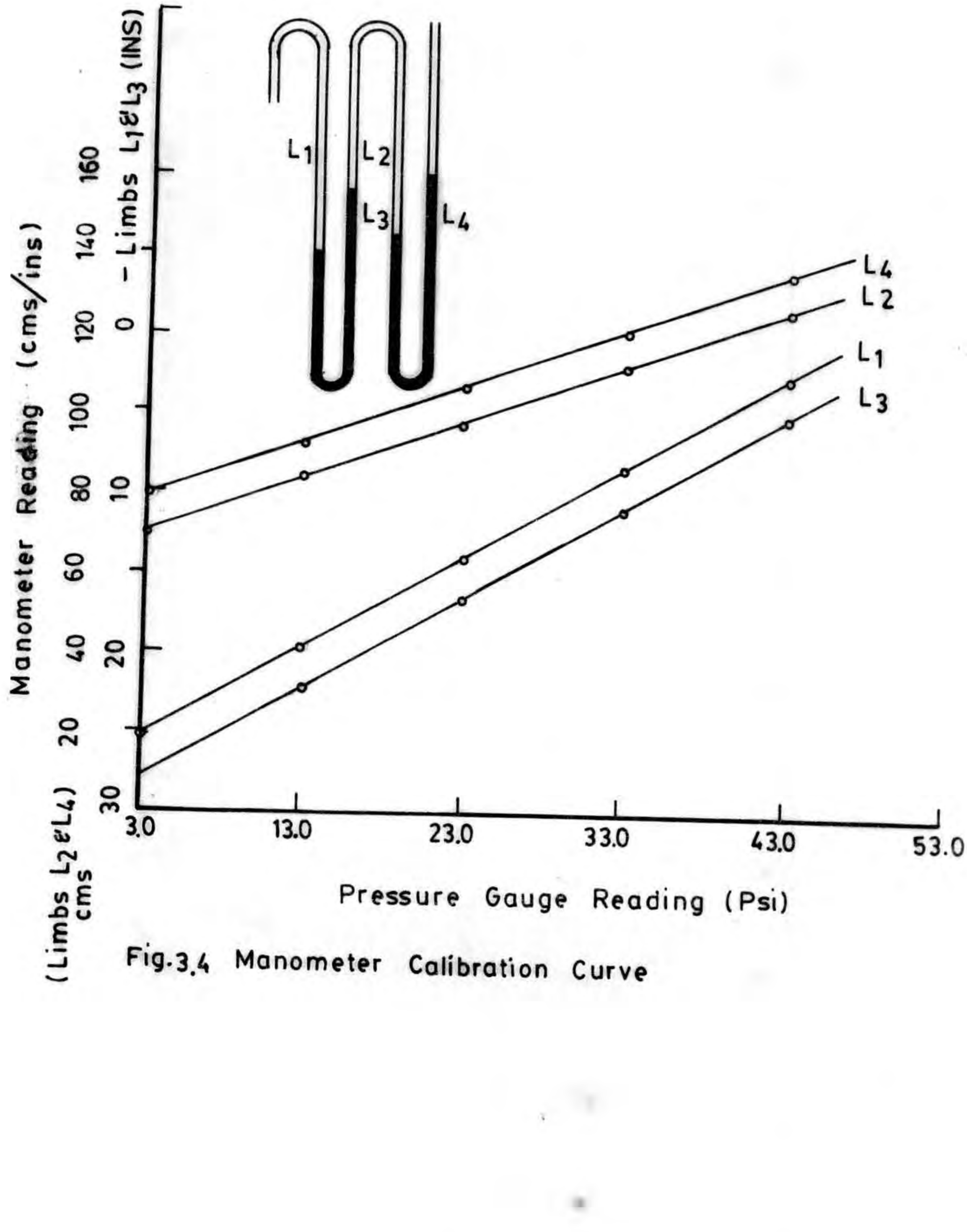

Fig.3.4 Manometer Calibration Curve

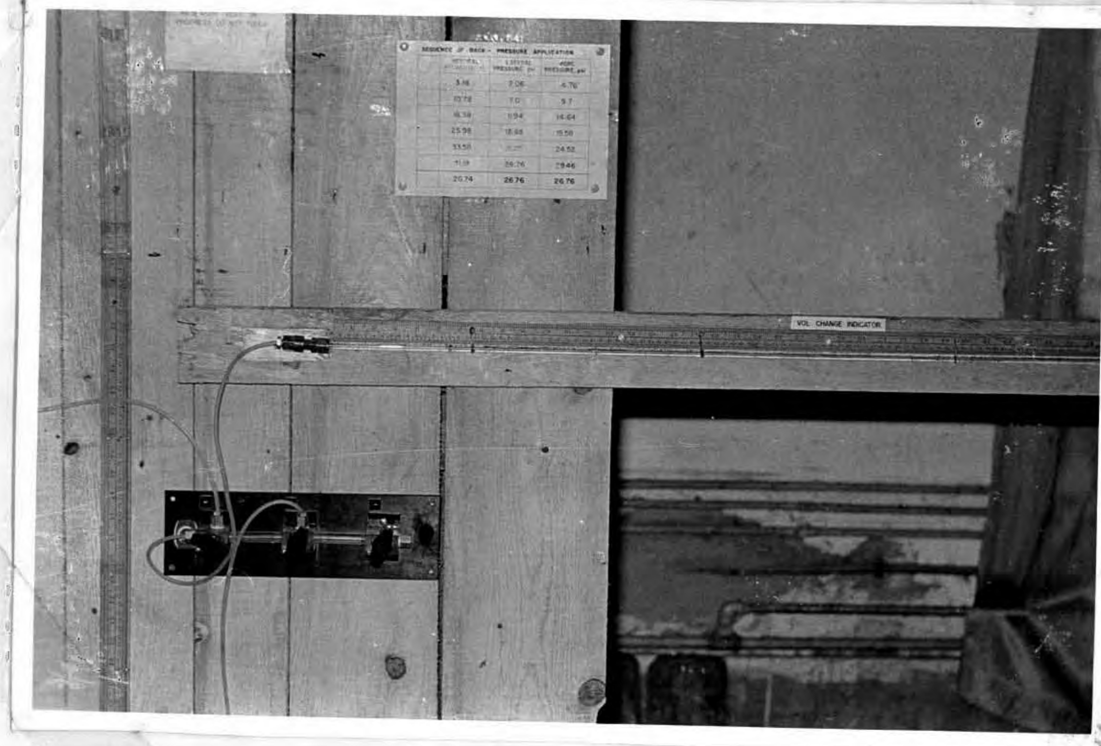

Plate 3.4 The Volume Change Indicator.

Plate 3.5 The Top Mercury Pot.

type mercury control (Fig. 3.6), which is used to provide back pressure to the pore-water system. This pot is filled with water on top of the mercury and the water continues through the flexible pipe to the graduated tube.

The movement of the meniscus along this tube gives the volume change of the specimen during consolidation. The movement of the meniscus along the horizontal tube has no effect on the constancy of the back pressure. The scale of the volume change indicator is graduated in centimeters and millimeters and a calibration factor of 0.00539 c.c/mm was obtained for the indicator.

3.5 Set-up for Stress-Path Tests

In the stress-path method of settlement analysis a soil specimen is tested in the laboratory by applying as closely as possible the same sequence of stress changes as those to which the soil will be subjected in the field. The stages of an idealized experimental program are presented in Fig. 3.5. When a sample is removed from the ground, the total stresses are reduced to zero and a negative pore-water pressure develops. In the first stage, therefore, the insitu stresses should be restored to obtain the condition before sampling. Then in the second stage a set of stresses equal to those to which the sample will be subjected owing to foundation loading should be applied under undrained conditions, and both the vertical strain and pore-water pressure measured. The sample then should be allowed to

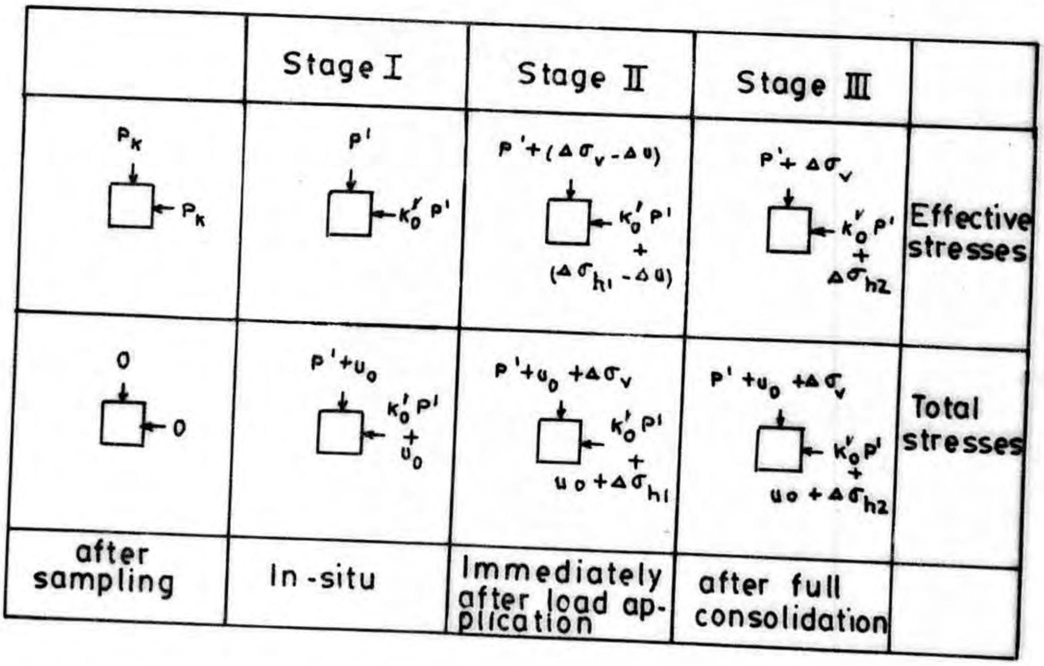

Fig.3.5 Stages of an Ideal Experimental Programme for Settlement Analysis.

consolidate against a back pressure equal to the equillibrium pore-water pressure u_o, and at the same time the horizontal stress should be decreased to its final value.

For this study a test setup was chosen so that all the stages of a stress-path test could be carried out conveniently. Fig. 3.6 shows the layout of the set-up and the photograph is shown in Plate 3.6.

Procedure to carryout a stress path test using the set-up of Fig. 3.6 is as follows:

(i) The sample A is placed in the K_o-cell, B, in such a way so that no air bubble is trapped between the sample and the platens of the top and bottom drains.

(ii) The zero reading of the null indicator, F, is obtained using pressure gage, I or manometer, J, keeping the water level in pipette G, at the same level as the midheight of the sample, A. This is done by opening coocks e, f and l.

(iii) Cocks e and l are closed and g, i and j are opened. The upper pot M of the Bishop type mercury control is adjusted so that the manometer/pressure gage reads the neutral pressure u_o in excess of the zero reading. The cocks g, i and j are then closed.

(iv) The bleed screw Q is then operated to bring back the manometer to zero reading.

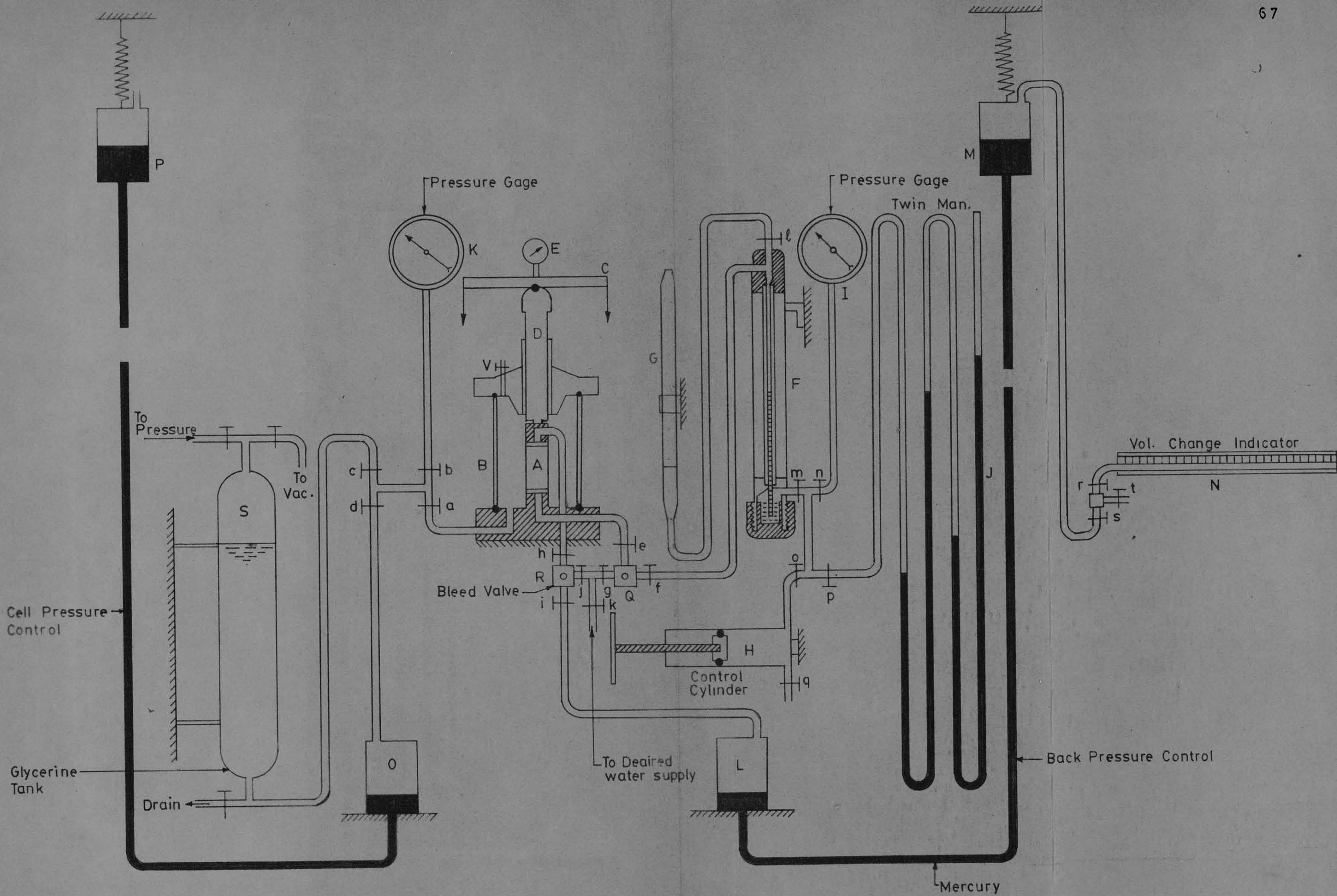

Fig. 3.6 Lay-out of Apparatus for Stress-Path Testing

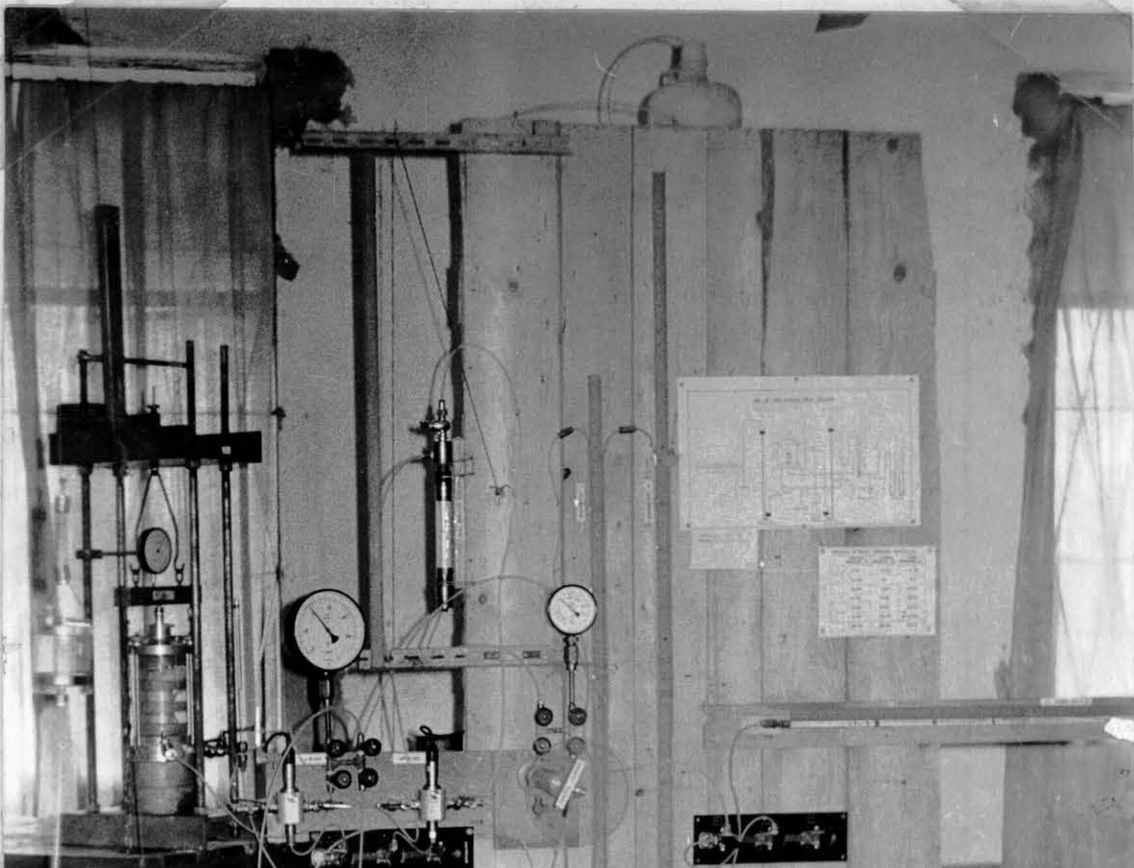

Plate 3.6 The Test Set-up.

(v) The K_o-cell is then filled with glycering from tank S, by opening cocks a and c and operating bleed valve, v when the cell is completely filled with glycerine cocks a and d are closed.

(vi) This is the stage-I of the stress-path test. To bring back the sample to the insitu state of stress the plunger is loaded for a pressure $p' + u_o$, keeping cocks e and f open to enable porewater pressure measurement through the bottom drain. When the full porewater pressure has been developed, cocks h and i is opened to allow drainage through the top drain under a back-pressure equal to u_o. The volume change readings during consolidation is obtained from the volume change indicator N. The vertical strain during consolidation can be obtained from the vertical dial E, capable of reading upto 0.0001 in. After full dissipation of pore-water pressure the soil element is at the insitu state of stress with the vertical total stress equal to $p' + u_o$ and horizontal total stress equal to $K_o' \, p' + u_o$. Now cock h is closed and cocks b and d opened. The cell pressure gage reading is brought to $K_o' \, p' + u_o$ by adjusting the upper pot P of the cell pressure control and then cock a is opened.

(vii) This is stage II of stress-path test. The axial stress at this stage is increased by $\Delta\sigma_v$ equal to the net increase in the vertical stress due to foundation loading and simultaneously the horizontal stress is increased by $\Delta\sigma_{h1}$, which is the net increase in horizontal stress under undrained condition.

The vertical dial reading and pore-water pressure is recorded which is due to the undrained foundation loading.

(viii) This is stage III and the last stage of a stress path test. After full development of the pore water pressure cock h is opened. As the pore pressure dissipates the horizontal stress is changed from $\Delta\sigma_{h1}$ to $\Delta\sigma_{h2}$ which is due to decrease in Poisson's ratio under drained condition. This is done by adjusting the upper pot P of the cell pressure control. During consolidation the vertical dial readings, the manometer readings and the volume change indicator readings are taken time to time to obtain the pattern of dissipation.

CHAPTER IV

EXPERIMENTAL INVESTIGATION

4.1 Field Investigation and Collection of Soil Samples

A couple of priliminary bore-holes and inspection of open cuts nearby revealed that the subsoil profile is more or less uniform at the upper layers of the site of the proposed water tower. On the basis of the preliminary field investigation it was decided to drill two boreholes at a distance of thirty feet on centres. Each of the boreholes were carried to 70' below ground level. One of the boreholes was drilled for undisturbed sampling and the samples were collected in $3\frac{1}{2}$ in. and 4 in. inside diameter Shelby tubes having 1/16 in. wall thickness. The other borehole was drilled mainly for subsurface sounding which was done by performing Standard Penetration Test (SPT) at intervals of five feet. Disturbed but representative samples were collected from this borehole and preserved in polythene bags for subsequent laboratory investigation. A bore-log showing the stratification, the position of the watertable, the Atterberg limits, the S.P.T values and the unconfined compressive strength is presented in Fig. 4.1.

4.2 Laboratory Investigation

The program for laboratory investigation may be divided into two broad categories:

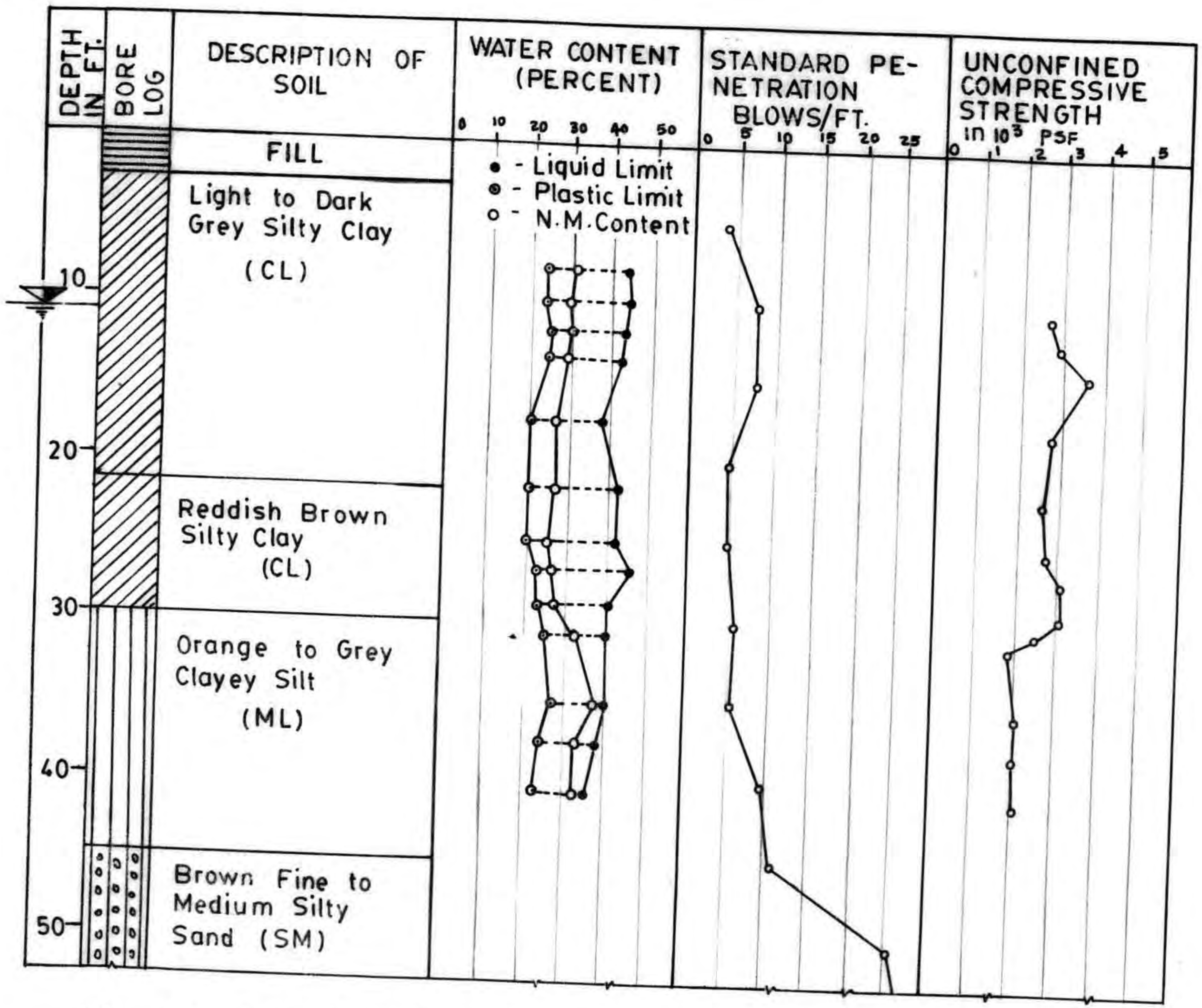

FIG. 4.1 Log of Boring

(i) Standard routine tests for determination of Atterberg limits, natural moisture content, specific gravity, unit weight, unconfined compression strength, consolidated undrained (CIU) triaxial tests and oedometer consolidation tests and

(ii) Special tests like K_o-test and stress-path triaxial consolidation tests in which soil specimens were tested following predetermined stress-paths.

4.3 Laboratory Tests-Specification and Procedure

Standard routine tests were performed inaccordance with the procedure specified by the ASTM except for the consolidated undrained triaxial tests. The test procedure followed for consolidated undrained triaxial tests is that described in details by Lambe (1951).

Test procedure for performing stress-path test has been discussed in Chapter III, where the use of the test set up was described. The K_o-test which is a part of the stress-path test has also been described there.

4.4 Laboratory Test Results

The test results of the soil samples collected from the borehole are discussed below:

4.4.1 Physical Properties

The results of Atterberg limits and natural moisture content test performed in the laboratory are incorporated in the bore log of Fig. 4.1. These values along with the plasticity index, dry and bulk density and specific gravity for samples at different depth are presented in Table 4.1.

From the physical properties and field investigation the sub-soil profile may be described as follows:

The surface layer extending upto approximately 5' below ground level was composed of fill material. The second layer which was found to extend from approximately 5' below ground level to approximately 21' below ground level was identified as light to drak grey silty clay of medium consistency. The third layer extending from 21' below ground level to approximately 30' below ground level was identified as reddish brown silty clay of medium consistency. Although both the second and third layers showed similar index properties, consistency and classification (CL by the unified classification system), they were different in colour. The fourth layer extending from 30' below ground level to approximately 45' below ground level was identified as light to dark grey clayey silt and was classified as ML. Below this layer a layer of medium compact silty fine to medium sand was encountered. The sand is coarser and denser with depth.

From grain size analysis the average clay content of the CL layer from 5' below ground level to 30' below ground level was obtained as 15 percent. The average clay content of ML layer was obtained as 8 percent.

Table 4.1. Summary of Physical Properties

Depth	L.L.	P.L.	P.I.	N.M.C.	Dry unit wt.	Wet unit wt.	Sp.Gr.
2'0" to 3'6"	-	-	-	18	101.7	120	-
5'6" to 7'0"	-	-	-	25	99.2	124	-
7'6" to 9'0"	44	25	19	29	96.9	125	2.66
9'6" to 11'0"	46	24	22	28	100.0	128	2.72
11'6" to 12'6"	44	26	18	31	93.1	122	2.71
13'0" to 14'6"	43	26	17	32	91.7	121	2.69
16'9" to 18'3"	39	21	18	28	96.9	124	2.66
20'6" to 22'0"	44	22	22	28	93.8	120	-
24'3" to 25'9"	43	21	22	26	101.6	128	2.72
26'3" to 27'9"	47	25	22	26	102.4	129	2.70
28'6" to 29'6"	42	24	18	26	100.8	127	2.72
30'0" to 31'6"	41	27	14	34	87.3	117	-
32'3" to 33'6"	-	-	-	35	83.7	113	-
34'3" to 35'6"	41	29	12	40	82.9	116	2.71
36'0" to 37'6"	39	26	13	35	85.2	115	2.70
39'9" to 41'3"	37	25	12	35	85.2	115	2.70

4.4.2 Shear Strength and Undrained Modulus

The unconfined compression test results are presented in Table 4.2. The strength shown are peak values of stress-strain curve and the corresponding strains are reported. In cases where peak did not occur strength at 20% strain is reported.

The depth of the foundation was choosen at 10' below ground level and as such tests were performed on samples from below this depth.

Samples from the CL layers showed substantial deformation before failure where as those from the ML layer failed at smaller strains.

Undrained elastic modulus was determined both from unconfined compression tests and consolidated undrained triaxial tests. The consolidated undrained triaxial tests were performed at a confining pressure equal to the existing effective overburden pressure. The undrained modulus values which are secant modulus at 50 percent of peak stress is presented in Table 4.3.

From unconfined compression test the average value of the undrained modulus was obtained as 366 psi for the CL layer and 221 psi for the ML layer.

From CIU triaxial compression test those values were obtained as 876 psi for the CL layer and 1610 psi for the ML layer. The scatter in case of results for samples from ML layer was high. The effect of confining pressure was found to be more

Table 4.2. Unconfined Compressive Strength Test Results

Depth	Unconfined compressive strength psf	Failure strain percent
9'6" to 11'0"	2759	20.0
11'6" to 12'6"	3006	16.0
13'0" to 14'6"	3672	20.0
16'9" to 18'3"	2605	14.0
20'6" to 22'0"	2675	16.0
24'3" to 25'9"	2752	12.0
26'3" to 27'9"	3456	11.5
28'6" to 29'6"	3168	10.0
30'0" to 31'6"	1830	5.0
34'3" to 35'6"	2130	8.0
36'0" to 37'6"	2016	9.5
39'9" to 41'3"	2125	8.5

Table 4.3. Undrained Modulus Obtained from Unconfined Compression and Consolidated Undrained Triaxial Compression Tests.

Depth	E_u in psi (from U.C. tests)	Av. E_u in psi (from U.C. tests)	E_u in psi (from CIU triaxial com. tests)	Av. E_u in psi (from CIU triaxial com. tests)
9'6" to 11'0"	305		-	
11'6" to 12'6"	349		845	
13'0" to 14'6"	445		846	
16'9" to 18'3"	356		-	
20'6" to 22'0"	375	366	877	876
24'3" to 25'9"	347		-	
26'3" to 27'9"	412		807	
28'6" to 29'6"	335		1005	
30'0" to 31'6"	280		1175	
34'3" to 35'6"	200	221	-	1610
36'0" to 37'6"	192		1505	
39'9" to 41'3"	213		2150	

pronounced in samples from the ML layer compared to those from CL layers.

4.4.3 Overconsolidation Ratio (OCR)

The overconsolidation ratio for samples from different depth was calculated by four different methods. Apart from the well known Casagrande graphical construction a graphical method using the void-ratio-reduction pattern suggested by Schmartmann (1955) was used.

The well known statistical relation $\frac{c_u}{\bar{p}_o} = 0.11 + 0.0037\ PI$ for normally consolidated clays advanced by Skempton (1957) was used as a method for determining the overconsolidation ratio. If the overconsolidation ratio is denoted as OCR, the actual apparent cohesion as c_{act}, and the cohesion for a normally consolidated clay as c_{norm}, then

$$\bar{P}_c = OCR \times \bar{P}_o \qquad 4.1$$

where $\bar{P}_c$ = maximum past preconsolidation pressure

$\bar{P}_o$ = existing effective overburden pressure.

At any value of plasticity index, the linear relationship between shear strength and vertical consolidating pressure gives,

$$\frac{\bar{P}_c}{\bar{P}_o} = \frac{c_{act}}{c_{norm}} \qquad 4.2$$

$$OCR = \frac{c_{act}}{c_{norm}} \qquad 4.3$$

The value of c_{act} was obtained by taking half of the unconfined compressive strength and the value of c_{norm} was obtained from the equation.

$$c_{norm} = \bar{P}_o \times (0.11 + 0.0037\ P.I.) \qquad 4.4$$

Substituting this value of c_{norm} in equation 4.3

$$OCR = \frac{c_{act}}{\bar{P}_o} \times \frac{1}{(0.11+0.0037\ P.I.)} \qquad 4.5$$

The calculation of OCR by Eq. 4.5 is shown in Table 4.4.

The overconsolidation ratio was also determined by using the undrained shear strength and liquid limit data by Eq. 4.6 (Simons 1974), which gives the maximum past preconsolidation pressure in the form

$$\bar{P}_c = \frac{S_u}{0.45\ LL} \qquad 4.6$$

where S_u = undrained shear strength

LL = liquid limit in percent

The overconsolidation ratio was then calculated from

$$OCR = \frac{\bar{P}_c}{\bar{P}_o}$$

The values of the overconsolidation ratio obtained by the methods described so far has been presented in Table 4.5.

Table 4.4. Overconsolidation Ratio from Undrained Shear Strength (after Skempton 1957)

Depth	c_{act} psf	$\bar{P}_o$ psf	P.I.	$\frac{c_{act}}{\bar{P}_o}$	$\frac{c_{norm}}{\bar{P}_o}$	OCR
7'6" to 9'0"	-	1000	19	-	0.1803	-
9'6" to 11'0"	1380	1250	22	1.104	0.1914	5.8
11'6" to 12'6"	1503	1438	18	1.045	0.1766	5.9
13'0" to 14'6"	1836	1563	17	1.175	0.1729	6.8
16'9" to 18'3"	1303	1781	18	0.732	0.1766	4.1
20'6" to 22'0"	1338	2031	22	0.659	0.1914	3.44
24'3" to 25'9"	1376	2250	22	0.612	0.1914	3.2
26'3" to 27'9"	1728	2375	22	0.728	0.1914	3.8
28'6" to 29'6"	1584	2500	18	0.634	0.1766	3.6
30'0" to 31'6"	915	2668	14	0.343	0.1618	2.1
34'3" to 35'6"	1065	2825	12	0.377	0.1544	2.44
36'0" to 37'6"	1008	2930	13	0.344	0.1581	2.2
39'9" to 41'3"	1063	3114	12	0.341	0.1544	2.2

Table 4.5. Overconsolidation Ratio by Different Methods

Depth	Overconsolidation ratio			
	Casagrande (1936)	Schmertmann (1955)	Skempton (1957)	Simons (1974)
7'6" to 9'0"	5.0	4.9	-	-
9'6" to 11'0"	4.6	7.2	5.8	5.3
11'6" to 12'6"	2.3	5.9	5.9	5.3
13'0" to 14'6"	1.5	3.6	6.8	6.1
16'9" to 18'3"	2.7	3.5	4.1	4.2
20'6" to 22'0"	-	-	3.44	3.3
24'3" to 25'9"	-	-	3.20	3.20
26'3" to 27'9"	1.38	1.4	3.80	3.50
28'6" to 29'6"	1.5	1.34	3.60	3.40
30'0" to 31'6"	-	-	2.1	1.86
34'3" to 35'6"	1.45	2.9	2.4	2.04
36'0" to 35'6"	1.76	2.4	2.2	1.96
39'9" to 41'3"	1.47	1.5	2.2	2.05

Both the emperical methods in which the overconsolidation ratio was calculated from undrained shear strength and Atterberg limits showed resonably close agreement.

The overconsolidation ratio by the graphical methods did not differ very greatly except for some scattered values for shallow depths.

A resonably good agreement has been obtained for values of the OCR determined for the ML layer but at shallow depths in the CL layer OCR calculated from the emperical methods were higher than those obtained from graphical methods.

The OCR obtained from all the four approaches showed the general tendency of decrease in its value with depth.

4.4.4 Oedometer Consolidation Properties

The one dimensional consolidation properties obtained from oedometer test results are presented in Tables 4.6 and 4.7.

Table 4.6 shows the values of the coefficient of volume compressibility, m_{v1}, and the coefficient of consolidation, C_{v1}, appropriate for the stress range to which soil elements at different depths will be subjected considering one-dimensional consolidation. In all the tests C_{v1} was determined by square root t fitting method as more consistent plots were obtained by this method compared to the log t fitting method.

Table 4.6. Coefficient of Volume Compressibility, m_{v1} and Coefficient of Consolidation, C_{v1}, from Oedometer Consolidation Test Results

Depth	Coeff. of vol. compr. m_{v1} in 10^{-5} ft^2/lb	Coeff. of consolidation c_{v1} in 10^{-5} $ft^2/min.$
9'6" to 11'0"	1.443	11.04
11'6" to 12'6"	1.344	8.31
13'0" to 14'6"	1.248	20.11
16'9" to 18'3"	1.06	15.20
26'3" to 27'6"	0.672	21.82
28'6" to 29'6"	0.693	42.23
34'3" to 35'6"	1.183	208.00
36'0" to 37'6"	1.023	258.50
39'9" to 41'3"	1.026	282.00

The values of m_{v1} showed a gradual decrease with depth for both the CL and ML layers. On the basis of m_{v1} values, the soil layer from 10' below ground level to 45' below ground level may be divided into three layers like that already shown in the bore-log of Fig. 4.1. The first layer from 10' below ground level to 21'-6" below ground level having average $m_{v1} = 1.274 \times 10^{-5}$ ft^2/lb. The second layer from 21'-6" below ground level to 30' below ground level having average $m_{v1} = 0.683 \times 10^{-5}$ ft^2/lb. The third layer from 30' to 45' having $m_{v1} = 1.077 \times 10^{-5}$ ft^2/lb.

Although the coefficient of consolidation C_{v1} values showed some scatter a resonably good average could be made for all practical purpose. On the basis of the C_{v1} values the whole soil profile can be divided into two major layers. The first layer consisting of the CL layer from 10' below ground level to 30' below ground level having average $C_{v1} = 15.30 \times 10^{-5} ft^2/min$ and the second layer consisting of the ML layer from 30' below ground level to 45' below ground level having average C_{v1} = 2.50×10^{-3} ft^2/min.

To investigate the effect of sample disturbance on the compressibility of the soil the field e-log p relation was reconstructed from the laboratory curve in a manner described in details by Schmartmann (1955). The values of the initial void ratio, compression index, C_{CL}, obtained from the laboratory compression curve, the recompression index C_{CR} and the virgin compression index C_{CF}, obtained from the reconstructed field curve are presented in Table 4.7.

Table 4.7 Consolidation Characteristics From Laboratory and Field e-log p Relation

Depth	Initial void ratio e_o	Compression index from lab.comp. curve C_{CL}	Recompression index from lab.rebound curve, C_{CR} (Schmartmann 1955)	Virgin Comp. index from reconstructed field curve, C_{CF} (Schmartmann 1955)
7'6" to 9'0"	0.712	0.164	0.0350	0.205
9'6" to 11'0"	0.701	0.150	0.0405	0.190
11'6" to 12'6"	0.832	0.211	0.0500	0.343
13'0" to 14'6"	0.883	0.220	0.0435	0.300
16'9" to 18'3"	0.768	0.320	0.0395	0.430
26'3" to 27'6"	0.667	0.143	0.0205	0.158
28'6" to 29'6"	0.701	0.135	0.0175	0.150
34'3" to 35'6"	1.160	0.334	0.0530	0.520
36'0" to 37'6"	0.965	0.294	0.0438	0.440
39'9" to 41'3"	1.008	0.320	0.0440	0.360

4.4.5 Three Dimensional Consolidation Characteristics

Two distinct layers were identified on the basis of physical properties, consistency and one-dimensional consolidation characteristics. The layers are, the CL layer from 10' below ground level to 30' below ground level and the ML layer from 30' below ground level to 45' below ground level.

To find the elastic parameters for three dimensional settlement calculation Davis and Poulos (1968) emphasized the need for obtaining a representative sample from a representative depth. They observed that as the compressibility decreases with depth the upper portion of the layer that is the layer above the midplane will contribute more to the overall settlement. So the representative depth to obtain a representative sample should be choosen at less than half of the full stratum depth. They suggested the representative depth as 1/3 to 1/4 of full stratum depth.

Taking these into consideration and on the basis of the one-dimensional consolidation properties one sample was choosen from each layer for performing stress-path tests and two specimens were tested from each sample. The position of the samples with respect to the layer depth and the one dimensional consolidation properties of the layer is presented in Table 4.8.

The samples were tested following the procedure outlined in Chapter III. The test program for the two samples are presented in Table 4.9 which should be read in conjunction with Fig.3.5.

Table 4.8. One Dimensional Consolidation Properties of the Representative Samples

Sample No.	Specimen No.	Depth	Depth of layer	Depth ratio	m_{v1} in 10^{-5} ft^2/lb		C_{v1} in 10^{-5} ft^2/min	
					Sample	Average for the layer	Sample	Average for the layer
S-2	S-2a S-2b	16'9" to 18'3"	10'0" to 30'0"	0.375	1.06	1.077	15.2	15.295
S-4	S-4a S-4b	36'0" to 37'6"	30'0" to 45'0"	0.47	1.023	1.077	285.5	249.5

Table 4.9. Test Program for Sample Nos. S-2 and S-4 (Fig.3.5)

Sample No.	Existing effective O.B. press. P' in psi	Neutral Pressure u_o in psi.	Increment in vertical press. due to foundation loading $\Delta\sigma_v$ in psi.	Increment in horizontal pressure due to foundation loading $\Delta\sigma_h = \Delta\sigma_{h1} = \Delta\sigma_{h2}$ in psi.
S-2	12.37	2.82	13.39	6.93
S-4	20.35	11.28	6.74	0.76

In addition to the samples for stress-path testing, two samples one from each of the two layers were tested for the determination of K_o and pore-pressure parameter A. The samples are designated S-1 which was taken from a depth of 11'6" to 12'6" below ground level and S-3 which was taken from a depth of 34'3" to 35'6" below ground level.

Apart from the experimental determination, the coefficient of earth pressure at rest, K_o' was also determined from the over consolidation ratio and the Atterberg limits values using the empirical relationship given by Brooker and Ireland (1965) and Sherif and Koch (1970). Brooker and Ireland related K_o with OCR and the plasticity index whereas Sherif and Koch related K_o with OCR and liquid limit. The relationship presented by Brooker and Ireland is shown in Fig. 4.2. According to Sherif and Koch the coefficient of earth pressure at rest may be expressed as

$$K_o' = \lambda + \alpha \,(\mathrm{OCR}-1) \qquad 4.7$$

$$\text{where } \log \lambda = 0.00275\,(\mathrm{LL}-20) + \log\,(0.54) \qquad 4.8$$

$$\text{and } \log \alpha = 0.00745\,(\mathrm{LL}-20) + \log\,(0.08) \qquad 4.9$$

The values of K_o' obtained by using these relationship and experimental test results is presented in Table 4.10. The OCR values for calculating K_o' from the emperical formulae was judged from those presented in Table 4.5.

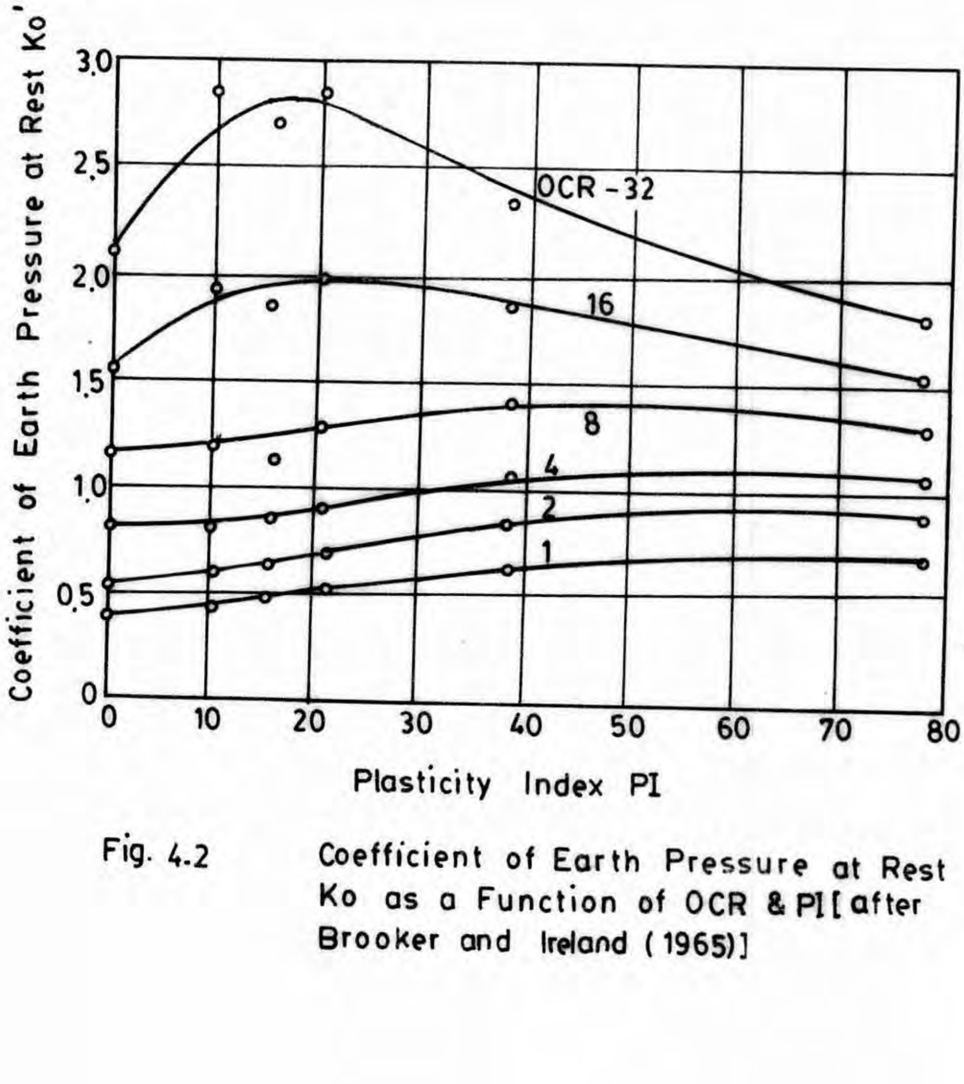

Fig. 4.2 Coefficient of Earth Pressure at Rest Ko as a Function of OCR & PI [after Brooker and Ireland (1965)]

Table 4.10 The Coefficient of Earth Pressure at Rest, K'_o

Sample No.	Depth	OCR	K'_o (Brooker and Ireland 1965)	K'_o (Sherif and Koch 1970)	K'_o (from experiment)
	7'6" to 9'0"	5.0	0.9	1.11	-
	9'6" to 11'0"	5.0	0.95	1.14	-
S-1	11'6" to 12'6"	4.0	0.85	0.99	0.69
	13'0" to 14'6"	3.6	0.80	0.93	-
S-2	16'9" to 18'3"	3.0	0.80	0.83	0.70
	26'3" to 27'6"	1.4	0.65	0.69	-
	28'6" to 29'6"	1.4	0.6	0.67	-
	30'0" to 31'6"	2.0	0.7	0.73	-
S-3	34'3" to 35'6"	2.0	0.65	0.73	0.60
S-4	36'0" to 37'6"	1.75	0.6	0.69	0.58
	39'9" to 41'3"	1.5	0.58	0.65	-

The values of K_o' obtained from experimental results were found to be lower than those obtained from empirical relationships.

The pore-pressure parameter A was obtained from results of stress path tests on samples S-2 and S-4. Undrained compression test with pore-pressure measurement was performed on samples S-1 and S-3 to obtain the value of A. The values obtained for the four samples are presented in Table 4.11.

Table 4.11. Pore-Pressure Parameter A

Sample No.	S-1	S-2	S-3	S-4
Pore-pressure parameter A	0.47	0.435	0.59	0.616

From the values of applied stresses and measured strains during stress-path tests the elastic settlement parameters were calculated for all the four specimens and are presented in Table 4.12.

4.5 Summary of Test Results

From the physical properties, consistency and consolidation characteristics a fairly accurate conclusion could be made that the subsoil from 10' below ground level to 45' below ground level is composed of two distinct layers. The layer, which may be termed as Layer A extends from 10' to 30' below ground level.

Table 4.12. Three-dimensional Settlement Parameters from Stress-Path Tests

Sample No.	Specimen	Axial strain due und. loading ϵ_{1u} in 10^{-3} in/in	Axial strain due to consolidation ϵ_{1c} in 10^{-3} in/in.	Undrained Elastic modulus E_u psi.	Drained Elastic modulus E' psi.	Drained Poisson's ratio ν'	Cofficient of consolidation (3 Dimn.) C_{v3} in 10^{-5} ft^2/min.
S-2	S-2a	7.17	10.46	901	476	0.36	9.03
	S-2b	7.32	11.10	883	441	0.38	11.07
S-4	S-4a	2.17	5.68	2758	801	0.30	157.00
	S-4b	2.23	5.43	2678	818	0.31	169.00

This layer can be classified as silty clay of low to medium plasticity (CL-group). The other layer, which may be termed as layer B extends from 30' to 45' below ground level. This layer can be classified as clayey silt having low plasticity (ML-group) (Fig. 4.3).

A check in the OCR values show that layer A is composed of soil which is slightly to moderately overconsolidated. Soils from layer B showed lesser degree of overconsolidation and may be termed as slightly overconsolidated. The OCR values showed the general tendency of decrease with depth.

The average physical and consolidation properties for the two layers are summarized in Tables 4.13 and 4.14.

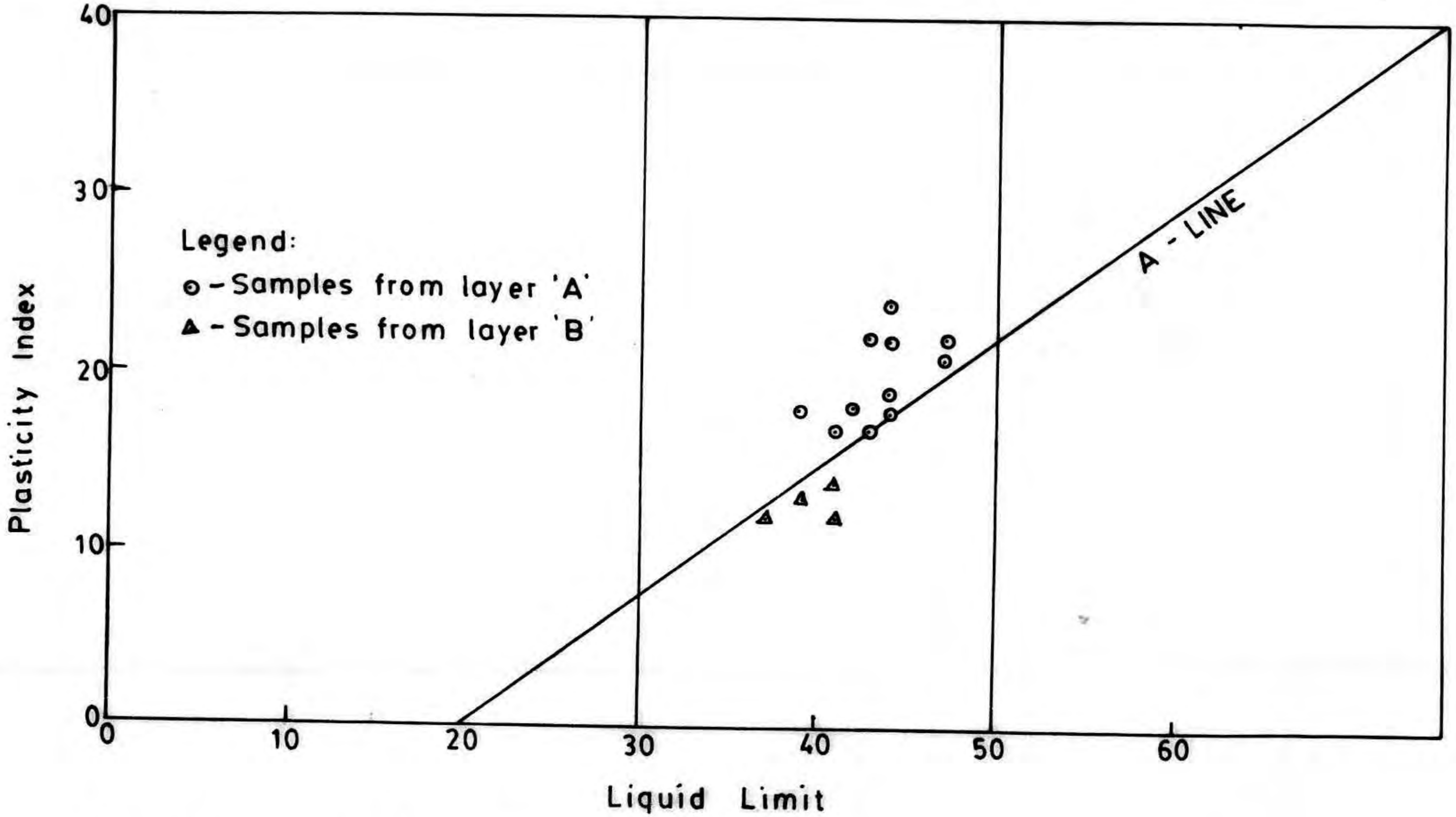

Fig 4.3 Plasticity Chart

Table 4.13 . Summary of Physical Properties

Layer	L.L.	P.L.	P.I.	Clay content %	Activity	Group symbol
A	44	24	20	15.0	1.33	CL
B	40	27	13	8.0	1.63	ML

Table 4.14. Summary of Consistency and Consolidation Characteristics

Layer	S_u psf	m_{v1} in $10^{-5} ft^2/lb$	C_{v1} in $10^{-5} ft^2/min.$	K'_o	A	E_u psi form CIU test	E_u psi from stress-path test	E' psi	ν'	C_{v3} in 10^{-5} ft^2/min	OCR range
A	1500	1.077	15.25	0.70	0.45	876	892	459	0.37	10.04	1.4 to 5
B	1000	1.077	249.50	0.59	0.60	1610	2718	810	0.31	163.00	1.5 to 2

CHAPTER V

ANALYSIS OF SETTLEMENT

5.1 General

A flexible circular permeable foundation forty feet in diameter and founded at a depth of ten feet below ground level was considered for the analysis of settlement. The net soil pressure at the base of the foundation was choosen as 2016 psf (14 psi) which offered a factor of safety of more than four against a general shear failure and a factor of safety of more than two against initiation of local yield in the soil mass (Fig. 2.5).

To calculate the distribution of stresses due to foundation loading the elastic stress distribution theory was used which considers the soil as a homogeneous, isotropic, elastic semi-infinite continuum. By the elastic theory the vertical and horizontal stresses developed along the centre line of a uniformly loaded flexible circular area is given by equations

$$\Delta\sigma_v = p\left[1 - \left(\frac{1}{1+(r/z)^2}\right)^{3/2}\right] \qquad 5.1$$

and $$\Delta\sigma_h = \frac{p}{2}\left[1 + 2\nu - 2(1+\nu)\left(\frac{z}{\sqrt{(r^2+z^2)}}\right) + \left(\frac{z}{\sqrt{(r^2+z^2)}}\right)^{3/2}\right] \qquad 5.2$$

where $\Delta\sigma_v$ and $\Delta\sigma_h$ are net increase in vertical andhorizontal stresses respectively due to foundation loading.

p = load/unit area at the base of the foundation

r = radius of the foundation

z = depth below foundation level

ν = Poisson's ratio of the soil; taken equal to 0.5 for saturated clays under undrained condition.

The stress distribution due to foundation loading was also determined by the sector method presented by Poulos (1967a, 1967b) in which sector influence factors are used to calculate stresses. By the sector method the vertical and horizontal stresses are given by the equation

$$\Delta\sigma = \frac{p}{2\pi} \cdot I \qquad 5.3$$

where I is the influence factor appropriate for the stress component required.

For vertical stresses beneath the centre of a uniformly loaded circular foundation

$$I = 2\pi \, I_{sa} \qquad 5.4$$

where I_{sa} is the sector influence factor for vertical stresses for a sector radius equal to the radius of the circular foundation. For horizontal stresses beneath the centre of a uniformly loaded circular foundation

$$I = \pi \left[{}_{\sigma r}I_{sa} + {}_{\sigma\theta}I_{sa} \right] \qquad 5.5$$

where ${}_{\sigma r}I_{sa}$ and ${}_{\sigma\theta}I_{sa}$ are the sector influence factors for the tangential and bulk stresses respectively for a sector radius equal to the radius of the circular foundation. The sector influence factors were obtained from those presented by Poulos. This method presented results almost identical to those obtained by using Eqs. 5.1 and 5.2.

The distribution of vertical and horizontal stresses due to foundation loading and the distribution of existing effective overburden pressure along the centre line of the foundation is presented in Fig. 5.1.

In order to establish some form of relationship among a number of settlement parameters the results of oedometer consolidation test presented in Chapter IV was used. A plot of compression index, C_{CL} versus initial void ratio e_o is presented in Fig.5.2 from which the following equation was derived

$$C_{CL} = 0.44\ (e_o - 0.36) \qquad 5.6$$

which may be compared to similar relations obtained by Nishida (1956) and Sirajuddin and Ahmed (1967).

Nishida (1956) obtained the relationship as

$$C_{CL} = 0.54\ (e_o - 0.35) \qquad 5.7$$

whereas Sirajuddin and Ahmed (1967) obtained the relationship as

$$C_{CL} = 0.44\ (e_o - 0.30) \qquad 5.8$$

A plot of compression ratio, $\frac{C_{CL}}{1 + e_o}$ versus the initial void ratio e_o is presented in Fig. 5.3.

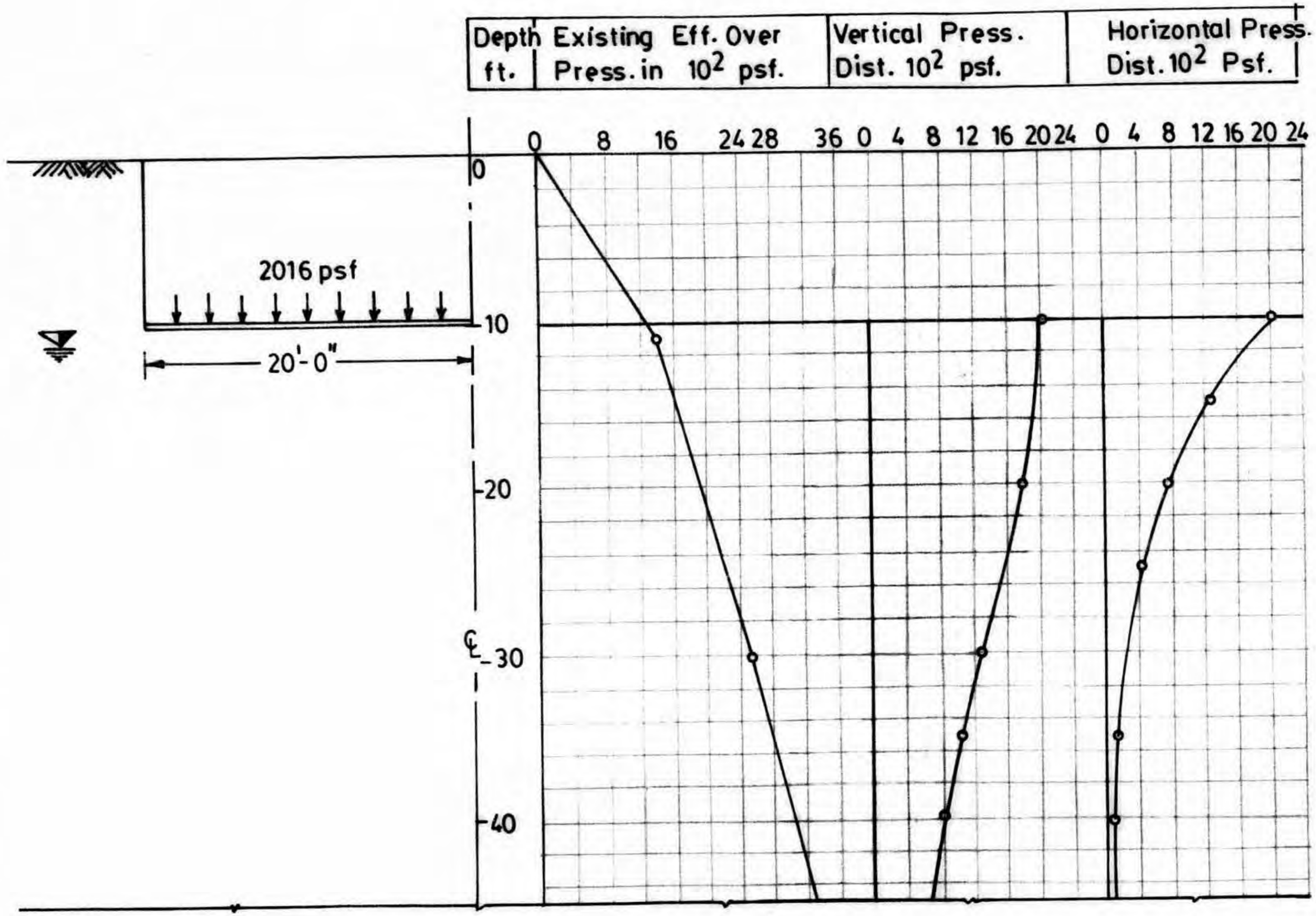

Fig. 5.1 Pressure Distribution Along the Centre Line of the Foundation

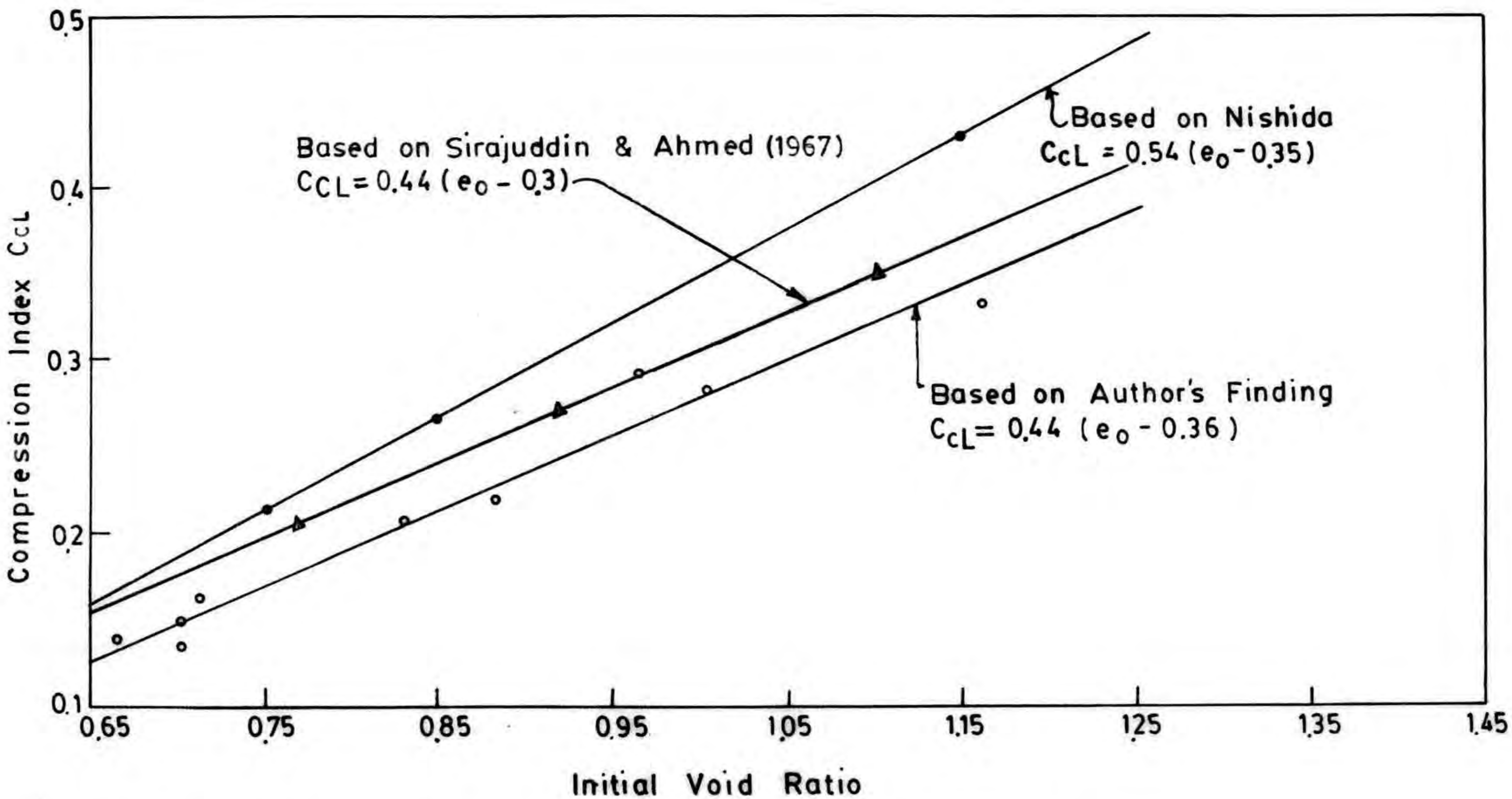

Fig. 5.2 Compression Index C_{cL}, Vs Initial Void Ratio, e_o, Plot

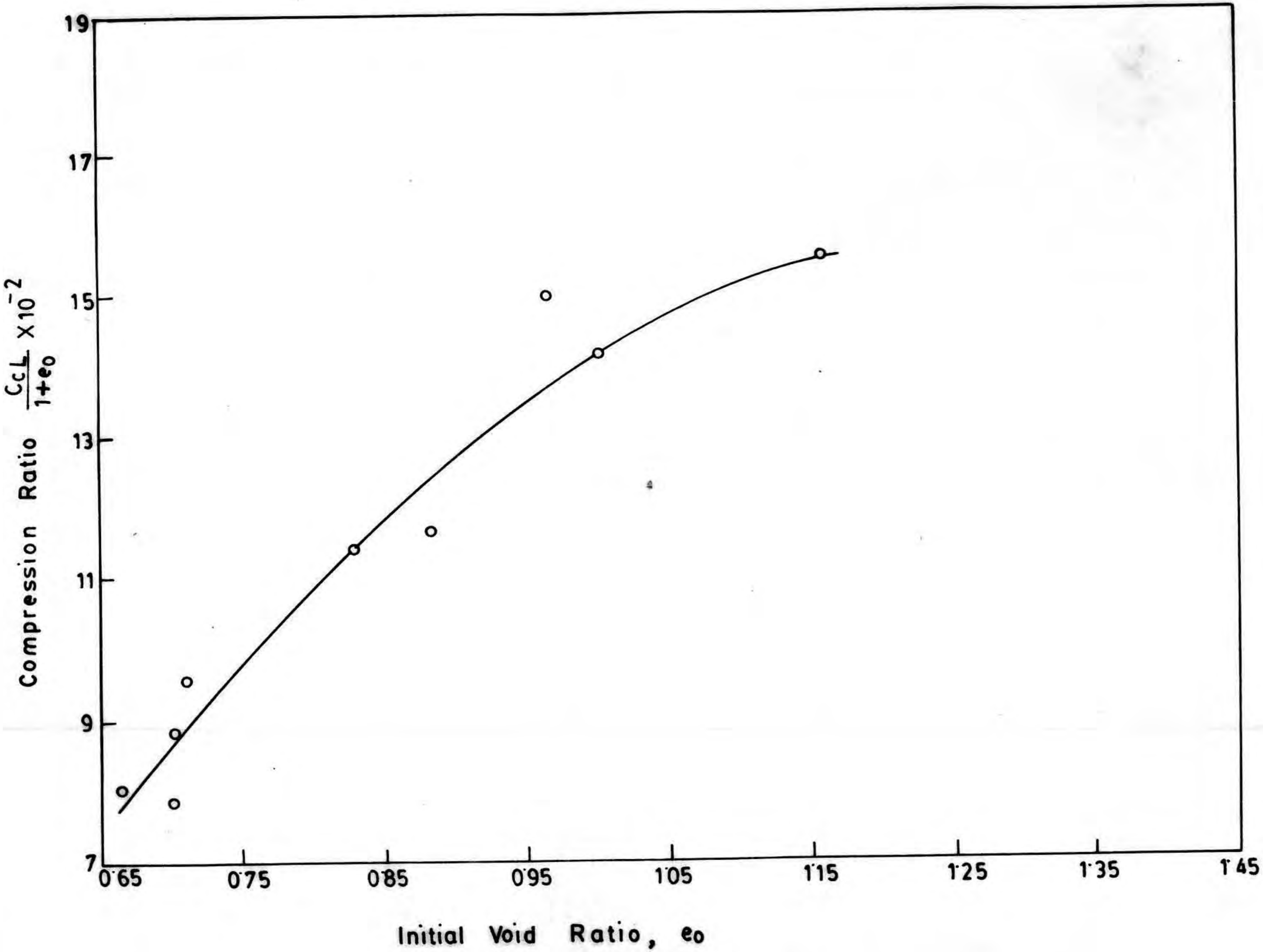

Fig. 5.3 Compression Ratio Vs Initial Void Ratio Plot.

5.2 Field Stress-Paths

Field stress-paths for the two samples designated S-2 and S-4 were determined using the values of K_o', pore-pressure parameter A (B was assumed equal to 1) and the pressure distribution obtained from the elastic theory. The effective and total stress-paths due to foundation loading for the two samples designated S-2 and S-4 is presented in Figs. 5.4 and 5.5 respectively. The in-situ state of effective stresses is represented by point A on the plot of vertical stress versus horizontal stress. Due to the application of foundation pressure under undrained condition the state of effective stress moves from point A to point B. During this process the effective vertical pressure increases but the effective horizontal pressure decreases due to development of pore-water pressure in the soil sample. The effective stress-path during this stage of undrained loading is given by line AB. As the sample starts to consolidate the stress-state moves from point B towards point C causing both the effective vertical and horizontal stress to increase by the amount equal to the magnitude of the pore-water pressure that is dissipated. After full consolidation i.e. full dissipation of excess porewater pressure the stress-point is at C and the effective stress-path due to consolidation of the sample is given by BC. The combined effective stress-path due to undrained loading and subsequent consolidation is given by ABC whereas the total stress point moves straight from point

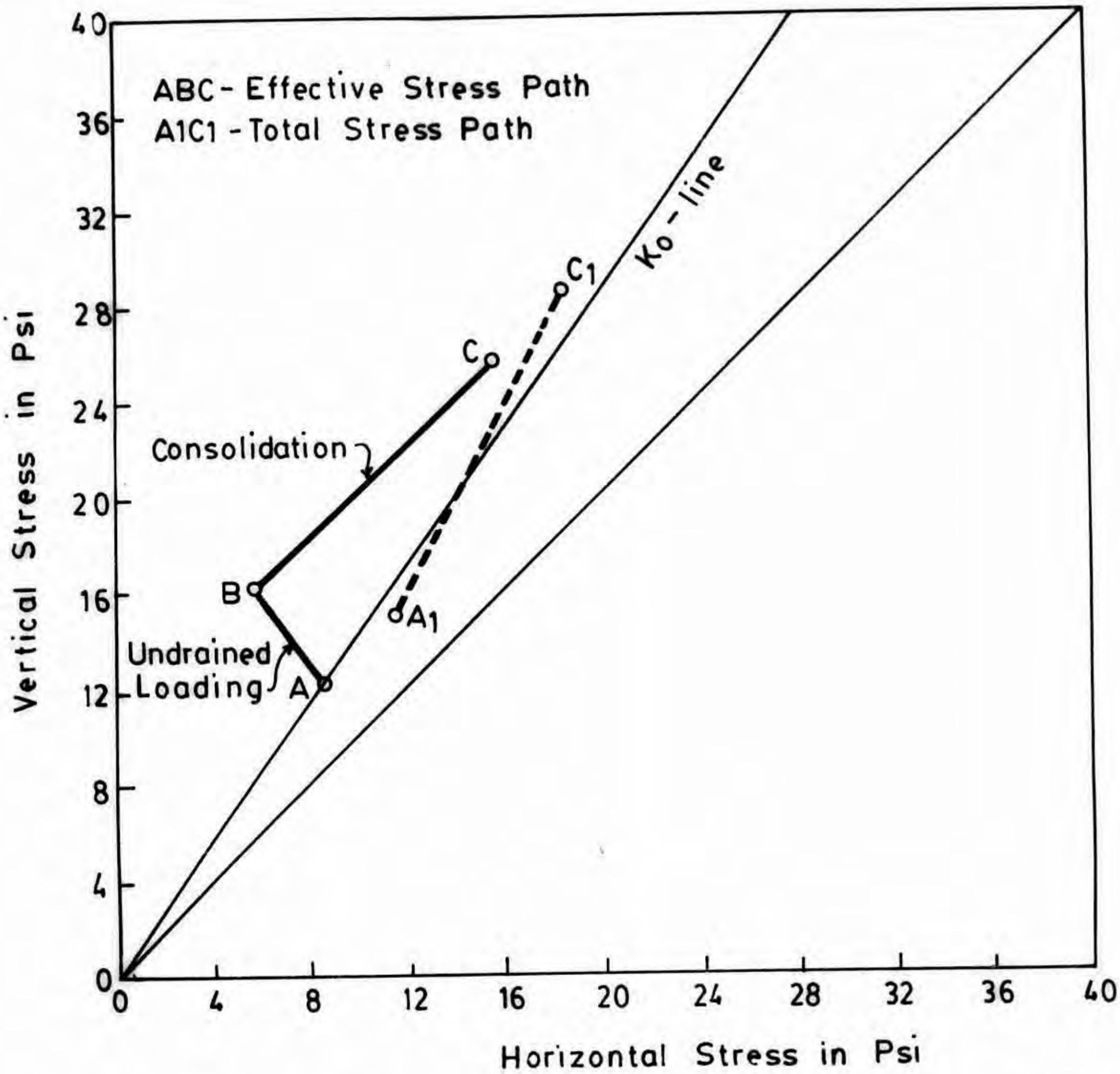

Fig. 5.4 Stress Path During Drained and Undrained Loading of Sample No. 2

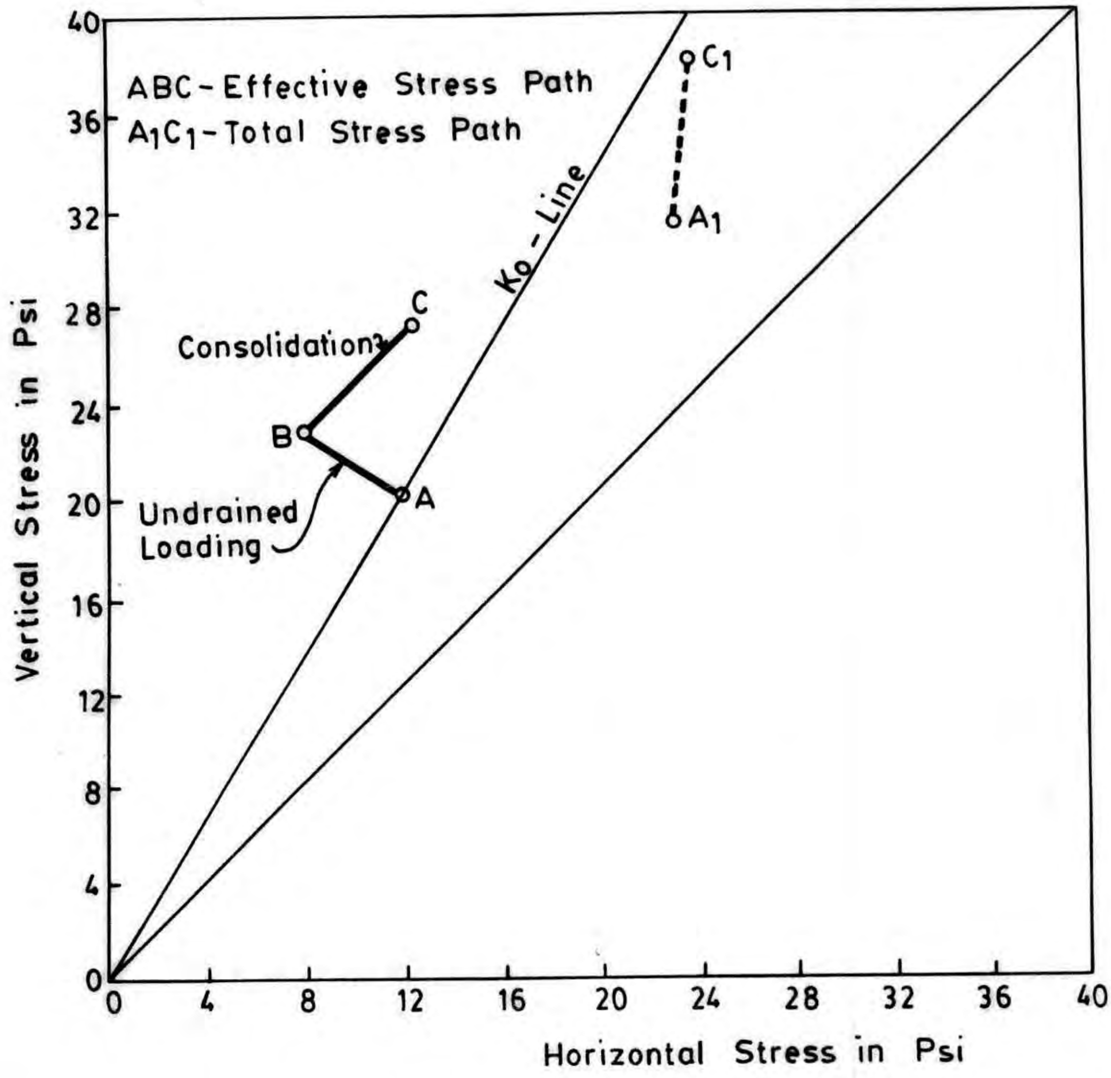

Fig. 5.5 Stress Path During Undrained and Drained Loading of Sample No. 4

A_1 to C_1 giving the total stress-path A_1C_1. The effect of change in horizontal stress-due to change in Poisson's ratio from the undrained value of $\nu = \nu_u = 0.5$ to $\nu = \nu'$ was neglected in this study.

5.3 Initial or Immediate Settlement

In the conventional and Skempton and Bjerrum methods the average immediate settlement was calculated from Eqs. 2.4 and 2.5. The average values of the undrained modulus E_u determined from CIU triaxial compression tests was obtained as 876 psi for layer A and 1610 psi for layer B. By using the principle of superposition in a manner presented by Simons and Menzies(1975) the contribution to the total average immediate settlement from each of the layer A and B was calculated. The immediate settlement at the centre of the flexible circular foundation was calculated using the following equation (Terzaghi 1943).

$$S_{u\ centre} = \frac{S_{u\ ave}}{0.85} \qquad 5.9$$

In the Davis and Poulos method the immediate settlement for the two layer system was calculated by using Eq. 2.20 which reduced to the form

$$S_u = \frac{1}{E_u} \int_0^z (\Delta\sigma_v - \Delta\sigma_h)\, dz \qquad 5.10$$

as in case of a circular loaded area $\sigma_x = \sigma_y = \Delta\sigma_h$

The average values of the undrained modulus E_u was determined from stress-path tests and was obtained as 892 psi for layer A and 2718 psi for layer B.

In the stress-path method the immediate settlement for the layer A and B was obtained by direct multipication of the axial strain due to undrained loading by the layer thickness under consideration. For layers A and B the average values of the axial strain due to undrained loading was calculated as 7.245×10^{-3} in/in and 2.2015×10^{-3} in/in respectively.

A summary of the magnitude of immediate settlement obtained by the different methods is presented in Table 5.1.

Table 5.1. Magnitude of Immediate Settlement at Centre of Foundation, S_u in ins.

Method / Layer	Conventional	Skempton and Bjerrum	Davis and Poulos	Stress-path
A	2.38	2.38	1.66	1.74
B	0.51	0.51	0.39	0.4
Total	2.89	2.89	2.05	2.14

5.4 Primary Consolidation Settlement

For the calculation of primary consolidation settlement by the conventional method Eq. 2.2 was used. To make the computation convenient layer A was divided into two layers A_1 and A_2 thus the whole stratum was divided into three layers viz A_1, A_2 and B and an average value of m_{v1} was assigned to each of three layers. The average value of m_{v1} for layer A_1 was obtained as 1.274×10^{-5} ft^2/lb and those for layers A_2 and B was obtained as 0.683×10^{-5} ft^2/lb and 1.077×10^{-5} ft^2/lb respectively.

In the Skempton and Bjerrum method Eq. 2.10 was used to determine the magnitude of primary consolidation settlement. The average value of the porewater pressure parameter A was calculated as 0.525 and with $\frac{H}{B}$ = 0.875 the value of coefficient μ was obtained equal to 0.7 from curves presented in Fig. 2.3.

The total final settlement by the Davis and Poulos method was calculated by using Eq. 2.18 which for a circular loaded area took the form

$$S_{TF} = \frac{1}{E'} \int_0^z (\Delta\sigma_v - 2\nu' \Delta\sigma_h) \, dz \qquad 5.11$$

as in this case $\sigma_x = \sigma_y = \Delta\sigma_h$

Average values of the elastic parameters E' and ν' were obtained for both the layers A and B. The average value of E' the modulus under drained condition was obtained as 459 psi and 810 psi for layers A and B respectively. The average value of Poisson's ratio ν' under drained condition was obtained as 0.37 and 0.31 for layers A and B respectively. The magnitude of primary consolidation settlement for each of the layers was obtained by subtructing the immediate settlement from the total final settlement for the layer under consideration.

In the stress-path method the primary consolidation settlement for each of the layers A and B was obtained by direct multiplication of the layer thickness with the axial strain during consolidation obtained from stress-path tests. The average axial strain during consolidation for the layers A and B was obtained as 10.78×10^{-3} in/in and 5.555×10^{-3} in/in respectively.

The magnitude of the primary consolidation settlement for the two layers under consideration, as obtained from different methods, is presented in Table 5.2.

Table 5.2. Magnitude of Primary Consolidation Settlement S_{CF} in ins. at the Centre of Foundation

Method / Layer	Conventional	Skempton and Bjerrum	Davis and Poulos	Stress-path
A	4.49	-	2.40	2.59
B	1.87	-	1.01	1.00
Total	6.36	4.45	3.41	3.59

5.5 Total Final Settlement

The total final settlement for each layer was calculated by adding the immediate and the consolidation settlement and that for the whole stratum was calculated by adding the contributions from each of the two layers. A summary of the magnitude of different settlement components obtained from different methods of settlement analysis is presented in Table 5.3.

5.6 Time Rate of Primary Consolidation Settlement

The one-dimensional consolidation theory was used to determine the time rate of settlement by the conventional and Skempton and Bjerrum method. For the calculation of time rate of settlement by these methods the whole strata was considered as a two layer system. The average values of C_{v1} for layers A and B were obtained as 15.25×10^{-5} ft^2/min and 249.5×10^{-5} ft^2/min respectively. An approximate method of analysis (NAVDOCKS DM-7) was used to determine the time rate of consolidation of the individual layers A and B as well as the combined layer. Fig. 5.6 shows the time-settlement relationship for the individual layers as well as the combined layer obtained in this manner.

The time rate of settlement under three dimensional condition was obtained by using the curves presented by Davis and Poulos (1972) which represents the solution of Eq. 2.38 for different drainage conditions. The curves which are similar to those presented in Fig. 2.10 were obtained for a circular footing of radius a resting on an elastic stratum of thickness h and Poisson's ratio $\nu = 0.5$. The curves relate, degree of settlement U_s with the logarithm of time factor T_v for different values of h/a ratio where, T_v is defined by

Table 5.3 Magnitude of Settlement by Different Methods

Method / Layer / Settlement	Conventional Eq. 2.1			Conventional Eq. 2.3			Skempton and Bjerrum			Davis and Poulos			Stress Path		
	A	B	Comb.	A	B	Comb.	A	B	Comb.	A	B	Comb.	A	B	Comb.
Immediate S_u ins.	0	0	0	2.38	0.51	2.89	2.38	0.51	2.89	1.66	0.39	2.05	1.74	0.40	2.14
Consolidation S_{CF} ins.	4.49	1.87	6.36	4.49	1.87	6.36	-	-	4.45	2.41	1.00	3.41	2.59	1.00	3.59
Total S_{TF} ins.	4.49	1.87	6.36	6.87	2.38	9.25	-	-	7.34	4.07	1.39	5.46	4.33	1.40	5.73

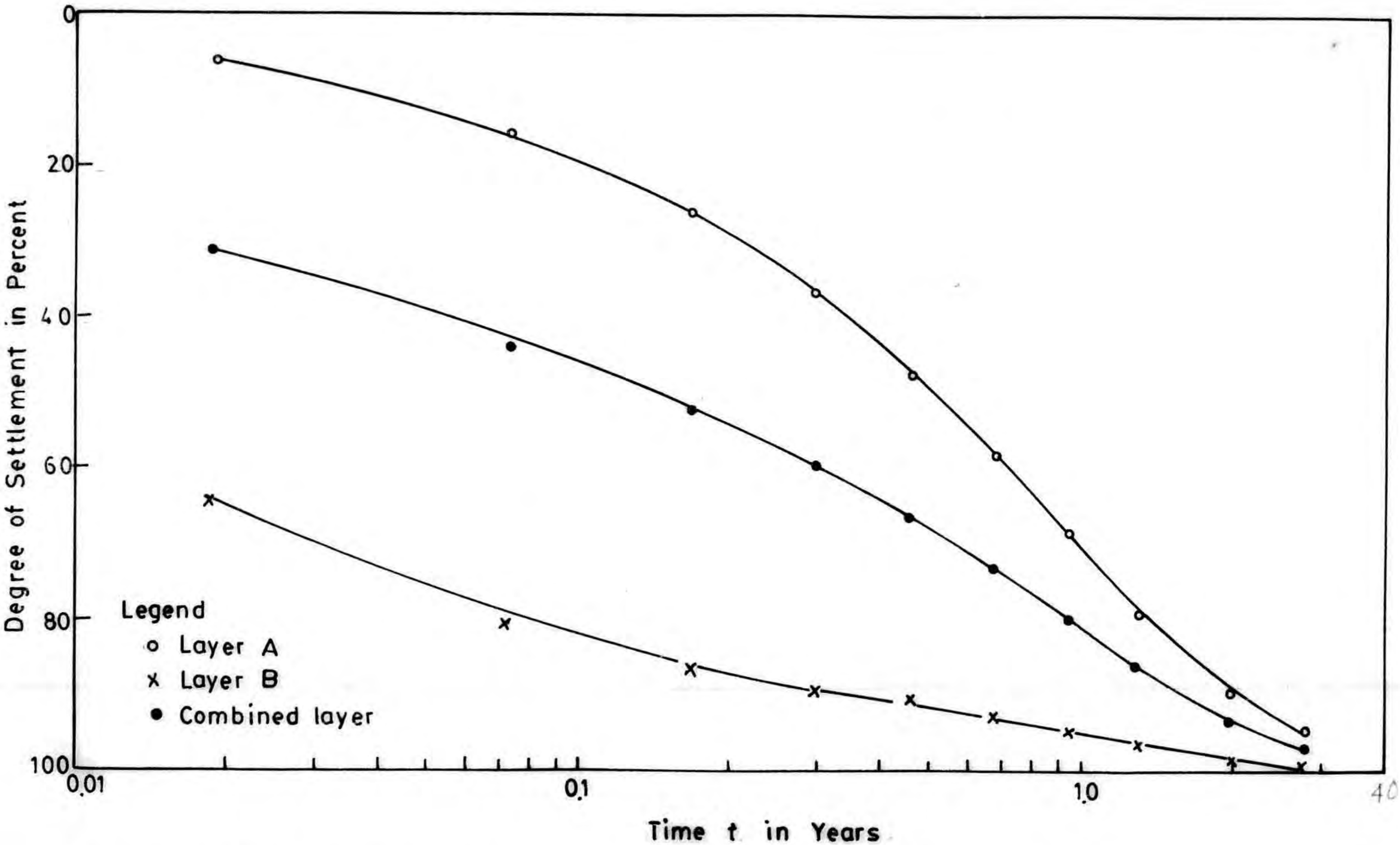

Fig. 5.6 Time Consolidation Curves Under One Dimensional Condition

$$T_v = \frac{C_{v1}\ t}{h^2} \tag{5.12}$$

where C_{v1} = one-dimensional coefficient of consolidation

h = full stratum depth

t = time

The solutions presented are for $\nu = 0.5$. For other values of Poisson's ratio Davis and Poulos writes that with T_v defined in terms of C_{v1}, the effect of ν on the degree of settlement is not very great, amounting to a maximum of 18% to the degree of settlement.

The same basis of solution as used under the one-dimensional condition was used in the solution of the rate of settlement of the two layer system under three-dimensional condition. The time settlement curves for the individual layers as well as the combined layer, under three-dimensional condition is presented in Fig. 5.7. In the Davis and Poulos and Stress-path method the three-dimensional consolidation theory was used to predict the time rate of settlement.

To compare the time rate of settlement obtained by the one-dimensional and the three-dimensional consolidation theories the time settlement relationship for the combined layer obtained from the two theories are presented in Fig. 5.8.

Finally the time settlement relation showing the progress of settlement with time by the different methods of settlement analysis was obtained which is presented in Fig. 5.9.

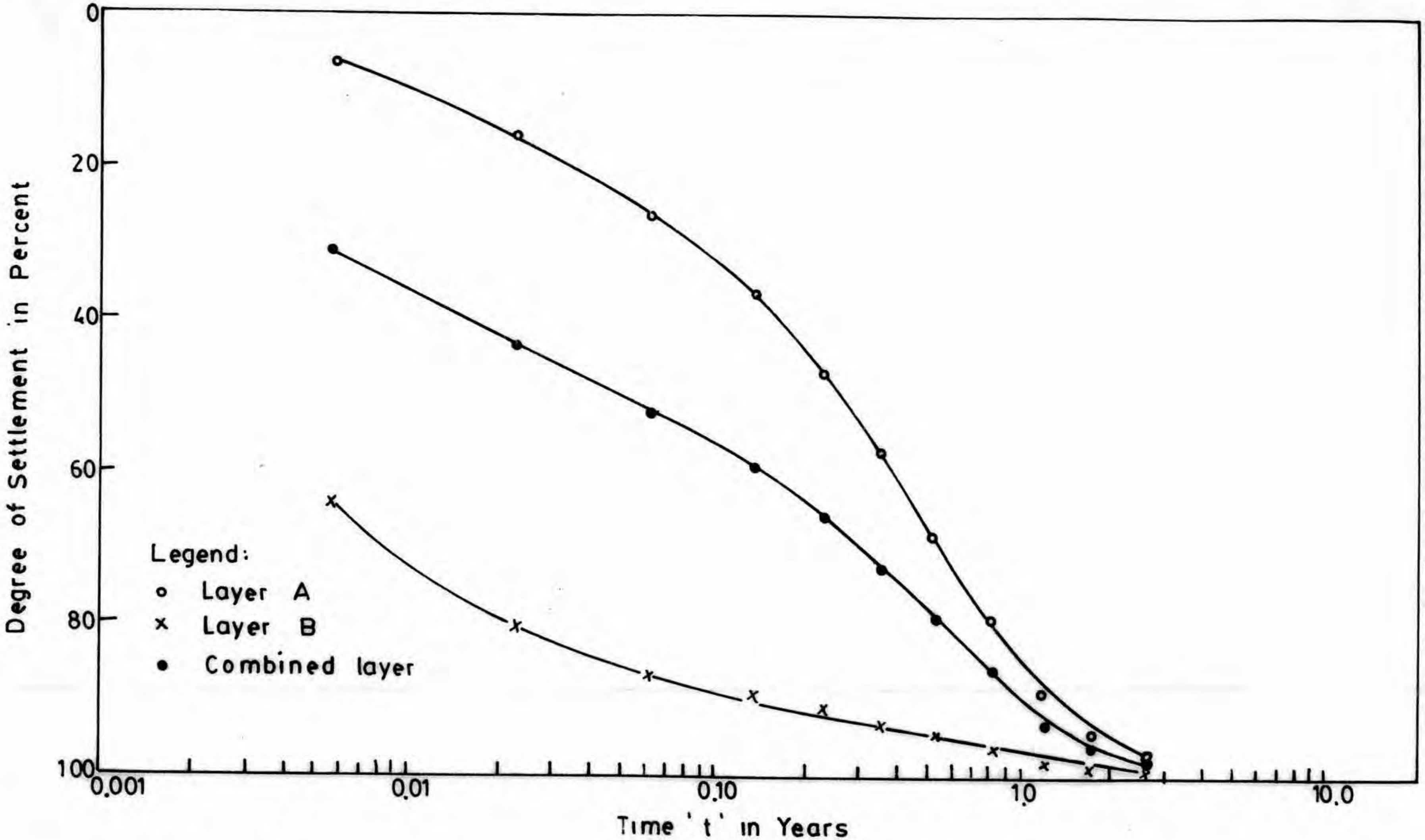

Fig. 5.7 Time - Consolidation Curves Under Three-Dimensional Conditions

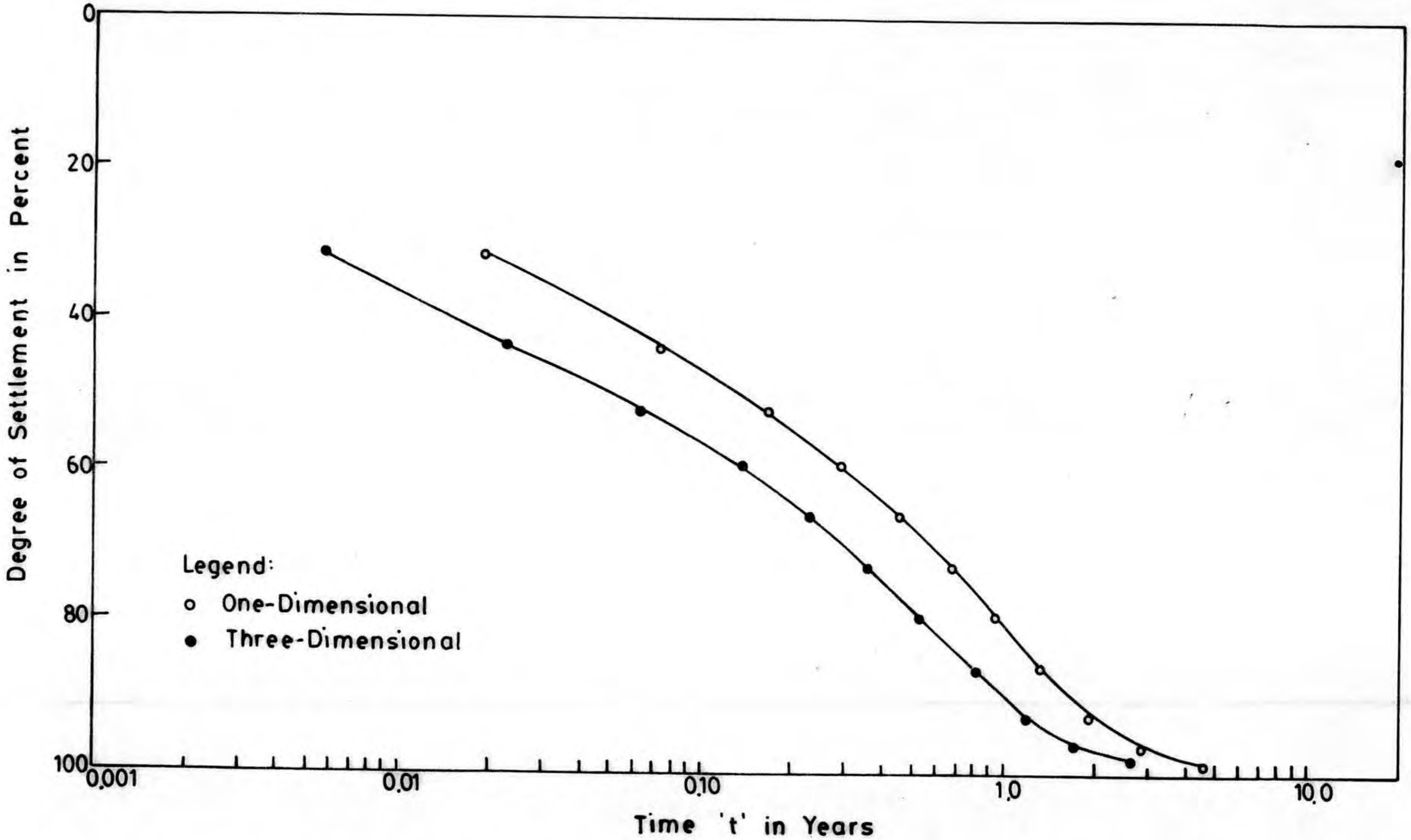

Fig. 5.8 Comparison of Time-Rate of Settlement Under One-and Three-Dimensional Conditions

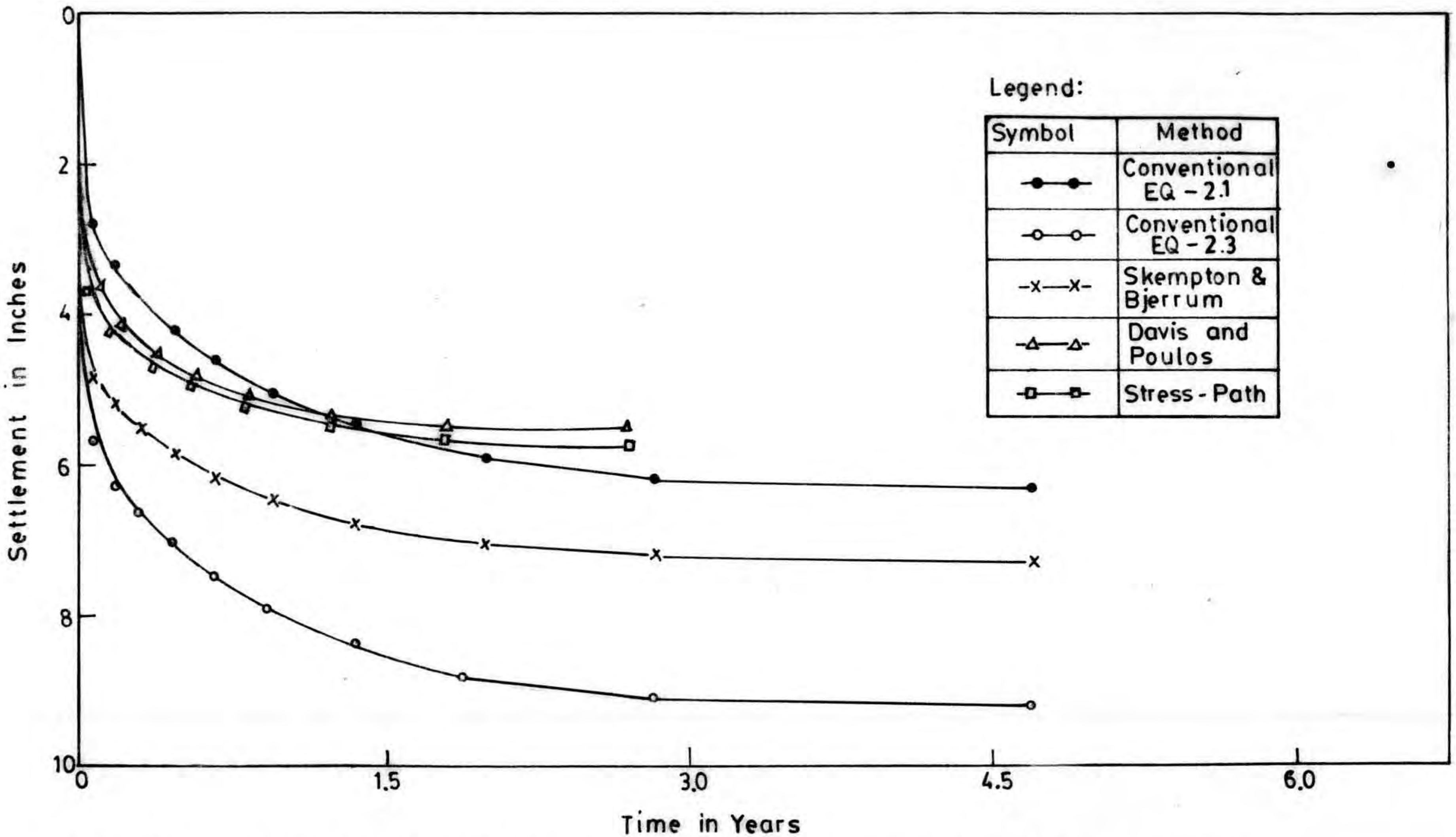

Fig. 5.9 Time-Settlement Curves by Different Methods of Settlement Analysis

5.7 Effect of Sample Disturbance

To study the effect of sample disturbance on the magnitude of primary consolidation settlement obtained by the conventional method, a method suggested by Schmartmann (1955) was used. Field e-log p relations were reconstructed from laboratory e-log p curves in a manner suggested by Schmartmann. The magnitude of primary consolidation settlement was then calculated from the field curves by the equations (Casagrande 1964),

$$S_{CF} = \frac{H}{1 + e_o} C_{CR} \log_{10} \frac{\bar{p}_o + \Delta p}{\bar{p}_o} \qquad 5.13$$

for $\bar{p}_o + \Delta p \leqslant \bar{p}_c$

and

$$S_{CF} = \frac{H}{1 + e_o} \left[C_{CR} \log_{10} \frac{\bar{p}_c}{\bar{p}_o} + C_{CF} \log_{10} \frac{\bar{p}_o + \Delta p}{\bar{p}_c} \right] \qquad 5.14$$

for $\bar{p}_o + \Delta p > \bar{p}_c$

where H is the thickness of the layer under consideration

Δp is the net increase in vertical pressure.

Using the OCR values obtained by the graphical method presented by Schmartmann and from the consolidation properties presented in Table 4.7, the magnitude of primary consolidation settlement was obtained as 2.41 in compared to 6.36 in obtained from laboratory curves.

5.8 Discussion on Test Results

As already pointed out in Chapter II, very little information is available to compare the stress path method with the other methods of settlement analysis for structures on heavily O.C. clay and even fewer data are available for structures on N.C. and slightly O.C. clays (Simons 1974).

Simons (1971) presented a comparison between the stress path method, the Skempton and Bjerrum method and the Conventional Method for a forty feet diameter flexible foundation established at twenty feet below ground level in heavily O.C. London clay. He concluded that "the actual stress path for an element of soil beneath a foundation in the field is in general quite different from that implied in standard methods of settlement computation based on the oedometer test. Since the axial deformation of an element of soil is dependent on the stress path followed, standard methods of settlement analysis cannot be expected to yield accurate predictions".

Lambe (1973) presented settlement studies on N.C. clay for the North-East Test Embankment. The test embankment was constructed on a thick layer of N.C. Boston Blue Clay. A comparison showed that in case of initial settlement there was closer agreement between the observed and predicted value by the conventional method while in case of primary consolidation settlement stress-path method gave better result.

A comparison of the total final settlement revealed that the elastic methods based on stress-path tests and the conventional method by Eq. 2.3 did not differ greatly. Lambe did not make any comment on the predicted and observed values of the total final settlement as the three settlement plates planted under the embankment offered very large differences in the observed primary consolidation settlement, which could not be explained. However, he opined that some of these discrepencies may be attributed to the large scatter in soil properties.

The foundation material in this study comprises a layer of slightly to moderately O.C. silty clay underlain by a layer of slightly O.C. clayey silt. Comparing the results obtained in this investigation with those obtained by Simons and Lambe, it is found that it fits well in between the two extreme cases of heavily O.C. London Clay and N.C. Boston Blue Clay. A comparison of the ratio of the different components of settlement obtained by the stress path method with those by the other methods for the three cases is presented in Table 5.4.

From the comparison presented it can be observed that the ratio obtained in this investigation for the lightly O.C. clay silt is always in between those obtained for heavily O.C. London Clay and N.C. Boston Blue Clay, except for the case of initial settlement. Lambe obtained a ratio of 1.22 for the initial settlement calculated by the conventional method to the observed value.

Table 5.4. Comparison of the Settlement Ratio Obtained by Simons, Lambe and the Author

Case	$\frac{S_{UCON}}{S_{USP}}$	$\frac{S_{CFCON}}{S_{CFSP}}$	$\frac{S_{CFSB}}{S_{CFSP}}$	$\frac{S_{TFCON}}{S_{TFSP}}$ Eq. 2.1	$\frac{S_{TFCON}}{S_{TFSP}}$ Eq. 2.3	$\frac{S_{TFSB}}{S_{TFSP}}$
Simons H.O.C. London Clay	1.9	2.7	1.9	1.9	2.4	1.9
Author Lightly O.C. Clay-silt	1.35	1.77	1.24	1.10	1.61	1.28
Lambe N.C. B.B.C	4.35	0.85	0.72	0.83	0.97	0.84

Notations:

S_{UCON} - Immediate settlement by Conventional Method

S_{CFCON} - Primary consolidation settlement by Conventional Method

S_{TFCON} - Total final settlement by Conventional Method

S_{CFSB} - Primary consolidation settlement by Skempton and Bjerrum Method

S_{TFSB} - Total final settlement by Skempton and Bjerrum Method

S_{USP} - Immediate settlement by stress-path method

S_{CFSP} - Primary consolidation settlement by stress-path method

S_{TFSP} - Total final settlement by stress-path method

Upto the local yield stress level the elastic method by Davis and Poulos and the stress path method are based on almost similar assumptions and it is expected that results obtained by these methods should not differ greatly provided the choice of 'average point' and representative depth' really represent the field condition. The values in Table 5.3 show that the agreement between the settlement by these two methods are very good.

From the range of literature reviewed by the author, except for the case of initial settlement of the test embankment described by Lambe (1973), the stress path method has been accepted to be more reliable and sophisticated compared to the other methods of settlement analysis. However, Lambe (1973) warned that the Engineer should not only be influenced by the sophistication of his predicting techniques but there are other factors like, quality of test data which may more than offset the sophistication of a technique and in such cases less sophisticated techniques may yield better results. The quality of test data depends on the degree of sample disturbances, sophistication of laboratory equipments and experience and skill of the laboratory technician.

In almost all the cases reviewed in this study the observed rate of settlement was found to be faster than the rate predicted by the conventional one-dimensional theory (Art.2.6). Very limited test data was available which presented relation between observed rate and that predicted by the three-dimensional theory. Davis and Poulos (1968, 1972) presented results of model footing tests which showed that the three-dimensional theory predicted reasonably accurately the observed rate of settlement. In this study a faster rate was obtained by the three-dimensional theory compared to that by the one-dimensional theory, so it is more likely that the actual rate of settlement will be closer to that obtained by the three-dimensional theory.

CHAPTER VI

CONCLUSIONS
AND
RECOMMENDATIONS FOR FUTURE RESEARCH

6.1 Conclusions

From the analysis and discussion of test results on the lightly O.C. clay layers investigated inthis study, the following conclusions may be drawn:

(i) The Conventional Methodsis likely to overestimate the actual immediate settlement in the field. It overestimated the immediate settlement by stress path and Davis and Poulos method by about 35 percent in this case.

(ii) The Skempton and Bjerrum method is likely to overestimate and the Conventional Method is likely to very much overestimate the actual field primary consolidation settlement. Primary consolidation settlement obtained by these methods were higher than that by stress path method by 24 and 77 percent respectively in this case.

(iii) The Conventional Method by Eqn. 2.1 is likely to overestimate and that by Eqn. 2.3 very much overestimate the actual total final settlement. These methods overestimated the total final settlement by 11 and 61 percent respectively over that estimated by stress path method. The Skempton and Bjerrum method is also likely to overestimate the actual total final settlement of the structure and it overestimated that by stress path method by 28 percent in this study.

(iv) Although the Conventional Method by Eqn. 2.1 overestimated the magnitude of total final settlement estimated by the stress path method by only about 11 percent, the stress path method provided more details which are very important for safe and economic design of foundations. About 37 percent of the total final settlement by the stress path method was instantaneous indicating a substantial part of the total settlement occuring during construction. On the other hand the Conventional Method assumes a gradual final settlement.

(v) A faster time-rate of consolidation was obtained by the three-dimensional theory compared to that by one-dimensional theory. It is more likely that the actual time-rate of consolidation in this particular study will be closer to that obtained by the three-dimensional theory than that by one-dimensional theory. The time-rate of consolidation by the three-dimensional theory was found to be much faster at the initial stages of consolidation than at the later stages compared to that by one-dimensional theory, the rate being 70 percent faster at 30 percent consolidation and 40 percent faster at 96 percent consolidation.

(vi) Elements of soil under foundation loading are likely to follow geometrically similar stress paths to those shown in Figs. 5.4 and 5.5.

(vii) Due to sample disturbance during transportation, handling and sampling by a standard Shelby tube, the computed value of the primary consolidation settlement obtained from oedometer test results may be very much higher than the actual settlement.

6.2 Recommendations for Future Research

Although the objective of this study was set to make a comparison of the stress path method of settlement analysis with other methods applied to a lightly O.C. clay, due to time constraints no field observation could be made to finally confirm the theoretically established points. Again the work was limited to settlement studies on lightly O.C. clay-silt from one site. On the basis of these and from the experience gathered from this study, the following recommendations are made for future research:

(i) A water tower is going to be constructed soon at the site from which the samples were collected for this study. Arrangements may be made to keep settlement records to check the validity of the conclusions made herein.

(ii) Settlement studies on lightly O.C. clays from other sites may be taken up to further check the validity of the results obtained from this study.

(iii) Systematic laboratory and field studies may be taken up for other types of soil for comparison of the stress-path method of settlement analysis with the other available methods.

(iv) Works may be taken up with a view to arriving at an appropriate value for the deformation modulus of the soil rather than using the e-log p relation to predict settlement characteristics.

(v) Reliable determination of preconsolidation pressure is still an unsolved problem, particularly if the sample is considerably disturbed. Efforts may be made to find methods for reliable determination of preconsolidation pressure which is very important for reliable settlement analysis.

(vi) The effect of sample disturbance on the settlement parameters may be investigated with special attention to the effect of sample disturbance on the undrained elastic modulus of clays.

REFERENCES

Biot, M.A., (1941) "General Theory of Three-dimensional Consolidation" Jnl. Appl. Phys. 12, 155.

Bishop, A.W., and Eldin, A.K.G., (1950) "Undrained Triaxial Tests on Saturated Sands and their Significance in the General Theory of Shear Strength" Geotechnique, 2:13-32.

Bishop, A.W., and Henkel, D.H., (1962) "The Measurement of Soil Properties in the Triaxial Test" Edward Arnold (Publ.) Ltd., London.

Brooker, E.W., and Ireland, H.O., (1965) "Earth Pressure at Rest Related to Stress History" Can. Geotech. Jnl., Vol. 2, No.1: 1-15.

Casagrande, A. (1936) "The Determination of Pre-consolidation Load and its Practical Significance" Ist. I.C.S.M.F.E., Vol. 3, Cambridge: 60-64.

Casagrande, L. (1964) "Effect of Preconsolidation on Settlements" P.A.S.C.E., J.S.M.F.D., Vol. 90, S.M.5: 349-362.

Cooling, I.F., and Gibson, R.E., (1955) "Settlement Studies on Structures in England" Conf. Corr. between Cal. and Obs. Str. and Displ. of Structures, I.C.E. Prelim. Vol:295-317.

D'Appolonia, D.J., Poulos, H.G. and Ladd, C.C. (1971) "Initial Settlement of Structures on Clay" P.A.S.C.E., J.S.M.F.D., Vol. 97, S.M.10: 1359-1377.

Davis, E.H. and Poulos, H.G. (1963) "Triaxial Testing and Three-dimensional Settlement Analysis" Proc. Fourth Aust.-NZ. C.S.M.F.E: 233-243.

Davis, E.H. and Poulos, H.G. (1968) "The Use of Elastic Theory for Settlement Prediction Under Three-dimensional Conditions" Geotechnique, Vol. 18: 67-91.

Davis, E.H. and Poulos, H.G. (1972) "Rate of Settlement Under Two- and Three-dimensional Conditions" Geotechnique, Vol. 22: 95-114.

Flaate, K. (1963) General Report on "Settlement on Cohesive Soils Observations and Comparison with Predictions" Opening Session, Euro. C.S.M.F.E., Wiesbaden.

Fox, E.N. (1948) "The Mean Elastic Settlement of Uniformly Loaded Area at a Depth Below the Ground Surface" Proc. Second I.C.S.M.F.E., Rotterdam, Vol.1: 129-136.

Gibson, R.E. and Lumb, P. (1953) "Numerical Solution of Some Problems in the Consolidation of Clay" Jnl. I.C.E.I, Part 1, 182.

Haswell, C.K. (1963) "Predicted and Actual Settlement of Selected Thermal Generating Stations" Euro. C.S.M.F.E., Wiesbaden: 111-117.

Hoeg, K., Christian, J.T. and Whitman, R.V. (1968) "Settlement of Strip Load on Elastic-Plastic Soil" P.A.S.C.E., J.S.M.F.D., Vol. 94, S.M.2: 431-445.

Hruban, K. (1948) "Sources of Error in Settlement Estimate" Proc. Second I.C.S.M.F.E., Rotterdam, Vol.1: 127-128.

Janbu, N., Bjerrum, L. and Kjaernsli, B. (1956) "Veiledning ved Lsning av Fundamenteringsoppgaver" N.G.I. Publ.No.16.

Lambe, T.W. (1951) "Soil Testing for Engineers" John Wiley and Sons Inc. (Publ.) New York.

Lambe, T.W. (1964) "Methods of Estimating Settlement" P.A.S.C.E., J.S.M.F.D., Vol. 90, S.M.5: 43-67.

Lambe, T.W. (1967) "Stress Path Method" P.A.S.C.E., J.S.M.F.D., Vol. 93, S.M.6: 309-331.

Lambe, T.W. (1973) "Predictions in Soil Engineering" Thirteenth Rankine Lecture, Geotechnique, Vol. 23: 151-202.

Lambe, T.W. and Whitman, R.V. (1969) "Soil Mechanics" Wiley Eastern Private Ltd. (Publ.) New Delhi.

Lee, I.K. (1968) "Soil Mechanics: Selected Topics" Butterworths (Publ.) London: 150-154.

McNamee, J. and Gibson, R.E. (1960) "Plain Strain and Axially Symmetric Problems of the Consolidation of a Semi Infinite Clay Stratum" Q. Jnl. Mech. Appl. Math. 13, Part 2,: 210-227.

NAVDOCKS DM-7 (1962) "Design Manual - Soil Mechanics, Foundations and Earth Structures" Dept. of Navy, Bureau of Yards and Docks, Washington.

Nishida, Y. (1956) "A Brief Note on the Compression Index of Soil" P.A.S.C.E., J.S.M.F.D., Vol. 82, S.M.3: 5.

Poulos, H.G. (1967a) "The Use of Sector Method for Calculating Stress and Displacements in an Elastic Mass" Proc. Fifth Aust.- N.E.C.S.M.F.E., 23.

Poulos, H.G. (1967b) "Stresses and Displacements in an Elastic Layer Underlain by a Rough Rigid Base" Geotechnique, 17, No.4, : 378-410.

Schmertmann, J.H. (1955) "The Undisturbed Consolidation, Behaviour of Clay" T.A.S.C.E, Vol. 120, 1201-1233.

Scott, R.F. (1963) "Principles of Soil Mechanics" Addison-Wesley Publishing Co., Massachusetts.

Serajuddin, M. and Ahmed, A. (1967) "Studies on Engineering Properties of East Pakistan Soils" Proc. First S.E.A.R.C.S.E., Bangkok: 9-22.

Sherif, M.A. and Koch, D.E. (1970) "Coefficient of Earth Pressure at Rest as Related to Soil Precompression Ratio and Liquid Limit" High. Res. Rec. 323,H.R.B., Washington: 39-48.

Simons, N.E. (1957) "Settlement Studies on Two Structures in Norway" Fourth I.C.S.M.F.E., London, Vol. 1: 431-436.

Simons, N.E. (1963) "Settlement Studies on a Nine Story Apartment Building atØkernbraten, Oslo" Proc. Euro. C.S.M.F.E., Wiesbanden, Vol. 1, : 179-191.

Simons, N.E. (1971) "The Stress-Path Method of Settlement Analysis Applied to London Clay" Proc. Roscoe Mem. Symp. on Stress-strain Behaviour of Soils, Cambridge, 241-252.

Simons, N.E. (1974) General Report on "Normally Consolidated and Lightly Overconsolidated Cohesive Materials" Session 2, Conf. on Settlement of Structures, Cambridge.

Simons, N.E. and Som, N.N. (1969) "The Influence of Lateral Stresses on the Stress Deformation Characteristics of London Clay" Proc. Seventh I.C.S.M.F.E., Maxico City, Vol. 1, : 369-377.

Simons, N.E. and Som, N.N. (1970) "Settlement of Structures on Clay With Particular Emphasis on London Clay" C.I.R.I.A. Report 22.

Simons, N.E. and Menzies, B.K. (1975) "A Short Course in Foundation Engineering" IPC Science and Technology Press (Publ.) London.

Skempton, A.W. (1957) "Discussion: The Planning and Design of the New Hong Kong Airport" Proc. I.C.E. Vol.7., 305-307.

Skempton, A.W., Peck, R.B. and MacDonald, D.H. (1955) "Settlement Analysis of Six Structures in Chicago and London" Proc. I.C.E. Pt. 1, Vol. 4, No.4., 525-544.

Skempton, A.W. and Bjerrum, L. (1957) "A Contribution to the Settlement Analysis of Foundations on Clay" Geotechnique, Vol. 7, : 168-178.

Som, N.N. (1970) "Lateral Stresses During One-dimensional Consolidation of an Over-consolidated Clay" Proc. Second S.E.A.C.S.E., Singapore: 295-307.

Terzaghi, K. (1943) "Theoretical Soil Mechanics" John Wiley and Sons (Publ.) New York.

APPENDIX-A

COMPUTATION OF BEARING CAPACITY AND SETTLEMENT

Bearing Capacity:

Taking average value of undrained shear strength for the two layers A and B

$$C_u = 1250 \text{ psf}$$

Ultimate bearing capacity,

$$q_u = 5(1+0.2B/L)(1+0.2\ D/B)\ C_u$$
$$= 5\times1.2\times1.05\times1250$$
$$= 7875 \text{ psf}$$

In this case

$B = L = 40'\text{-}0''$

$D = 10'\text{-}0''$

$B/L = 1$ & $D/B=0.25$

For layer A: $K'_o = 0.70$; $C_u/\bar{p} = 0.8$ (Av.)

Initial shear ratio, $f = \dfrac{(1 - K'_o)}{2\ C_u/\bar{p}} = \dfrac{0.3}{2\times0.8} = 0.1875$

Entering Fig. 2.5(b) with $C_u/\bar{p} = 0.8$ and $K'_o = 0.70$, a factor of safety of 2 against ultimate bearing capacity failure to prevent local yield is obtained, Fig. 2.5(a).

Choosing a net foundation pressure of 2016 psf (14 psi).

Factor of safety against ultimate bearing capacity failure

$= \dfrac{7875}{2016} = 3.91 \approx 4.$

Factor of safety against initiation of local yield = 4/2 = 2.

Considering two layer system having undrained shear strength of 1500 psf for layer A and 1000 psf for layer B.

$C_A/C_B = \dfrac{1500}{1000} = 1.5$ $T/B = 20/40 = I.5$

where T = Depth of interface of layers A and B from base of foundation.

$N_C = 5.69$ (for strip footing)

for $D/B = 0.25$; $N_{CD}/N_C = 1.075$

where N_{CD} is the bearing capacity factor which includes the effect of depth of footing.

$\therefore \; N_{CD} = 1.075 \times 5.69 = 6.12$

bearing capacity factor for a circular footing

$N_{CR} = 1.2\, N_{CD} = 1.2 \times 6.12 = 7.344$

$q_u = C_A\, N_{CR} = 1500 \times 7.344 = 11{,}016$ psf

F.S. against ultimate bearing capacity failure

$= \dfrac{11{,}016}{2016} = 5.5$

F.S. against initiation of local yield

$= 5.5/2 = 2.75$

Immediate Settlement

Conventional and Skempton and Bjerrum Method (Ref. Fig. 2.1 and Simons and Menzies, 1975).

Layer, A -

$D/B = 0.25$; $E_{UA} = 876$ psi

$H/B = 20/40 = 0.50$

μ_0 (from Fig. 2.1) = 0.945 ; μ_1 = 0.28

$$\text{Average } S_{UA(876)} = 0.28 \times 0.945 \times \frac{14 \times 40 \times 12}{876}$$

$$= 2.03 \text{ in}$$

At centre from Eq. 5.9

$$S_{UA(876)} = \frac{2.03}{0.85} = 2.38 \text{ in.}$$

Layer, B -

Assuming that layer B extends to the surface,

$$H/B = 35/40 = 0.875 \quad \text{and } E_{UB} = 1610 \text{ psi}$$

where $\mu_1 = 0.39$, $\mu_0 = 0.945$

Average settlement for the entire depth

$$S_{UAB(1610)} = 0.945 \times 0.39 \times \frac{14 \times 40 \times 12}{1610} = 1.538 \text{ in}$$

the average settlement of layer A if $E_{UA} = E_{UB} = 1610$ psi

$$S_{UA(1610)} = 0.28 \times 0.945 \times \frac{14 \times 40 \times 12}{1610} = 1.104 \text{ in}$$

average settlement for layer B,

$$S_{UB(1610)} = S_{UAB(1610)} - S_{UA(1610)}$$

$$= (1.538 - 1.104) = 0.434 \text{ in}$$

at Centre,

$$S_{UB(1610)} = \frac{0.434}{0.85} = 0.51 \text{ in}$$

Davis and Poulos Method

$$S_u = \int_{z_1}^{z_2} \frac{\Delta\sigma_v - 2\nu_u \Delta\sigma_h}{E_u} \, dz$$

ν_u = 0.5 (for saturated clays)

$$S_u = \int_{z_1}^{z} \frac{\Delta\sigma_v - \Delta\sigma_h}{E_u}$$

Putting the values of and from Eqs. 5.1 and 5.2

for $\nu = \nu_u = 0.5$,

$$S_u = \frac{3p}{2E_u} \int_{z_1}^{z_2} \left[\frac{z}{\sqrt{(r^2 + z^2)}} - \frac{z^3}{(r^2 + z^2)^{3/2}} \right] dz$$

Integrating

$$S_u = \frac{3p}{2E_u} \left[\frac{p^2}{\sqrt{(r^2+z^2)}} \right]_{Z_2}^{Z_1} \qquad \text{Eq.(A)}$$

Layer A,

E_u = 892 psi p = 14 psi

r = 20'-0" Z_1 = 0, Z_2 = 20'-0"

$$S_{UA} = \frac{3 \times 14}{2 \times 892} \left[\frac{400}{20} - \frac{400}{\sqrt{(400+400)}} \right]$$

= 1.66 in

Layer B,

E_u = 2718 psi, p = 14 psi, Z_1 = 20'-0", Z_2 = 35'-0"

r = 20'-0"

Putting these values in Eq. (A)

$S_{UB} = 0.391$ in

$S_u = S_{UA} + S_{UB} = 1.66 + 0.39 = 2.05$ in

Stress-path Method

Layer, A, $S_{UA} = \epsilon_{1U} \times H_A$

$= 0.007245 \times 20 \times 12 = 1.74$ in

Layer, B, $S_{UB} = 0.0022015 \times 15 \times 12 = 0.396$ in 0.4 in

$S_u = S_{UA} + S_{UB} = 1.74 + 0.4 = 2.14$ in

Consolidation Settlement

Conventional Method

$$S_{oed} = \int_{z_1}^{z_2} \Delta \sigma_v \, m_{v1} \, dz$$

Putting the value of $\Delta \sigma_V$ from Eq. 5.1 and integrating

$$S_{oed} = p \, m_{v1} \left\{ z \Big|_{z_1}^{z_2} - \sqrt{(z^2+r^2)} \Big|_{z_1}^{z_2} + \frac{r^2}{\sqrt{(z^2+r^2)}} \Big|_{z_1}^{z_2} \right\}$$

... Eq. (B)

Layer A,

$p = 2016$ psf, $m_{v1} = 1.27375 \times 10^{-5}$ ft^2/lb,

$Z_1 = 0$, $Z_2 = 11.5'$, $r = 20'-0''$

Putting these values in Eq. (B)

$$S_{oed}\ A_1 = 0.2848 \text{ ft}$$

Layer A_2,

$P = 2016$ psf, $z_1 = 11.5'$, $z_2 = 20'$, $m_{v1} = 0.6825 \times 10^{-5}\ ft^2/lb$

$r = 20'\text{-}0''$

Putting these values in Eq. (B)

$$S_{oed}\ A_2 = 0.0892 \text{ ft}$$

Layer B,

$p = 2016$ psf, $z_1 = 20'$, $z_2 = 35'$, $m_{v1} = 1.077 \times 10^{-5}\ ft^2/lb$

$r = 20'\text{-}0''$

Putting these values in Eq. (B)

$$S_{oed}\ B = 0.1562 \text{ ft} = 1.87 \text{ in}$$

Layer A,

$$S_{oed}\ A = S_{oed}\ A_1 + S_{oed}\ A_2 = 0.2848 + 0.0892$$

$$= 0.374 \text{ ft} = 4.49 \text{ in}$$

Total consolidation settlement

$$S_{oed} = S_{oedA} + S_{oedB} = 1.87 + 4.49 = 6.36 \text{ in}$$

Skempton and Bjerrum Method

Average value of pore-pressure parameter A for the whole depth

$A = 0.525$

For a circular footing with B = 40'-0", H = 35'-0",

H/B = 1.875 and A = 0.525

From Fig. 2.3, $\mu = 0.70$

So

$$S_{CF} = \mu\, S_{oed} = 0.70 \times 6.36 = 4.45$$

Davis and Poulos Method

Total final settlement.

$$S_{TF} = \frac{1}{E'} \int_{z_1}^{z_2} (\Delta\sigma_v - 2\nu' \Delta\sigma_h)\, dz$$

putting the values of $\Delta\sigma_v$ and $\Delta\sigma_h$ from Eqs. 5.1 and 5.2 and integrating,

$$S_{TF} = \frac{p}{E'} \left[(1-2\nu')z + (2\nu'-1)\sqrt{(r^2+z^2)} - (1+\nu') \frac{r^2}{\sqrt{(r^2+z^2)}} \right]_{z_1}^{z_2} \quad \text{Eq. (C)}$$

Layer, A,

$E' = 459$ psi, $= 0.37$, $p = 14$ psi

$z_1 = 0$, $z_2 = 240$ in $r = 240$ in.

Putting these values in Eq. (C)

$$S_{TFA} = 4.06 \text{ in}$$

Layer, B,

$E' = 810$ psi, $= 0.31$, $p = 14$ psi

$z_1 = 240$ in, $z_2 = 420$ in, $r = 240$ in

Putting these values in Eq. (C)

$$S_{TFB} = 1.40 \text{ in}$$

$$S_{CFA} = 4.06 - 1.66 = 2.40 \text{ in}$$

$$S_{CFB} = 1.40 - 0.39 = 1.01 \text{ in}$$

Total consolidation settlement.

$$S_{CF} = S_{CFA} + S_{CFB} = 2.40 + 1.01 = 3.41 \text{ in}$$

Stress-path Method:

Layer A, $S_{CFA} = \epsilon_{1C} \times H_A = 0.01078 \times 20 \times 12 = 2.59 \text{ in}$

Layer B, $S_{CFB} = 0.005555 \times 15 \times 12 = 1.00 \text{ in}$

Total consolidation settlement.

$$S_{CF} = S_{CFA} + S_{CFB} = 2.59 + 1 = 3.59 \text{ in}$$

Rate of Settlement

The rate of settlement was calculated for the individual layers A and B as well as for the combined layer. The computations were based on an approximate method presented in the Design Manual NAVDOCKS DM-7. For calculation of the rate of settlement under three-dimensional condition a solution presented by Davis and Poulos (1968, 1972) was used. The same basis of calcula tion as used for one-dimensional case for the two layer system was used for the three-dimensional case.

One-dimensional Condition:

Layer A:

$m_{VA} = 1.077\times10^{-5}\ ft^2/lb \qquad H_A = 20\ ft$

$C_{VA} = 15.295\times10^{-5}\ ft^2/min. \qquad 0.22\ ft^2/day$

$K_{VA} = 1.48\times10^{-4}\ ft/day$

Layer B:

$m_{VB} = 1.077 \times 10^{-5}\ ft^2/lb \qquad H_B = 15\ ft$

$C_{VB} = 2.495\times10^{-5}\ ft^2/min = 3.59\ ft^2/day$

$K_{VB} = 1.68\times10^{-3}\ ft/day$

Ratios:

$$R_H = \frac{H_A}{H_B} = \frac{20}{15} = 1.33$$

$$R_K = K_A/K_B = 0.0881$$

$$R_{mv} = m_{VA}/m_{VB} = 1.0$$

Step-1.

$$K_{AVE} = \frac{R_{H+1}}{R_H+R_K}\ (K_A)$$

$$= \frac{(1.33 + 1)}{(1.33+0.0881)} \times 1.48\times10^{-4} = 2.43\times10^{-4}\ ft/day$$

$$m_{VAVE} = \frac{R_H\ R_{mv} + 1}{R_H + 1}\ (m_{VB})$$

$$= \frac{1.33\times1+1}{1.33+1} \times 1.077\times10^{-5} = 1.077\ \times10^{-5}\ ft^2/lb$$

$$C_{VAVE} = \frac{K_{AVE}}{m_{VAVE} \times \gamma_w} = \frac{2.43\times10^{-4}}{1.077\times10^{-5}\times62.4} = 0.362 \text{ ft}^2/\text{day}$$

Step 2.

Equivalent drainage distance

$$H' = \tfrac{1}{2}\,(H_A + R_K\,H_B)$$

$$= \tfrac{1}{2}\,(20 + 0.0881 \times 15) = 10.66 \text{ ft.}$$

Step 3.

Equivalent thickness ratio

$$D_A = \frac{H_A}{H'} = \frac{20}{10.66} = 1.88$$

$$D_B = \frac{R_K\,H_B}{H'} = \frac{1.322}{10.66} = 0.124$$

Step 4.

From well known Terzaghi solution

Case A. at $\bar{u} = 20\%$ $T_V = 0.031$ (sample calculation)

$$t = T_V\,\frac{H^2}{C_{VAVE}} = 0.031 \times \frac{\left(\frac{35}{2}\right)^2}{0.362} \qquad (2H = 35'\text{-}0'')$$

$$= 26.23 \text{ days} = 0.0728 \text{ year}$$

Case B. at $\bar{u} = 70\%$ $T_V = 0.403$

$$t = \frac{T_V \times H^2}{C_{VAVE}} = \frac{0.403 \times \left(\frac{35}{2}\right)^2}{0.362}$$

$$= 340.94 \text{ days} = 0.947 \text{ years.}$$

Step 5.

To compute $\Delta \bar{u}_B$, percent consolidation of portion $R_K H_B$ of equivalent thickness H', the following equations are used

(i) when $\bar{u} \leqslant 33.3\%$ and $D_B \leqslant \frac{3\,\bar{u}}{100}$

$$\Delta \bar{u}_B = D_B - \frac{100}{3\,\bar{u}}(D_B{}^2) + \frac{10,000}{27\,\bar{u}^2}(D_B)^3$$

(ii) When $\bar{u} \leqslant 33.3\%$ and $D_B \geqslant \frac{3\bar{u}}{100}$ $\Delta \bar{u}_B = \bar{u}$

(iii) When $\bar{\mu} > 33.3\%$

$$\Delta \bar{u}_B = D_B - \left(\frac{100 - \bar{u}}{200}\right)\left[3(D_B)^2 - (D_B)^3\right]$$

Case A.

$$\bar{u} = 20\% < 33.3\%$$

$$D_B = 0.124 < \frac{3\bar{u}}{100} = \frac{3 \times 20}{100} = 0.6$$

$$\Delta \bar{u}_B = 0.124 - \frac{100}{3 \times 20}(0.124)^2 + \frac{10,000}{27 \times 20^2}(0.124)^3$$

$$= 0.1001 = 10.01\%$$

Case B.

$$\bar{\mu} = 70\% > 33.3\%$$

$$\Delta \bar{u}_B = D_B - \left(\frac{100 - \bar{u}}{200}\right)\left[3D_B{}^2 - D_B{}^3\right]$$

$$= 0.124 - \frac{(100-70)}{200}\left[3 \times (0.124)^2 - (0.124)^3\right]$$

$$= 0.1174 = 11.74\%$$

Step 6.

$$\Delta \bar{u}_A = 2\bar{u} - \Delta \bar{u}_B$$

Case A. $\Delta \bar{u}_A = 2\times 20 - 10.01$

$= 40 - 10.01 = 29.99\%$

Case B. $\Delta \bar{u}_A = 2\times 70 - 11.74$

$= 128.26\%$

$$\bar{u}_A = \frac{\Delta \bar{u}_A}{H_A/H'} , \qquad \bar{u}_B = \frac{\Delta \bar{u}_B}{R_K H_B/H'}$$

$$\bar{u}_{AB} = \frac{R_H \bar{u}_A + \bar{u}_B}{R_H + 1}$$

Case A.

$$\bar{u}_A = \frac{29.99}{20/10.66} = 15.98\% \qquad \bar{u}_B = \frac{10.01}{1.3215/10.66} = 80.75\%$$

$$\bar{u}_{AB} = \frac{R_H \bar{u}_A + \bar{u}_B}{R_H + 1} = \frac{1.33 \times 15.98 + 80.75}{1.33 + 1} = 43.78\%$$

Case B.

$$\bar{u}_A = \frac{128.26}{20/10.66} = 68.36\%$$

$$\bar{u}_B = \frac{11.74}{1.3215/10.66} = 94.70\%$$

$$\bar{u}_{AB} = \frac{1.33\times 68.36 + 94.70}{2.33} = 79.66\%$$

<u>Settlement Parameters From</u>

<u>Three-dimensional Triaxial Test:</u> (Sample calculation)

Sample No. S-2a

$L_o = 2.8$ in $\qquad V_o = 70.63$ cc

K_o - loading = 12.37 psi

Immediate compression = 42.00 (dial reading)

Dial reading at the end of K_o - consolidation

= 810.5

Vol. gage reading - 36.5 cm

$$\epsilon_v = \frac{36.5 \times 0.0539}{70.63} = 0.0279 \text{ cc/cc}$$

Vertical dial = 0.08105

$$\epsilon_1 = \frac{0.08105}{2.8} = 0.0289 \text{ in/in}$$

Length after K_o test = 2.8 - 0.08105 = 2.72 in

Vol after K_o - test = ∂0.63 - 1.97 = 68.66 cc.

Undrained loading

$\Delta\sigma_1$ = 13.39 psi

$\Delta\sigma_3$ = 6.93 psi

$\Delta\sigma = \Delta\sigma_1 - \Delta\sigma_3 = 13.39 - 6.93$

$= 6.46$ psi

$\Delta_L = 0.0195$ Dial reading = 195

$$\epsilon_{1U} = \frac{0.0195}{2.72} = 7.17 \times 10^{-3} \text{ in/in}$$

$$E_u = \frac{6.46}{7.17 \times 10^{-3}} = 901 \text{ psi}$$

L = 0.0195 in

Length after undrained loading

L = 2.72 - 0.0195 = 2.7005in

Consolidation:

$\Delta\sigma_1 = 13.39$ psi $\quad \Delta\sigma_3 = 6.93$ psi

$\Delta\sigma = 6.46$ psi

dial change = 282.5

$$\epsilon_{1C} = \frac{0.02825}{2.7005} = 0.01046$$

$$\epsilon_1 = 0.00717 + 0.01046 = 0.01763$$

Vol. gage reading = 20.4

$$\epsilon_V = \frac{20.4 \times .0539}{68.66} = 0.01601 \text{ cc/cc}$$

$$\epsilon_V = \epsilon_1 + 2\epsilon_3$$

$$\epsilon_3 = \frac{\epsilon_V - \epsilon_1}{2} = \frac{0.01605 - 0.01763}{2}$$

$$= -0.00081 \text{ in/in}$$

$$\nu' = \frac{\epsilon_1 \Delta\sigma_3 - \epsilon_3 \Delta\sigma_1}{\epsilon_1(\Delta\sigma_3 + \Delta\sigma_1 - 2\epsilon_3 \Delta\sigma_3)}$$

$$= \frac{0.01763 \times 6.93 + 0.00081 \times 13.39}{.01763(13.39+6.93) + 2\times 0.00081\times 6.93}$$

$$= \frac{0.133}{0.3695} = 0.36$$

$$E' = \frac{(\Delta\sigma_1 - 2\nu'\Delta\sigma_3)}{\epsilon_1} = \frac{13.39 - 0.72 \times 6.93}{0.01763}$$

$$= 476 \text{ psi}$$

APPENDIX-B

ONE- AND THREE-DIMENSIONAL CONSOLIDATION TEST RESULTS

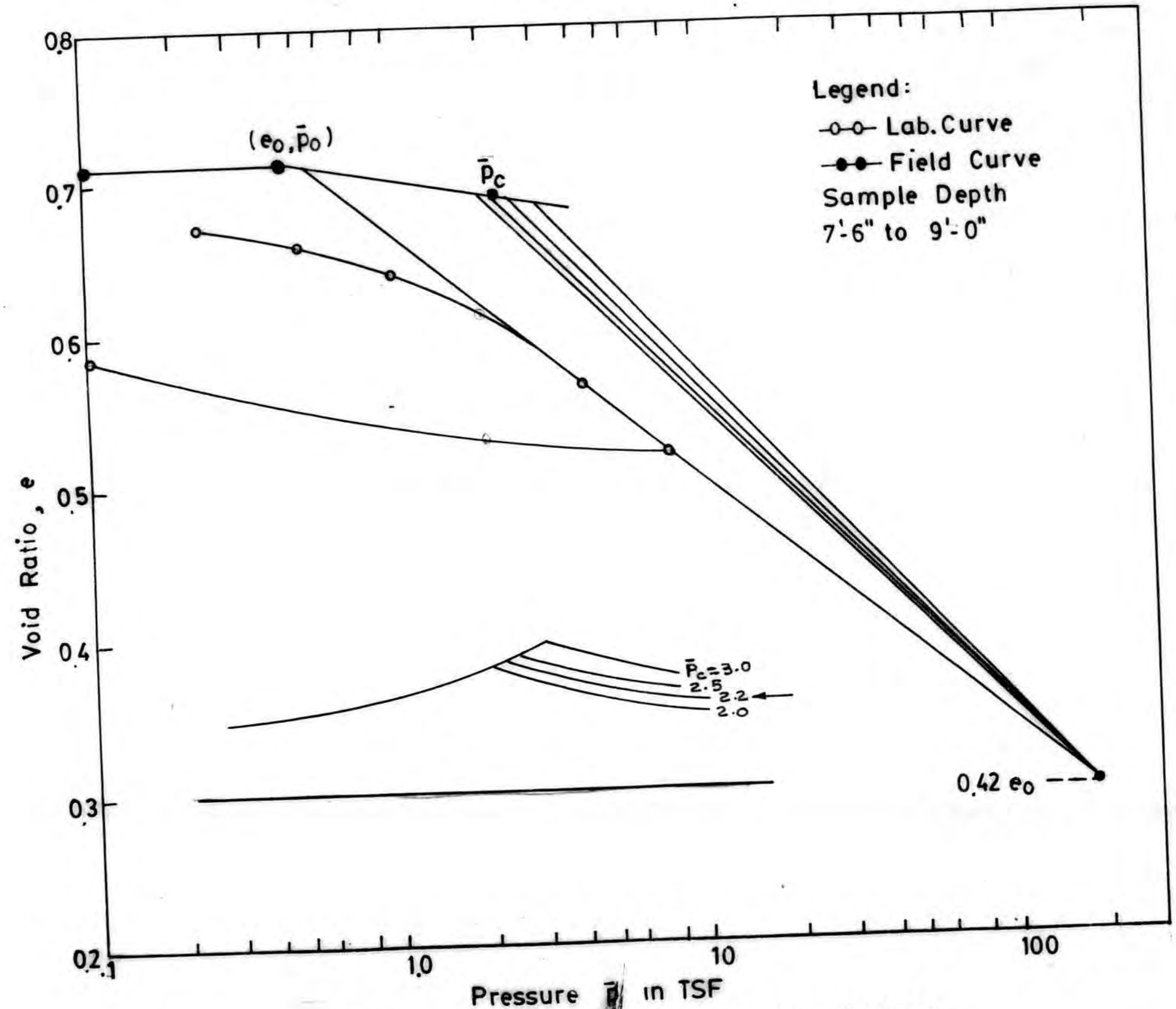

Fig. B-1 e-log p̄ Relation and Void-ratio - reduction Pattern

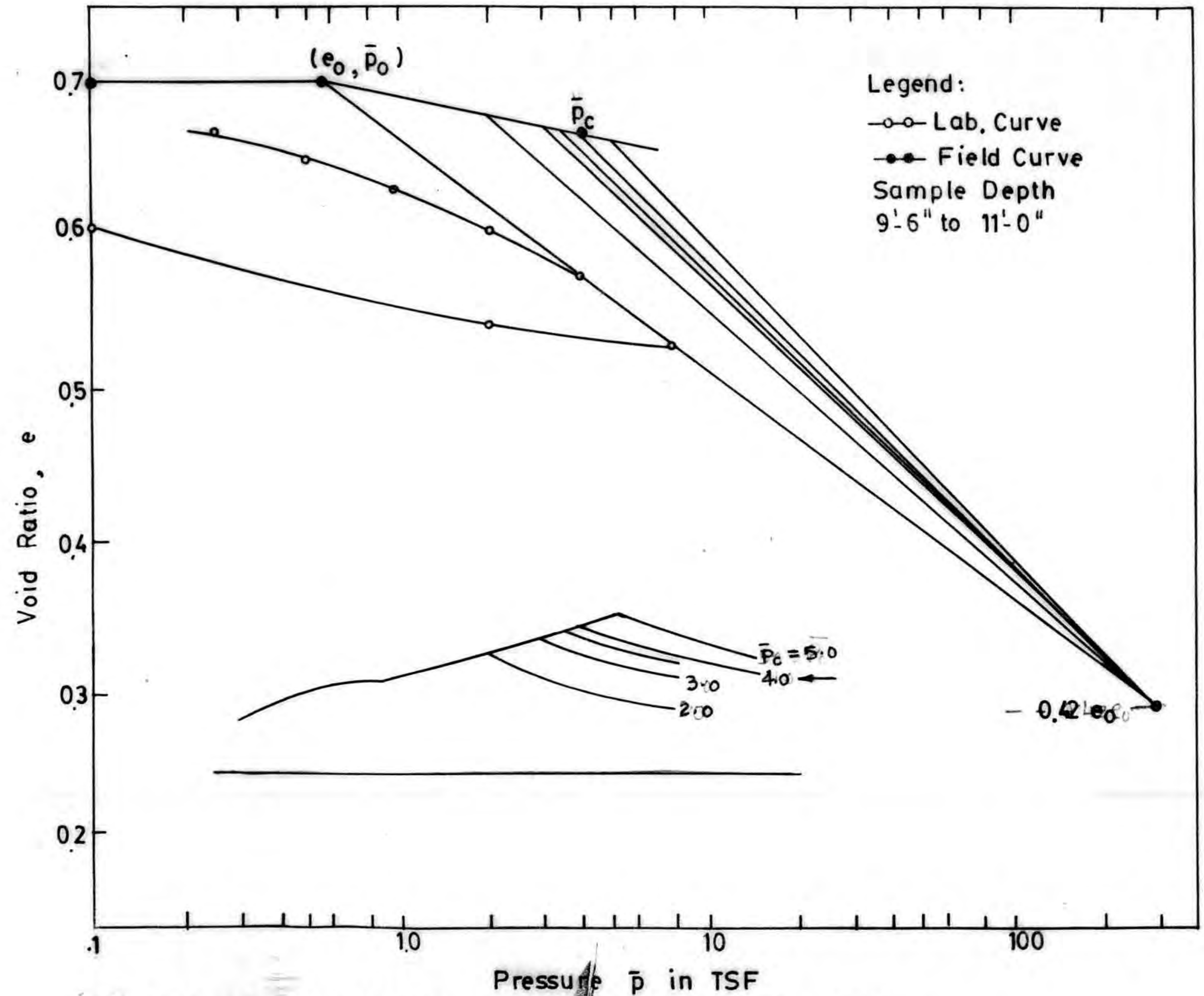

Fig. B-2 e-log $\bar{p}$ Relation and Void-ratio-reduction Pattern

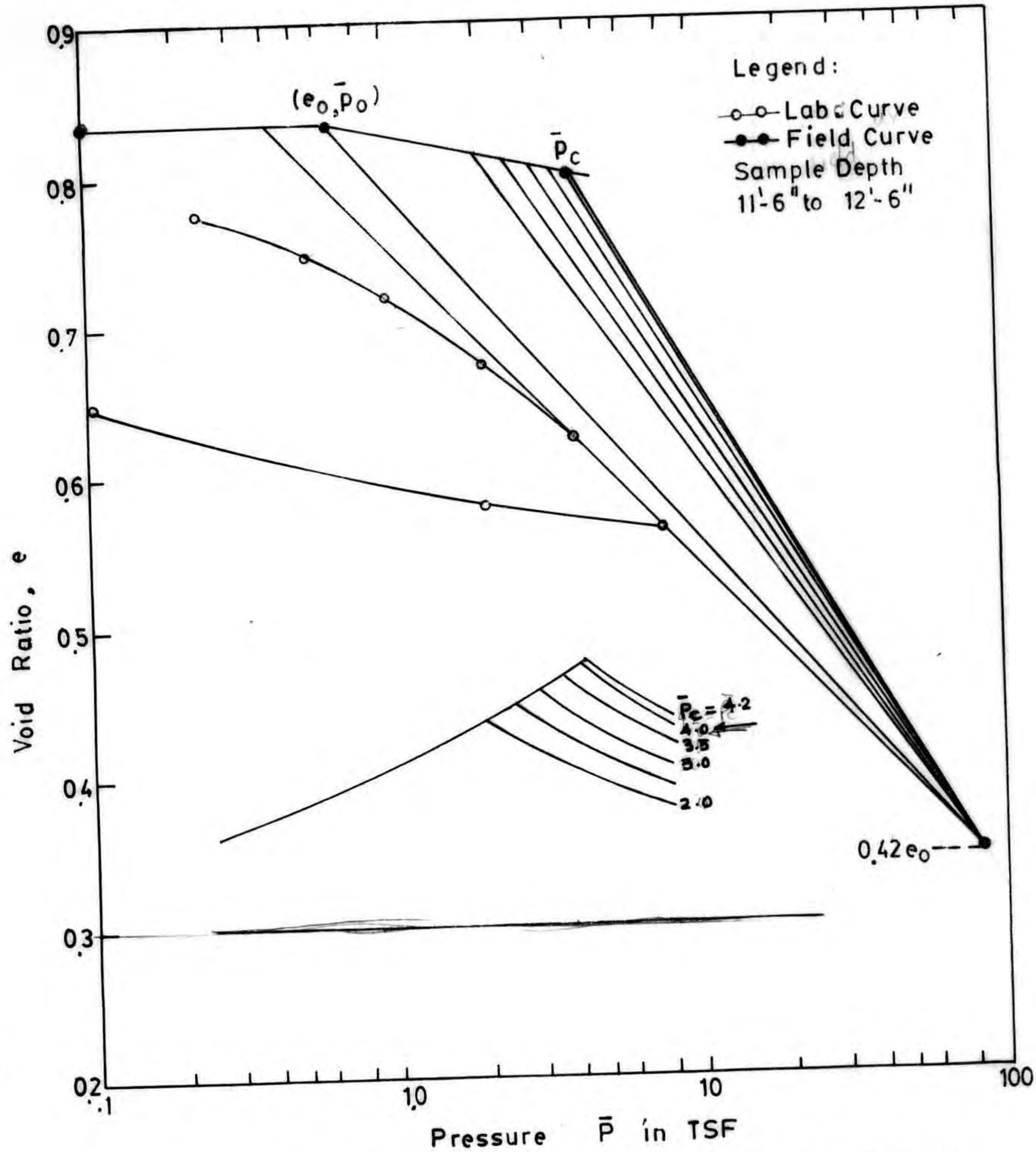

Fig.B-3 e - log $\bar{p}$ Relation and Void-ratio-reduction Pattern

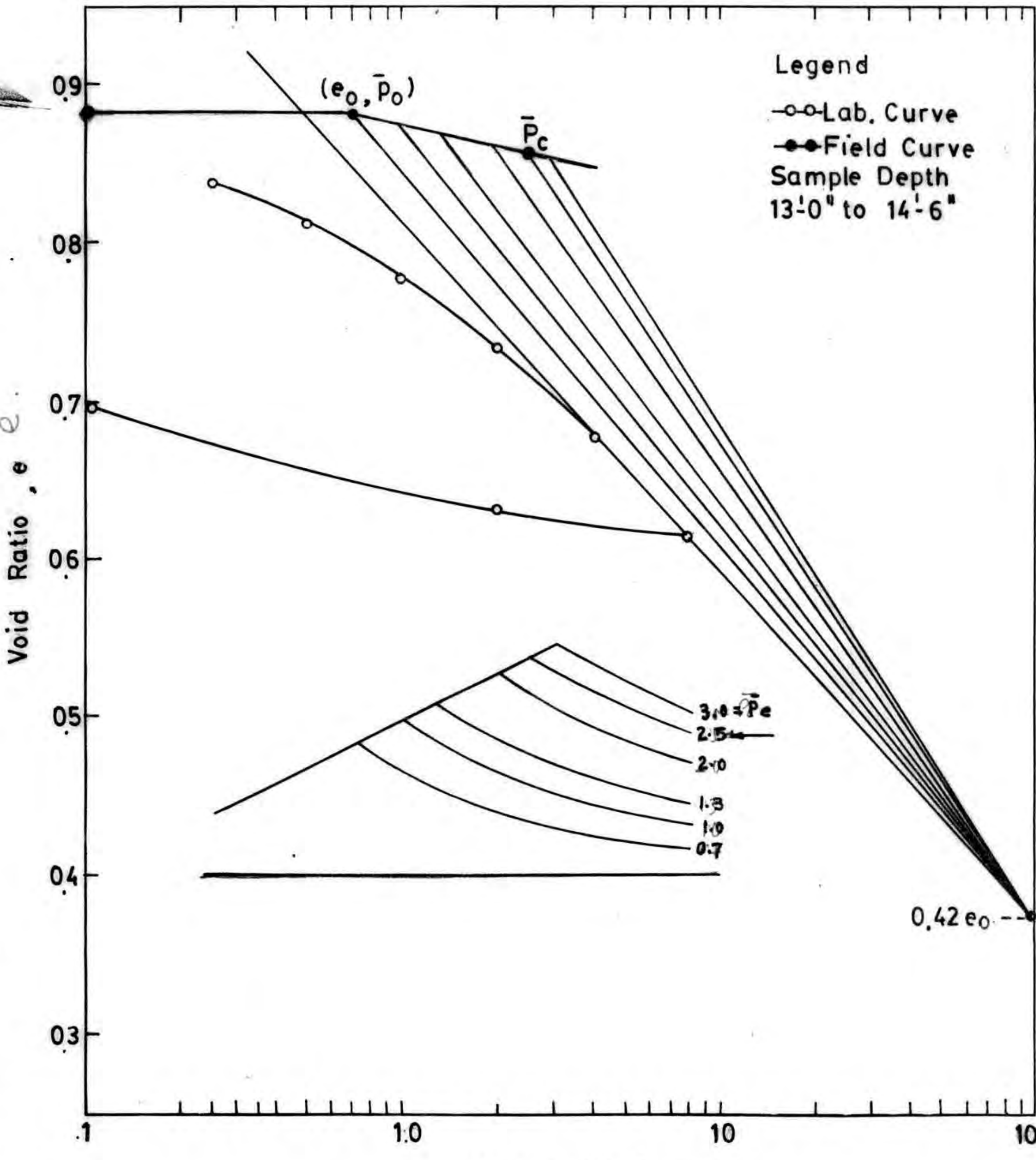

Fig.B-4 e - log $\bar{p}$ Relation and Void-ratio - reduction Patter

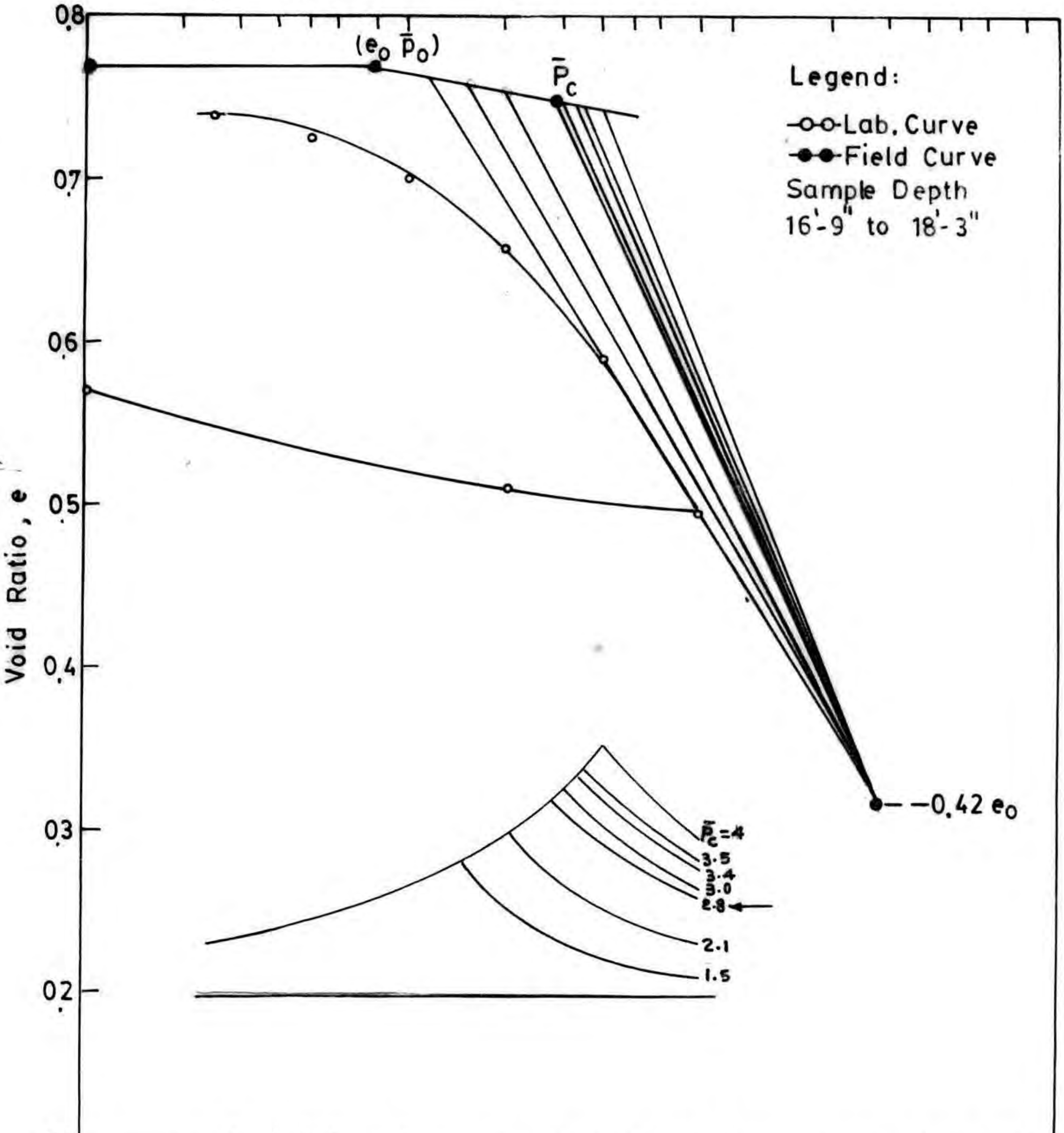

Fig. B-5 e – log $\bar{p}$ Relation and Void-ratio-reduction Pattern

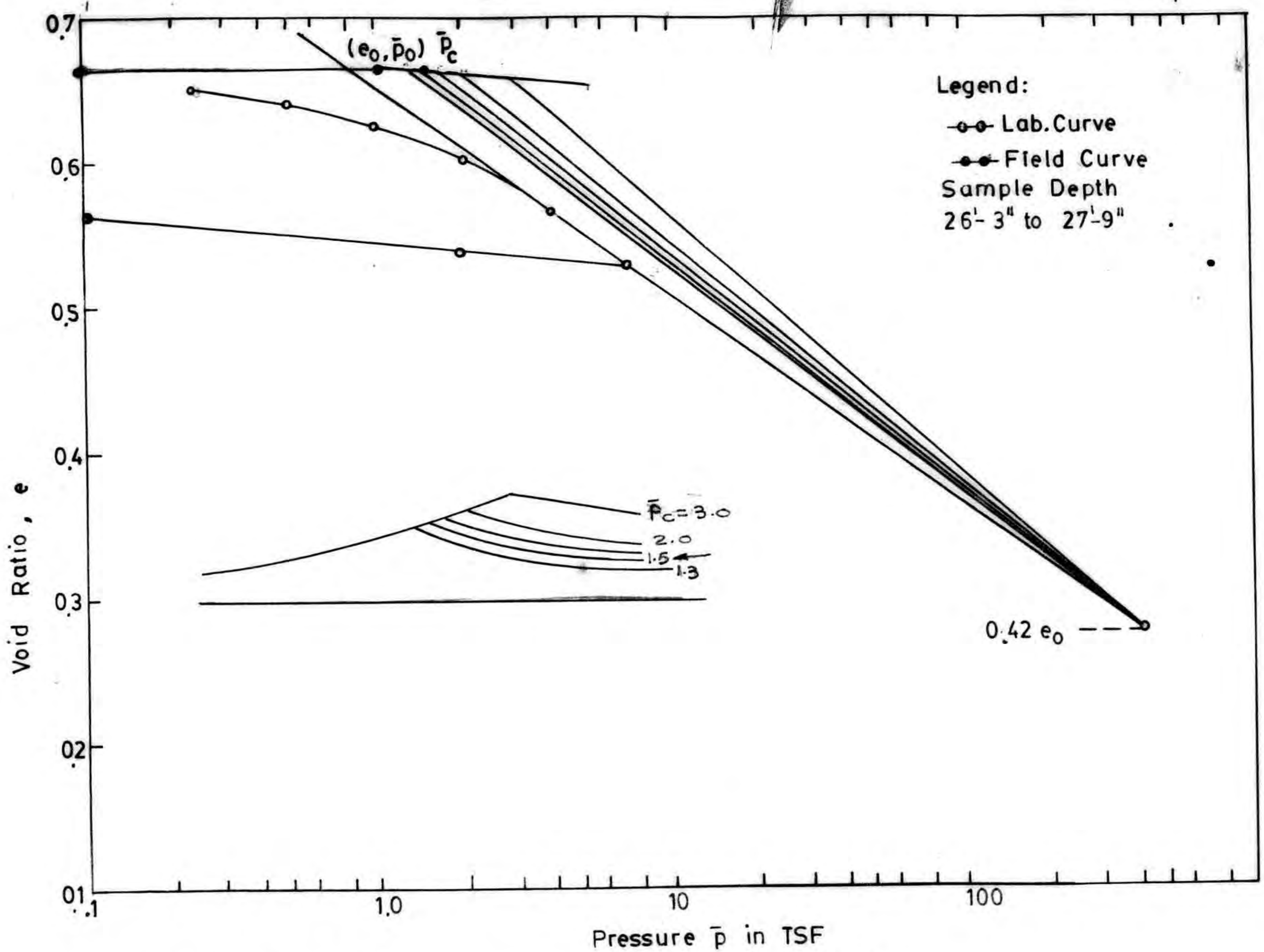

Fig. B-6 e-log $\bar{p}$ Relation and Void-ratio-reduction Pattern

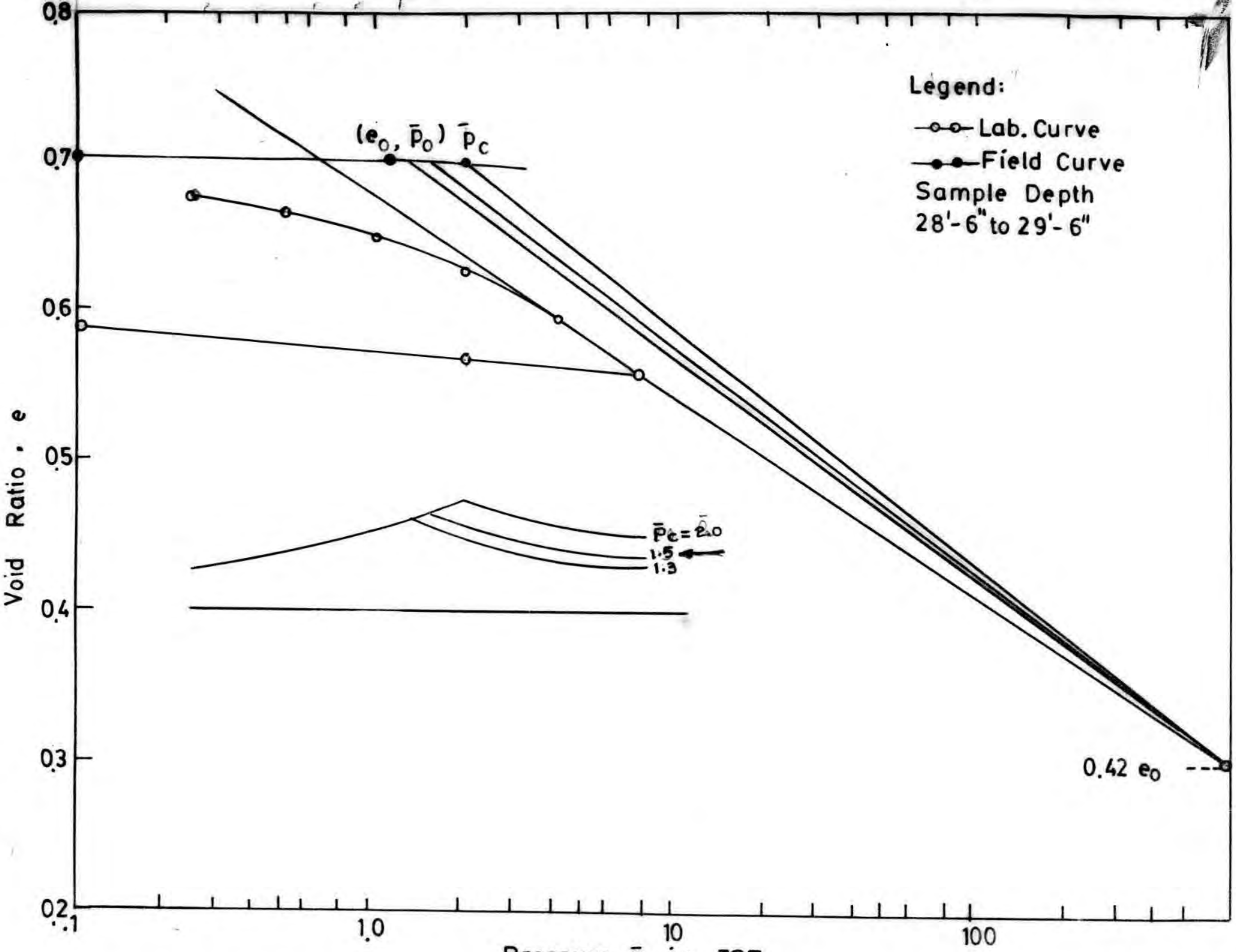

Fig. B-7 e-log $\bar{p}$ Relation and Void-ratio-reduction Pattern

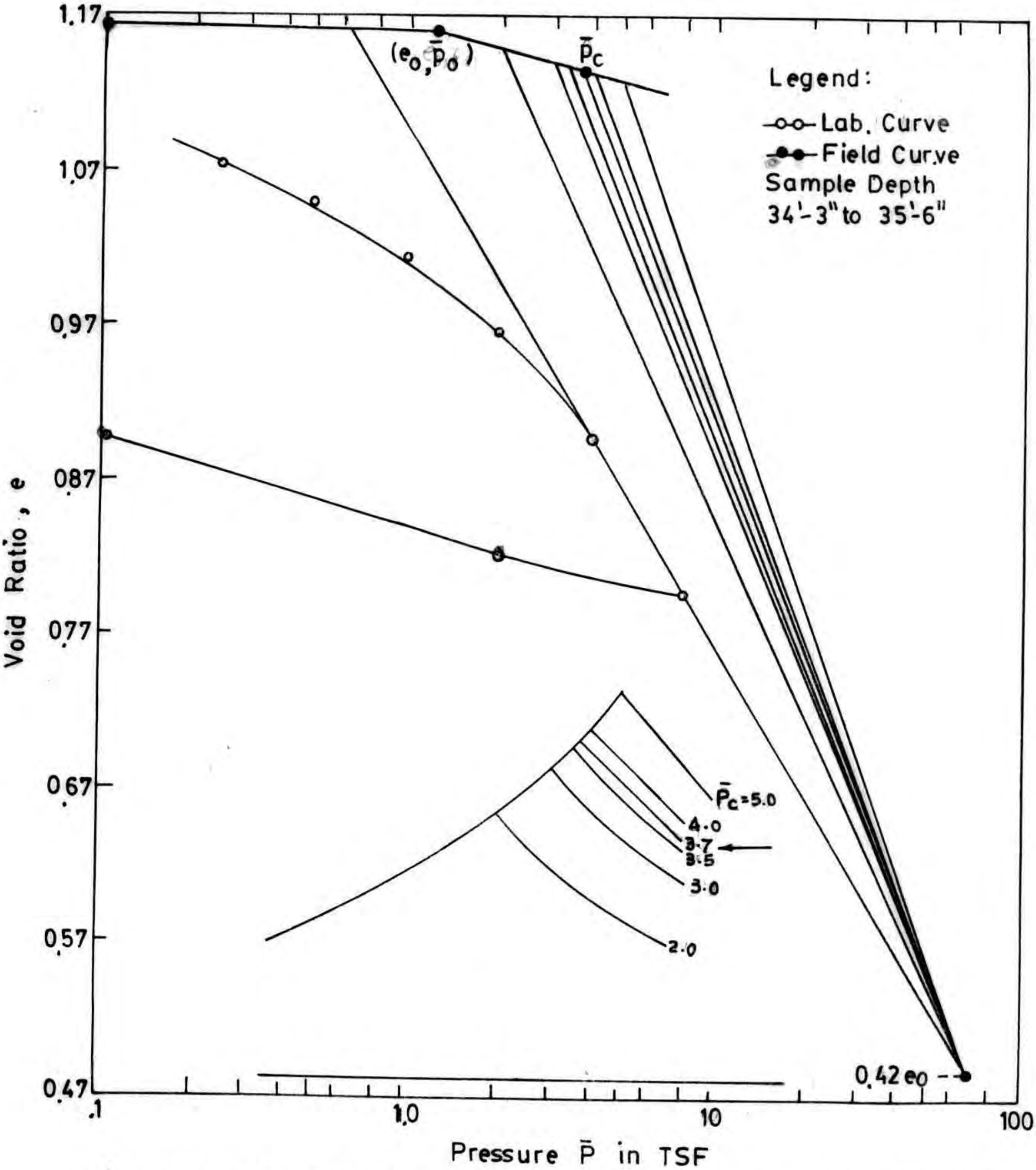

Fig. B-8 e – log $\bar{p}$ Relation and Void-ratio-reduction Pattern

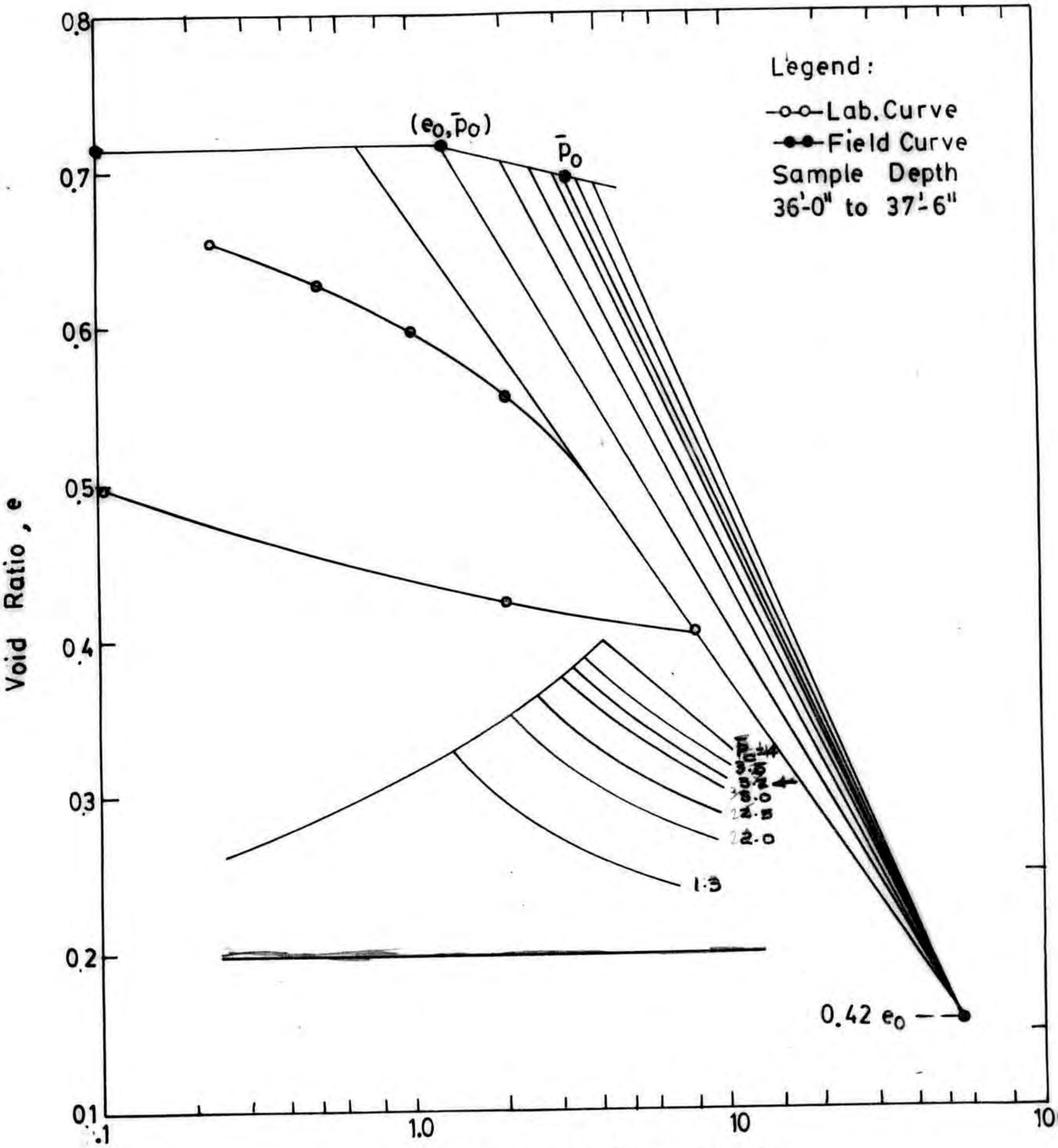

Fig. B 9 e - log $\bar{p}$ Relation and Void - ratio - reduction Pattern

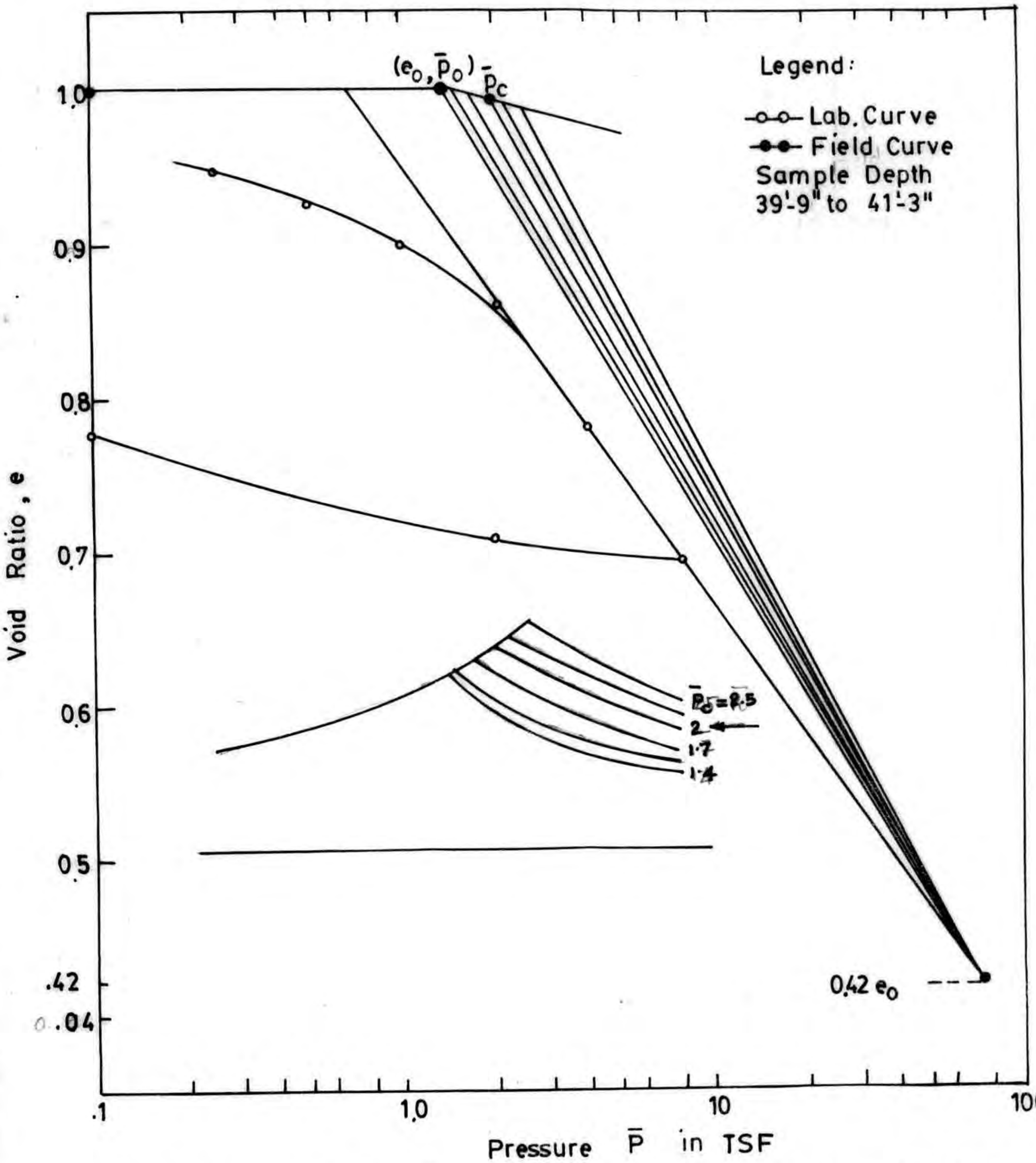

Fig. B-10 e - log $\bar{p}$ Relation and Void - ratio - reduction Pattern

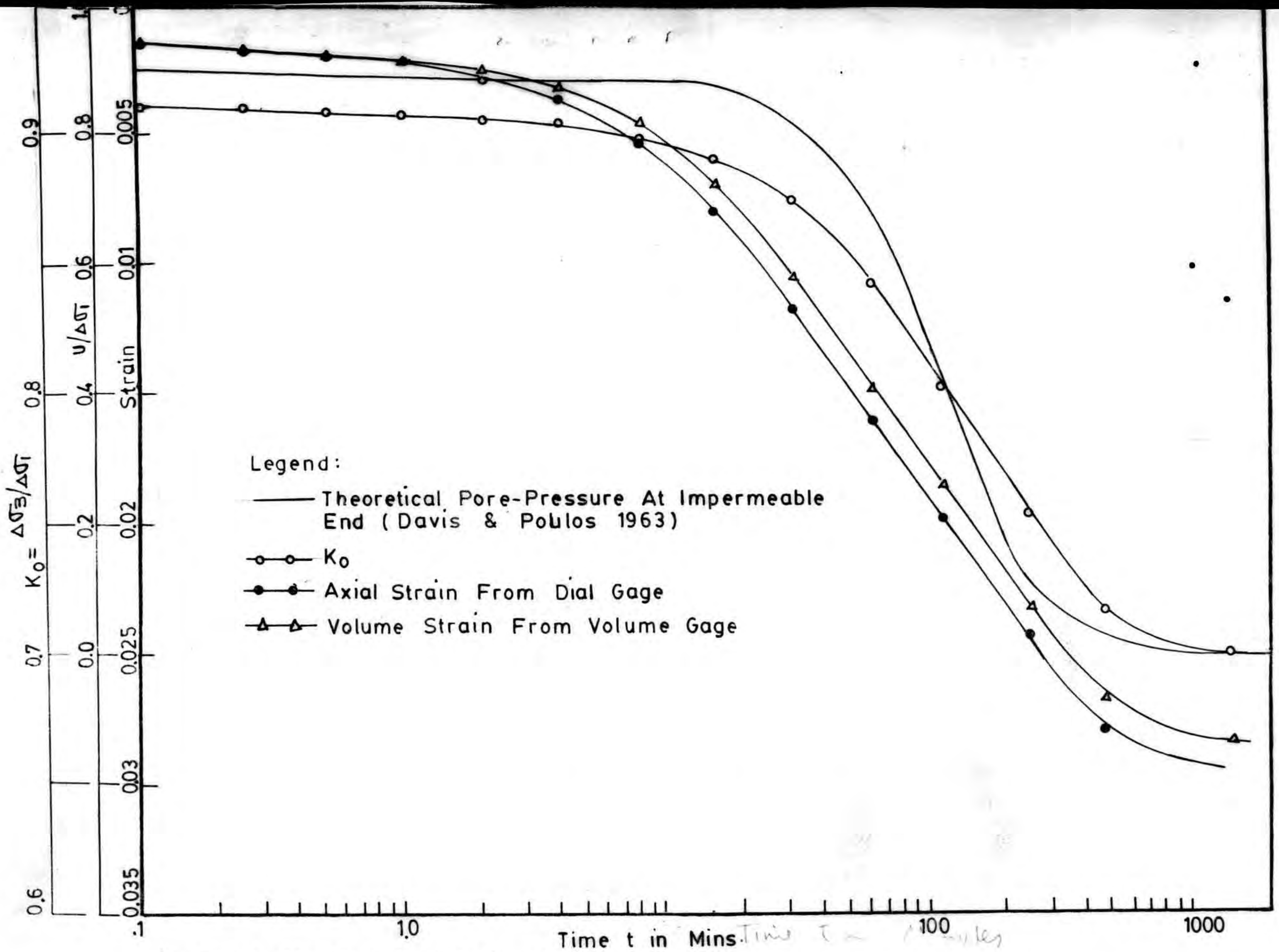

Fig. B - 11 K_o - Test Result Sample No. S-2a

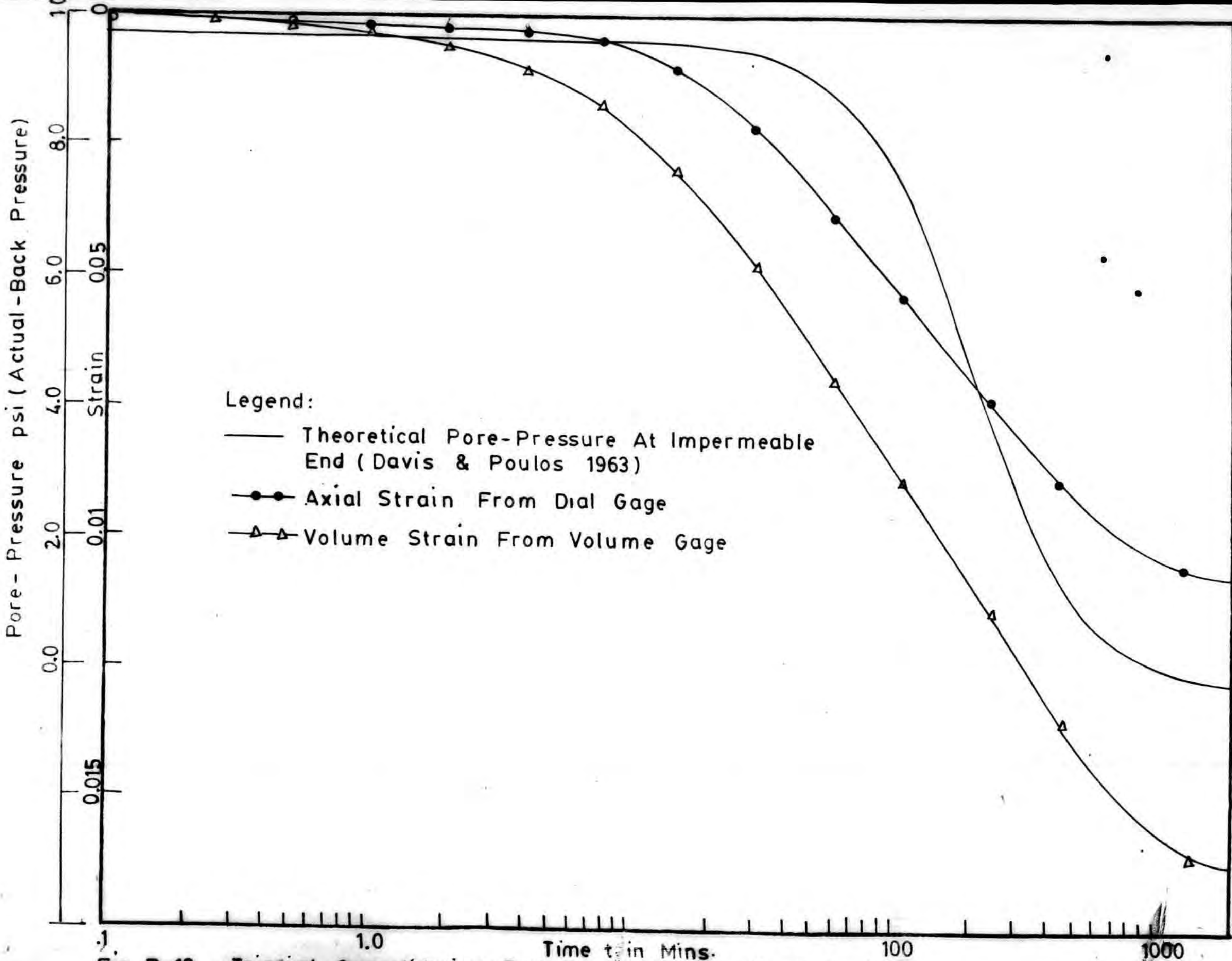

Fig. B-12 Triaxial Consolidation Test Result Sample No. S-2a

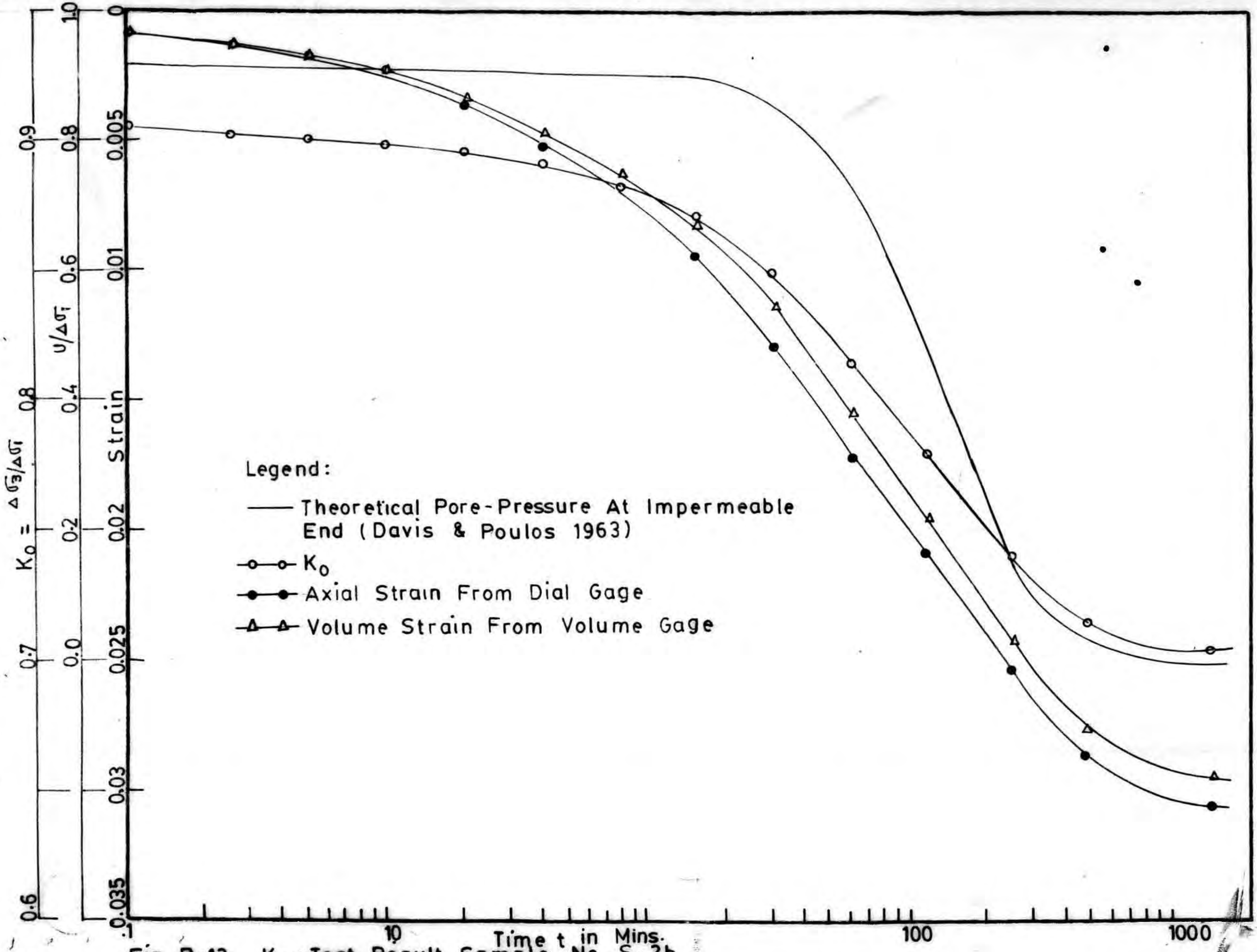

Fig. B-13 K_o–Test Result Sample No. S-2b

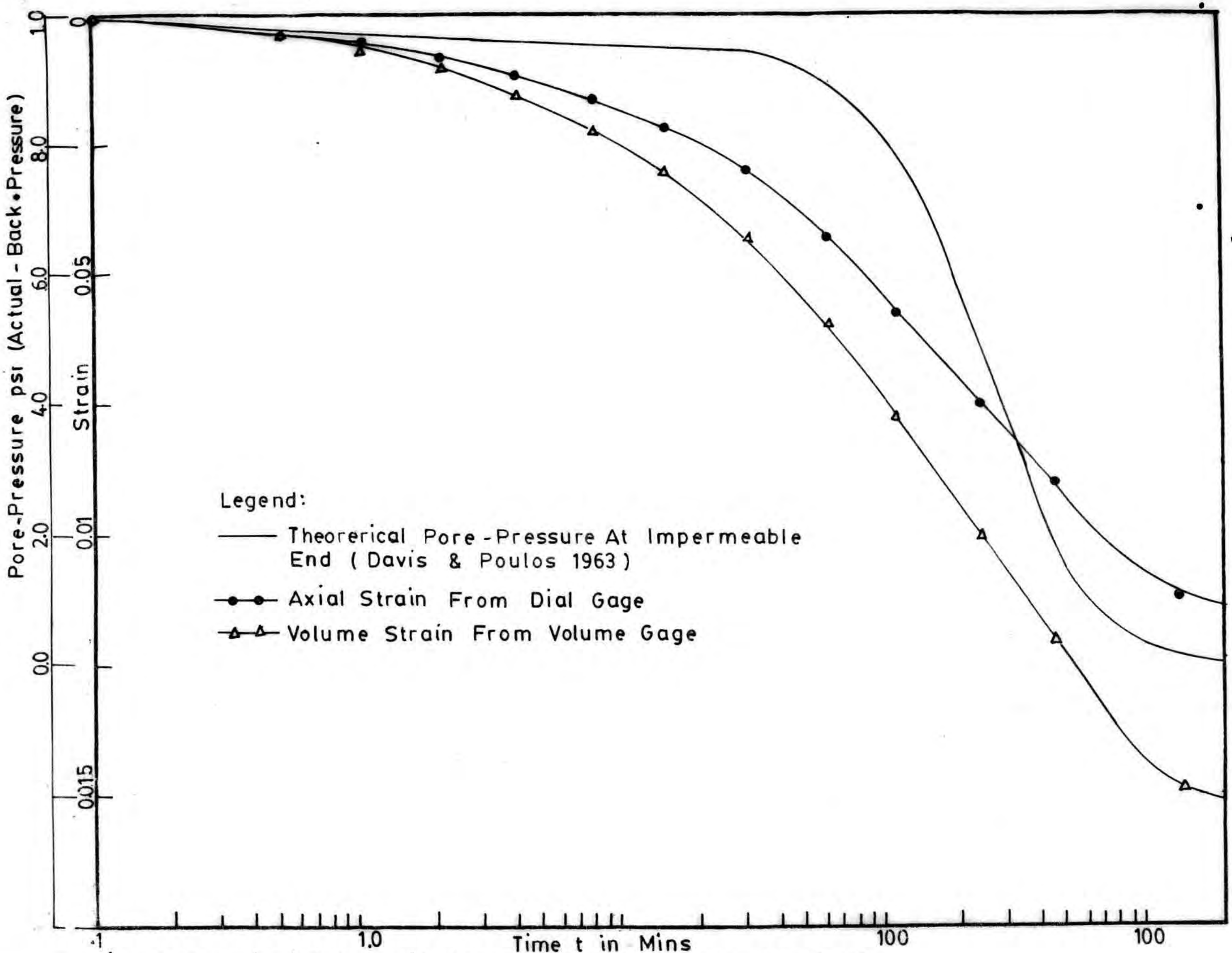

Fig. B- 14 Triaxial Consolidation Test Result Sample No. S - 2b

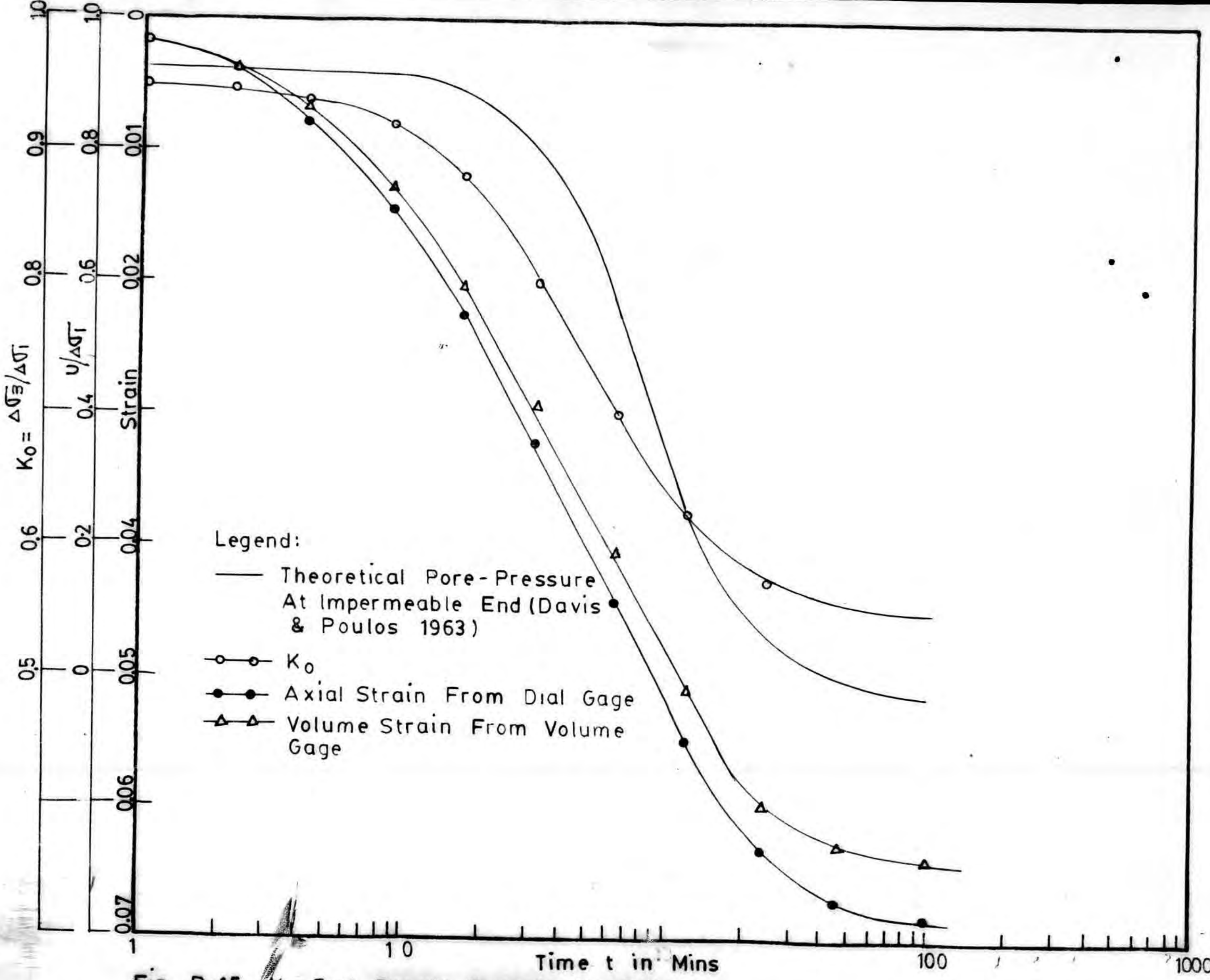

Fig. B-15 K_0-Test Result Sample No. S-4a

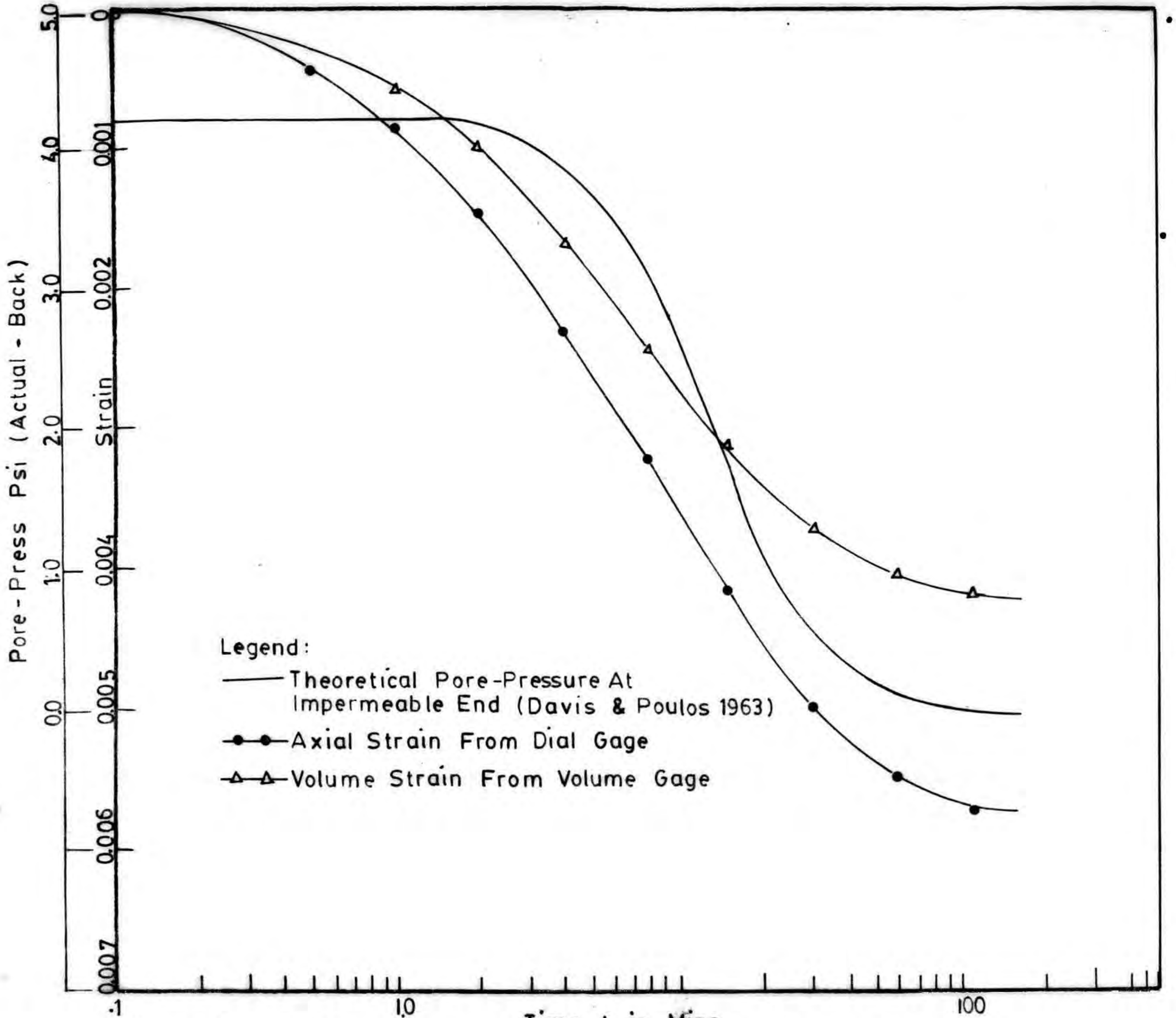

Fig. B-16 Triaxial Consolidation Test Result Sample No S-4a

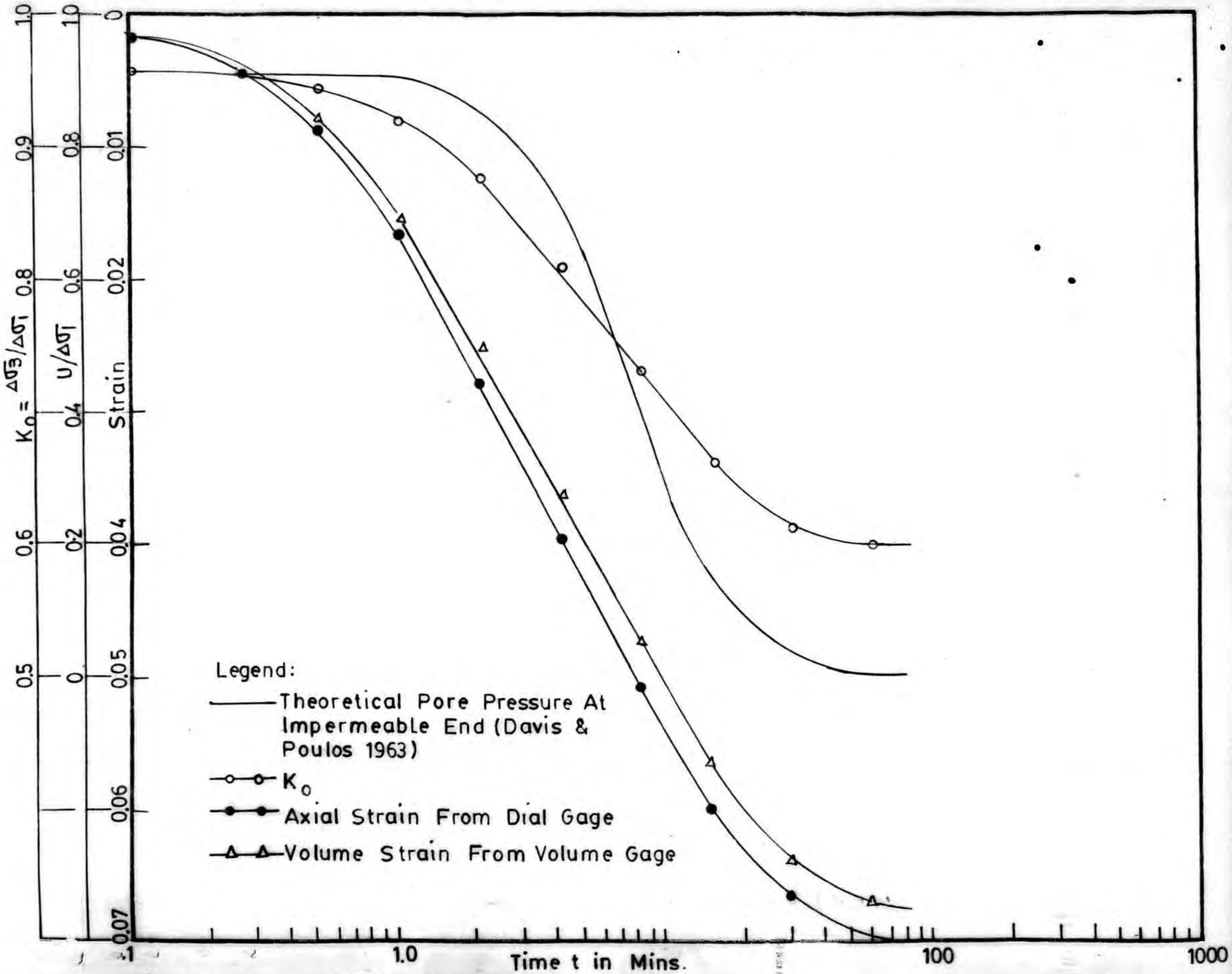

Fig. B - 17 K_o – Test Result Sample No. S - 4b

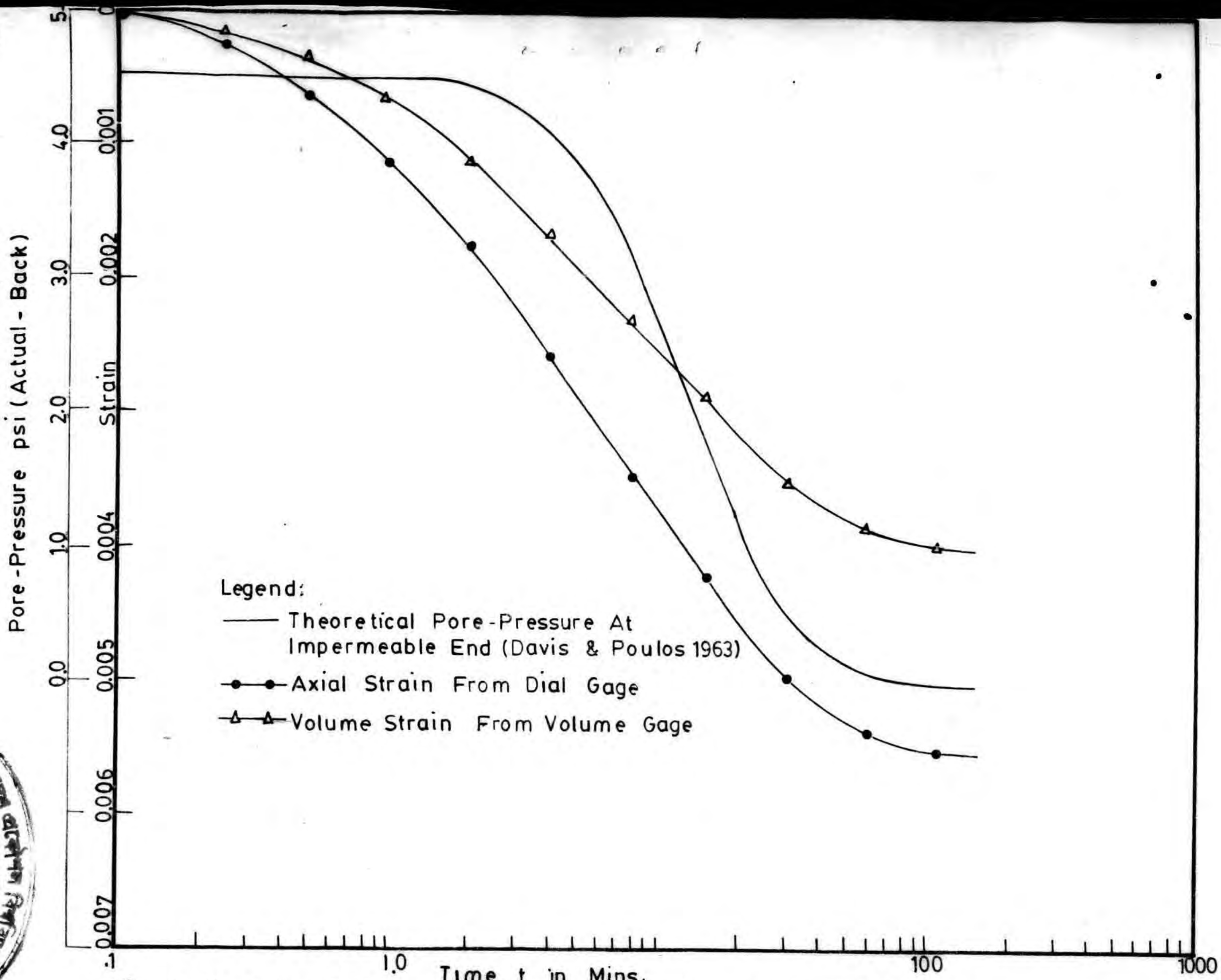

Fig. B-18 Triaxial Consolidation Test Result Sample No. S-4b